PROTEIN MODIFICATION: A PROPOSED MECHANISM FOR THE LONG-TERM PATHOGENESIS OF TRAUMATIC BRAIN INJURY

by

Rachel C. Lazarus

Dissertation submitted to the Faculty of the
Neuroscience Graduate Program
Uniformed Services University of the Health Sciences
In partial fulfillment of the requirements for the degree of
Doctor of Philosophy, 2015

UNIFORMED SERVICES UNIVERSITY, SCHOOL OF MEDICINE GRADUATE PROGRAMS
Graduate Education Office (A 1045), 4301 Jones Bridge Road, Bethesda, MD 20814

APPROVAL OF THE DOCTORAL DISSERTATION IN THE
NEUROSCIENCE GRADUATE PROGRAM

Title of Dissertation: "Protein modification: A proposed mechanism for the long-term pathogenesis of traumatic brain injury"

Name of Candidate: Rachel Lazarus
Doctor of Philosophy Degree
June 4, 2015

DISSERTATION AND ABSTRACT APPROVED:

DATE: 6/19/15
Dr. Clifton Dalgard
DEPARTMENT OF ANATOMY, PHYSIOLOGY AND GENETICS
Committee Chairperson

06/04/2015
Dr. Gregory Mueller
DEPARTMENT OF ANATOMY, PHYSIOLOGY AND GENETICS
Dissertation Advisor

6/4/2015
Dr. Regina Day
DEPARTMENT OF PHARMACOLOGY
Dissertation Co-Advisor

4 June 2015
Dr. Diane Borst
DEPARTMENT OF ANATOMY, PHYSIOLOGY AND GENETICS
Committee Member

6/4/15
Dr. David Grahame
DEPARTMENT OF BIOCHEMISTRY AND MOLECULAR BIOLOGY
Committee Member

ACKNOWLEDGMENTS

This work reflects the efforts of many people who have guided and assisted me through this process. My growth at USUHS as both a professional and as a scientist is entirely due to an incredible group of teachers and researchers. I am grateful to them all.

I am deeply appreciative to Dr. Gregory Mueller for his mentorship over these last five years at USUHS. He not only gave me the opportunity to work in the laboratory, but also devoted countless hours and boundless energy to teaching me how to become a scientist. His unwavering optimism and patience inspired me to pursue meaningful research, and I am so grateful to him for his support. Thank you for shaping me into the researcher that I am today.

I am also incredibly grateful to my co-mentor, Dr. Regina Day. Dr. Day challenged me to grow as a successful science communicator and always made the time to speak with me about research, writing, and my future career in science.

I would like to thank the members of my dissertation committee, including Drs. Dalgard, Borst and Grahame. Their input and critical feedback regarding experimental design and data interpretation were invaluable to the development of this work.

I would also like to thank Dr. David Jacobowitz, who devoted an incredible amount of effort into training me in immunohistochemical techniques. I would also like to acknowledge Dr. Dennis McDaniel, whose teaching allowed me to appreciate the fundamentals of confocal microscopy.

I am particularly grateful to Mr. Mike Flora and Mr. Jim Freedy. Their work in experimental design and protocol optimization provided the technical backbone for this research. The expert skills of Ms. Tinghua Chen guided many aspects of the data

collection for this work, and her training allowed me to become a successful independent researcher.

An immense amount of gratitude is due to two former members of the lab, Dr. John Buonora and Mr. Mike Mousseau. Dr. Buonora contributed enormously to this work, with his tissue collection establishing the basis for this research. The work presented here would not have been possible without his ceaseless efforts. Mr. Mousseau's research laid the foundation for much of our work in protein carbonylation.

Finally, I would like to thank my friends and family. I am so grateful for the loving support of my parents, Ira and Ellen Lazarus, who have always encouraged me to pursue my education to the fullest. Thank you to my grandmother, Bunny Abrams, and my aunt, Wendy Abrams, who inspire me constantly with their cheer and positivity. Thank you to the Lutz and Jackson families, who have brought so much joy and friendship into my life. Finally, thank you to my best friend and husband, Alex Lutz, who has supported me over these last five years with endless encouragement and love.

DEDICATION

For my best friend, Alex.

COPYRIGHT STATEMENT

The author hereby certifies that the use of any copyrighted material in the dissertation manuscript entitled: "Protein modification: A proposed mechanism for the long-term pathogenesis of traumatic brain injury" is appropriately acknowledged and, beyond brief excerpts, is with the permission of the copyright owner.

Rachel C. Lazarus
Program in Neuroscience
August 4, 2015

ABSTRACT

Title of Dissertation: Protein modification: A proposed mechanism for the long-term pathogenesis of traumatic brain injury

by

Rachel C. Lazarus, Doctor of Philosophy, 2015

Thesis directed by: Dr. Gregory P. Mueller, Ph.D.
Professor and Vice Chairman for Research,
Department of Anatomy, Physiology and Genetics
Professor, Program in Neuroscience
Associate Dean for Graduate Education

Traumatic brain injury (TBI) is a major cause of long-term disability. Acute TBI prompts a constellation of dysfunctional processes, collectively known as "secondary injury" mechanisms. A hallmark secondary injury in TBI is a prolonged imbalance in calcium homeostasis, resulting in a dramatic influx of calcium into brain cells. This influx elicits the generation of damaging reactive oxygen species. Protein carbonylation and citrullination are pathological post-translational modifications that can result from intracellular calcium overload. These modifications have been proposed to play a role in neurodegenerative disorders, including Alzheimer's disease, and multiple sclerosis. Both carbonylation and citrullination can contribute to ongoing dysfunction, either through

direct loss of protein function or via immune-based mechanisms where proteins specifically modified by citrullination become targeted by the adaptive immune system.

This work investigated carbonylation and citrullination in a rodent model of TBI. We have identified specific regions and cell types susceptible to these modifications following TBI. While protein carbonylation was expressed in astrocytes of the lesion site and ependymal cells of specific periventricular regions, citrullination was found in astrocytes throughout the cerebral cortex, external capsule, and hippocampus. Unexpectedly, only a small subset of proteins in the entire brain proteome was affected by TBI. Four proteins were found to be carbonylated in response to injury, and these same proteins, along with 33 others, were found to be citrullinated following TBI. Many of these 37 proteins are known to be modified similarly in other neuropathologies. While the distribution and magnitude of protein citrullination was unaffected by gender, susceptibility to protein carbonylation was gender dependent, with males showing significantly greater protein carbonylation in ependymal cells distant from the injury lesion, as compared to females.

These findings show that carbonylation and citrullination are specific processes, with selective effects on regional, cellular, and proteomic susceptibility. Gender differences observed in carbonylation indicate that hormonal mechanisms may serve a protective role in TBI-induced oxidative stress. The dramatic expression of protein citrullination following injury may provide a basis for the development of autoimmune dysfunction in TBI pathology. Accordingly, persistent proteomic changes may underlie ongoing disability, either through direct loss-of-function or secondary immune-based pathological mechanisms.

TABLE OF CONTENTS

LIST OF TABLES xi

LIST OF FIGURES xii

CHAPTER 1: Introduction 1

Traumatic brain injury 1
Mechanisms of secondary injuries 2
Ionic imbalance and intracellular calcium overload following TBI 2
Oxidative stress and protein carbonylation 3
Calcium overload and protein citrullination 6
Pathological effects of carbonylation and citrullination 8
Summary 10

CHAPTER 2: Protein carbonylation after traumatic brain injury: cell specificity, regional susceptibility, and gender differences 13

Abstract 14
Introduction 16
Materials and Methods 17
Controlled Cortical Impact (CCI) 17
Immunoblotting: protein carbonylation detection and identification in brain tissue 18
Tissue collection and preparation 18
One-dimensional gel electrophoresis 18
Fluid-phase isoelectric focusing (IEF) 19
Postelectrophoretic detection of carbonylated proteins 20
Protein identification by peptide mass fingerprinting 21
Immunohistochemistry 22
Tissue collection and preparation 22
Detection of carbonylated proteins and cell-specific markers 22
Preadsorption control 23
Statistical analysis 24
Results 24
CCI increases protein carbonylation in specific regions of the brain 24
Cell specificity of CCI-induced protein carbonylation 30
Gender influences regional patterns of protein carbonylation 32
Discussion 37
Conclusion 43
Acknowledgments 43

CHAPTER 3: Protein citrullination: A proposed mechanism for long-term pathology in traumatic brain injury 44

Abstract 45
Introduction 47

Materials and Methods 49
Controlled Cortical Impact (CCI) 49
Immunohistochemistry 50
Tissue collection and preparation 50
Detection of cell-specific citrullination 50
Preadsorption control 51
Identification of citrullinated protein species in injured rat brain 52
Tissue collection and preparation 52
Fluid-phase Isoelectric Focusing (F-IEF) 52
Molecular weight fractionation 53
Immunoblotting 53
Protein identifications 54
In vitro model of protein citrullination following TBI-induced excitotoxicity in astrocytes 55
Results 56
Discussion 67
Acknowledgments 72

CHAPTER 4: Discussion 74

Region and cell-specific effects of TBI on protein carbonylation and citrullination 77
TBI induces protein carbonylation in ependymal cells of the dorsal third ventricle and median eminence 77
Region-specific protein carbonylation and citrullination within astrocytes following TBI 79
Neurons and oligodendrocytes do not express protein citrullination after TBI 83
Gender modulates protein carbonylation following injury 84
Selective modification of proteins following TBI 86
Potential long-term effects of protein carbonylation and citrullination on TBI pathology 90
Summary and Conclusions 92

REFERENCES 95

Appendix 1: Technical validation of 6B3 anti-citrullinated protein antibody 109

LIST OF TABLES

Table 1. Increased expression of selective protein carbonylation and citrullination in multiple neurodegenerative pathologies. Proteomic analyses in this investigation revealed several proteins carbonylated and citrullinated following TBI (blue column). Many of these proteins are modified in other pathological neural disorders, including Alzheimer's disease, prion disease, multiple sclerosis/EAE (experimental autoimmune encephalomyelitis), and aging brain tissue. Asterisk (*) indicates evidence of modification-induced autoantigenicity..... 89

LIST OF FIGURES

Figure 1. Mechanisms of protein carbonylation following mitochondrial dysfunction. In the wake of mitochondrial dysfunction driven by calcium overload, oxygen is reduced to hydroxyl radicals through a series of electron reductions catalyzed by enzymes such as NAD(P)H oxidase and superoxide dismutase. Hydroxyl radicals, as well as the intermediate molecules superoxide and hydrogen peroxide, are known as reactive oxygen species (ROS). ROS are highly reactive molecules that target polyunsaturated fatty acids, such as those in the lipid membranes of neural cells, forming breakdown products of lipid peroxidation. These products are categorized as reactive carbonyl species (RCS). Both ROS and RCS catalyze irreversible protein carbonylation..... 5

Figure 2. Mechanisms of protein citrullination following intracellular calcium overload. Peptidylarginine deiminase (PAD) enzymes are activated by high levels of intracellular calcium. Once activated, PAD enzymes catalyze the conversion of intrapeptidyl arginine residues to intrapeptidyl citrulline residues. Ammonia (NH_3) is released as a byproduct of this reaction. (Figure adapted from Tešija-Kuna & Žirović (2008))..... 8

Figure 3. Proposed model of proteomic changes following TBI-induced calcium overload. After traumatic injury, ischemia and mechanical damage (tearing, shearing, and hemorrhage) lead to increased extracellular glutamate, an excitatory amino acid (1). This causes significant ionic imbalance, prompting a dramatic influx of calcium into cells (2). High intracellular levels of calcium impair mitochondrial function, causing decreased energy metabolism (3). ATP depletion prevents the efflux of calcium to restore ionic homeostasis (4). In addition, calcium-induced mitochondrial dysfunction leads to the production of reactive oxygen species (ROS) (5). Two post-translational modifications, citrullination and carbonylation, are driven by calcium overload. Citrullination, the conversion of intrapeptidyl arginine to intrapeptidyl citrulline residues, is catalyzed by peptidylarginine deiminase, which is a calcium-dependent enzyme (top panel). Carbonylation, the conversion of an intrapeptidyl amino acid (Lys, Cys, His) to a carbonyl group, is driven by the effects of ROS (bottom panel). Both citrullination and carbonylation are irreversible proteomic modifications with significant effects on protein structure and function. 11

Figure 4. Effects of CCI on protein carbonylation in rat brain. Five days after experimentally administered CCI, extracts were obtained from dissected regions of brain containing the injury penumbra (I) and the corresponding contralateral control region (C). Lysates were analyzed (4.2 μg/lane) for protein carbonylation by one-dimensional gel electrophoresis followed by Western blotting. Coomassie staining of the protein remaining in the transferred gel was used to confirm equal protein loading (left). DNP Western blotting was performed to detect protein carbonylation in CCI-injured brain samples versus uninjured contralateral brain samples (right). Arrows indicate protein bands for which carbonylation was most affected by CCI. Images are representative of three independent experiments. A total of *n*=5 CCI animals were examined..... 25

Figure 5. Identification of rat brain proteins carbonylated after CCI. Proteins present in extracts of naïve rat brain (N) and contralateral (C) and ipsilateral (I) regions of CCI-injured rats were fractionated by fluid-phase IEF (p*I* ranges listed at bottom) and one-dimensional gel electrophoresis. Proteins were transferred to nitrocellulose, derivatized, and probed with anti-DNP antibody (right). Proteins remaining in the gel were visualized by Coomassie staining (left). Features showing increased carbonylation in response to TBI (numbered boxes, right) were mapped to the corresponding Coomassie features (left) and identified by peptide mass fingerprinting as: (1) GFAP (49,957 Da; p*I* 5.4), (2) CRMP2 (62,278 Da; p*I* 6.0), (3) ALDOC (39,284 Da; p*I* 6.7), and (4) ALDOA (39,352 Da; p*I*8.3). Images are representative of three independent experiments. A total of *n*=8 CCI and *n*=8 naïve animals were examined. 26
Figure 6. Effects of CCI on protein carbonylation immunohistochemistry in rat brain. Brain tissue was collected 5 days after CCI and evaluated by anti-DNP immunofluorescence. A whole-slice image (top, ×1 original magnification, scale bar indicates 2 mm) and an image of the lesion site (bottom, ×2.5 original magnification, scale bar indicates 2 mm) are shown. Images are representative of three independent experiments. A total of *n*=16 CCI animals and *n*=16 naïve animals were examined, with 16 slices per animal from bregma –2.12 mm to bregma –3.30 mm. 27
Figure 7. The CCI-induced increase in anti-DNP immunofluorescence is specific for protein carbonylation. Brain tissue was collected 5 days after CCI and evaluated by anti-DNP immunofluorescence. Anti-DNP immunofluorescence in the cerebral cortex contralateral to the injury and the CCI-injured cortex are depicted in (A) and (B), respectively (original magnification ×10, scale indicates 200 μm). Immunoneutralization of the anti-DNP antibody with (C) carbonylated and derivatized β-casein but not (D) unmodified β-casein resulted in reduced DNP immunohistochemical staining of the CCI-injured brain (original magnification ×20, scale bar, 100 μm). Images are representative of three independent experiments. A total of *n*=16 CCI animals and *n*=16 naïve animals were examined, with 16 slices per animal from bregma –2.12 mm to bregma –3.30 mm. 28
Figure 8. Effects of CCI on protein carbonylation in ependymal cells lining the dorsal third ventricle and median eminence. Brain tissue was collected 5 days after CCI and evaluated by anti-DNP immunofluorescence (A and C, naïve control; B and D, CCI). (A and B) Representatives of the dorsal third ventricle. (C and D) Representatives of the ventricle lining above the median eminence. After CCI, ependymal cells lining the dorsal third ventricle became highly immunoreactive, as did distinct cells located in the adjacent parenchyma of the paraventricular thalamic nucleus (B, arrows). Also after CCI, cells lining the ventricle of the median eminence showed an increase in protein carbonylation (D). (A and B) Original magnification ×20, scale 50 μm. (C and D) Original magnification ×40, scale 50 μm. Images are representative of three independent experiments. A total of *n*=16 CCI animals and *n*=16 naïve animals were examined, with 16 slices per animal from bregma –2.12 mm to bregma –3.30 mm. 30
Figure 9. CCI-induced protein carbonylation is most significantly associated with astrocytes in the region of a CCI lesion. Brain tissue was collected 5 days after CCI

and evaluated by coimmunofluorescence. (A–C) Representatives of the astrocyte and DNP detection at the injury site, (D–F) representatives of neuron and DNP detection at the injury site. Carbonylated proteins within the penumbra region were identified by anti-DNP immunohistochemistry (green, A and D). (B) and (E) represent anti-GFAP (astrocytes, red) and anti-NeuN (neurons, red) detection, respectively, in the injury lesion. (B) also illustrates counterstaining with DAPI (blue) for the detection of nuclei. Merged images (C and F) indicate the detection of carbonylated proteins and their relation to astrocytes (C) and neurons (F). Astrocytes containing carbonylated proteins are shown in yellow (C). Astrocyte bodies and processes (red) contained carbonylated proteins (green, A), resulting in a yellow colocalization signal as indicated by white arrows (C). Astrocyte processes surrounding degenerating cells that contained carbonylated proteins are indicated by pink arrows (C). Neurons were identified using anti-NeuN (red, E), and protein carbonylation was identified using anti-DNP (green, D). The merged image indicates locations where both labels occur (yellow, F). Arrows indicate neurons that contained carbonylated proteins. (A–C) Original magnification ×40, scale 50 μm. (D–F) Original magnification ×20, scale 100 μm. Images are representative of three independent experiments. A total of *n*=3 CCI animals and *n*=3 naïve animals were examined, with four slices per animal from bregma –2.12 mm to bregma –3.30 mm. 31

Figure 10. Representative images depicting the carbonylation scoring system. Brain tissue was collected 5 days after CCI and evaluated by anti-DNP immunofluorescence. Images show relative increments in anti-DNP immunofluorescence (0–3) observed in the penumbra/cortex, dorsal third ventricle, and median eminence regions. The distinguishing feature differentiating a score of 2 versus a score of 3 for the dorsal third ventricle was the anti-DNP labeling of peri-ependymal cells located in the parenchyma both lateral and ventral to the dorsal third ventricle. This observation reflected a stippled pattern of carbonylation-positive cells expanding approximately 10 to 50 μm into surrounding tissue from the ependymal lining of the ventricle. Penumbra/cortex and median eminence images, original magnification ×10; dorsal third ventricle images, original magnification ×20. Images are representative of three independent experiments. A total of *n*=16 CCI animals and *n*=16 naïve animals were examined, with 16 slices per animal from bregma –2.12 mm to bregma –3.30 mm. 33

Figure 11. Gender did not affect the degree of protein carbonylation in the cerebral cortex of control and CCI-lesioned rats. Brain tissue was collected 5 days after CCI and evaluated by anti-DNP immunofluorescence. As shown qualitatively for a representative (A) male and (B) female, and quantitatively in Figure 13, the degree of protein carbonylation after CCI in the penumbra region was not significantly affected by gender. Original magnification ×20, scale 100 μm. Images are representative of three independent experiments. A total of *n*=16 CCI animals (7 female, 9 male) were examined, with 16 slices per animal from bregma –2.12 mm to bregma –3.30 mm. 34

Figure 12. Effects of CCI on protein carbonylation in regions of the cerebral cortex of male and female rats. Brain tissue was collected 5 days after CCI and evaluated by anti-DNP immunofluorescence. Sections were scored for protein carbonylation as

described under Material and methods. Data indicate means ± SEM. A post hoc Tukey HSD analysis indicated a statistically significant difference (***p<0.001) between the scores of the penumbra versus other cortical regions of the injured and naïve animals. Graph is representative of three independent experiments. A total of n=16 CCI animals (7 female and 9 male) and n=16 naïve animals (9 female and 7 male) were examined, with 16 slices per animal from bregma –2.12 mm to bregma –3.30 mm. 35

Figure 13. Gender differences in the effects of CCI on protein carbonylation in the median eminence and dorsal third ventricle. Brain tissue was collected 5 days after CCI and evaluated by anti-DNP immunofluorescence. Sections were scored for protein carbonylation as described under Material and methods. Data indicate means ± SEM. N.S., not statistically significant; *p<0.05; **p<0.01. Regarding the median eminence, a one-way ANOVA indicated significantly different levels of protein carbonylation between the animal gender and the injury conditions (F(3,27) =13.096, p=0.000). A post hoc Tukey HSD analysis indicated a statistically significant difference between male naïve and male CCI protein carbonylation (*p<0.05), a statistically significant difference between male naïve and female naïve protein carbonylation (*p<0.05), and a statistically significant difference between male CCI and female CCI protein carbonylation (**p<0.01). There was not a statistically significant difference between female naïve and female CCI protein carbonylation (N.S., p=0.192). Regarding the dorsal third ventricle, a one-way ANOVA indicated significantly different levels of protein carbonylation between the animal gender and the injury conditions (F(3,28) =11.874, p=0.000). A post hoc Tukey HSD analysis indicated a statistically significant difference between male naïve and male CCI protein carbonylation (*p<0.05) and a statistically significant difference between male CCI and female CCI protein carbonylation (**p<0.01). There was not a statistically significant difference between male naïve and female naïve protein carbonylation (N.S., p=0.311) or between female naïve and female CCI protein carbonylation (N.S., p=0.996). Graph is representative of three independent experiments. A total of n=16 CCI animals (7 female and 9 male) and n=16 naïve animals (9 female and 7 male) were examined, with 16 slices per animal from bregma –2.12 mm to bregma –3.30 mm. 36

Figure 14. Injury upregulates the expression of citrullinated proteins in the cerebral cortex. Brain tissue was collected five days after CCI and evaluated for protein citrullination by anti-protein citrulline immunolabeling using mAB 6B3. The panels show immunolabeling in sections of control (left) and injured brain (right) (2X magnification). Data are representative of 15 control animals (8 males and 7 females) and 21 CCI animals (11 males and 10 females). No gender-based differences were observed. PB-cit: Protein-bound citrulline. 56

Figure 15. Specificity of anti-protein citrulline immunolabeling by mAb 6B3. Panels A and B show immunofluorescent signals from mAb 6B3 anti-protein citrulline labeling of the injured cerebral cortex (panel A) and ipsilateral hippocampus (panel B). Panels C and D show immunolableing of equivalent sections with mAb 6B3 that was preadsorbed with citrullinated protein standards. Panels E, F, and G show secondary-only control images of the cortex, external capsule, and corpus callosum /

cingulum (20x magnification). The control and immunoneutralized preparations of mAb 6B3 were treated identically, with the exception of the presence or absence of neutralizing citrullinated proteins. Data are representative of two independent experiments. Scale bar: 200 μm. 57
Figure 16. Increased protein citrullination in the cerebral cortex, hippocampus and external capsule following CCI. Anti-protein citrulline immunolabeling by mAb 6B3 is shown for the control brain regions (panels A, D, and G), regions ipsilateral to the lesion (panels B, E, H) and regions contralateral to the lesion (panels C, F, and G). Structures representated are the cerebral cortex (A-C), hippocampus (D-F), and external capsule (G-I). Data are representative of 15 control animals (8 males and 7 females) and 21 CCI animals (11 males and 10 females). No gender-based differences were observed. Scale bar: 200 μm. 59
Figure 17. Localization of CCI-induced protein citrullination to astrocytes. Panels on the left show the colocalization of mAb 6B3 labeling with anti-GFAP labeling in the external capsule. Panels on the right show the colocalization of mAb 6B3 labeling with anti-GFAP labeling in the cerebral cortex. Data are representative of 15 control animals (8 males and 7 females) and 21 CCI animals (11 males and 10 females). No gender-based differences were observed. Scale bar: 200 μm. PB-cit: Protein-bound citrulline. 60
Figure 18. CCI did not affect the status of protein citrullination in neurons, microglia or oligodendrocytes. Sections of cerebral cortex ipsilateral to CCI were probed with mAb 6B3 to label protein bound citrulline (PB-Cit; upper panels) and either anti-NeuN, Iba1, or MBP to label neurons, microglia, or oligodendrocytes, respectively (middle panels). The merge of the two signals is presented in the lower panels. Data are representative of 8 separate experiments. Scale bar = 200 μm. 61
Figure 19. Effects of CCI on protein citrullination in GFAP-positive cells of the ipsilateral and contralateral hippocampus. Colocalization of anti-protein citrulline and anti-GFAP labeling in astrocytes of the ipsilateral hippocampus is depicted in the pairs of panels presented on the left (A-C). Panel D shows the distinctive anti-citrullinated protein immunolabeling of large, rounded cells observed in the contralateral hippocampus of approximately 20% of CCI animals (4 of 21). While these cells lacked the classical stellate morphology of astrocytes, the anti-citrullinated protein labeling colocalized with GFAP immunolabeling (panels E-G). PB-cit: Protein-bound citrulline. 62
Figure 20. Specificity of anti-protein citrulline mAb 6B3 detection for western blotting. Displayed on the left are two Coomassie-stained profiles showing the protein composition of native fibrinogen (Fib) and citrullinated fibrinogen (C-Fib). The western blot (right) shows three immunoblots in which: citrullinated fibrinogen was probed with active mAb 6B3 (Active/C-Fib; left lane); citrullinated fibrinogen was probed with immunoneutralized mAb 6B3 (Neutralized/C-Fib; middle lane); and native fibrinogen was probed with active mAb 6B3 (Active/Fib; right lane). 63
Figure 21. Identification of proteins that are citrullinated in response to CCI. Extracts of control (C) and injured (I) cerebral cortex were fractionated by fluid-phase isoelectric focusing into defined pH ranges (shown at top) and then further resolved according to molecular weight using one-dimensional gel electrophoresis. Proteins were then transferred to nitrocellulose membranes and probed for protein-bound

citrulline (see Methods) (right panel, “Western blot”). Gels run in parallel were visualized with Coomassie (left panel). Sixteen features showing increased citrullination in response to CCI (black numbered boxes, right panel) were mapped to corresponding Coomassie features (red numbered boxes, left panel) and identified by peptide mass finger printing and tandem mass spectrometry. Proteins identified are listed in the lower panel. Images are representative of six independent experiments. A total of n = 4 CCI and n = 4 control animals were examined..... 65
Figure 22. Simulated brain injury in normal human astrocytes reveals a spectrum of GFAP breakdown products and the hyper-citrullination of one GFAP species. Normal human astrocytes were treated with ionomycin (10 μM; 4h) and analyzed for GFAP (left panel) and protein-bound citrulline immunoreactivity (right panel) by western blot. The results of three independent experiments (A, B, and C) are presented, showing the immunoreactivity in extracts prepared from untreated control cells (Control) and cells treated with ionomycin (+ Iono). The blue arrows indicate intact GFAP, while the orange arrows indicate the hyper-citrullinated GFAP breakdown product..... 66
Figure 23. Potential ongoing effects of protein carbonylation and citrullination in TBI pathology. Injury may induce long-term dysfunction through the calcium-mediated proteomic modifications, carbonylation and citrullination. These modifications can elicit a number of pathological outcomes, including the generation of antigenic epitopes (citrullination) and formation of cytotoxic aggregates (carbonylation). 74

CHAPTER 1: Introduction

TRAUMATIC BRAIN INJURY

Traumatic brain injury (TBI) is a major public health issue in the U.S., with over 1.7 million cases occurring annually. At least 5.3 million Americans are currently living with ongoing disability due to TBI (157). In civilians, these injuries are largely due to motor vehicle accidents (48), as well as falls, sports, and firearms (161). While on deployment, military populations are at disproportionate risk for blast-injury TBIs caused by improvised explosive devices in theater (61). These blast-induced injuries have become the signature injury of operations in Iraq and Afghanistan, with 10% – 20% of returning veterans reported to have suffered a TBI (46).

The long-term consequences of TBI can be complex and progressive, with 10% – 15% of individuals diagnosed with mild TBI going on to suffer from persistent symptoms, while as many as 50% of patients with moderate TBI experience long-term dysfunction (12). In addition to the development of cognitive deficits in attention, memory, and executive function (12), a chronic inflammatory state can persist in the brain for months, and even years, following TBI (107; 114). However, elucidating the mechanisms that underlie chronic dysfunction following TBI has proven challenging. Currently, it is not well understood how the acute mechanical injury of TBI can develop into long-term dysfunctions that may last for years. Present understanding of post-injury processes falls into two distinct phases: a first stage of "primary injury," and subsequent "secondary injury." Primary injury refers to the direct, physical disruption of neural tissue following impact, such as axonal strain and injury due to rotational acceleration-deceleration (137) or focal injuries such as skull fracture (117). Secondary injury refers to

the ensuing constellation of dysfunctional cellular and physiological processes following primary mechanical injury (161).

MECHANISMS OF SECONDARY INJURIES

Secondary injury consists of a delayed series of interdependent pathological processes triggered by primary injury (109; 161). Hemorrhage, edema, and raised intracranial pressure are hallmarks of primary injury (51; 161). Consequences of ischemia and hypoxia (86) involve complex cascades of cellular processes, including mitochondrial dysfunction, calcium overload, inflammation, and oxidative stress, which arise over the course of hours to weeks following TBI (157). These secondary injury processes can lead to serious cognitive dysfunction by disrupting synaptic plasticity, axonal structure, and by inducing cell death through apoptosis, necrosis, and autophagy (157). One important component of secondary injury is the disturbance of ionic homeostasis (101), which can lead to acute and ongoing changes in cellular physiology (52).

IONIC IMBALANCE AND INTRACELLULAR CALCIUM OVERLOAD FOLLOWING TBI

Primary injury from mechanical forces can lead to ionic imbalance in the brain, largely due to the effects of glutamate excitotoxicity following TBI. The dramatic increase of extracellular glutamate, an excitatory amino acid, is due to a number of post-injury effects, including the physical disruption of cell membranes and the impairment of energy-dependent glutamate uptake mechanisms (157). This glutamate-rich extracellular environment prompts the activation of a number of ionotropic glutamate receptors, including N-methyl-D-aspartate (NMDA) receptors (52). Over-activation of these receptors affects ionic balance in a number of ways, including increased potassium efflux

and the concurrent, dramatic influx of sodium, chloride, and calcium, causing neurons and glial cells to pathologically swell (117). Furthermore, intracellular magnesium levels are reduced, unblocking NMDA receptors and leading to an even greater influx of calcium across the cell membrane (157). This shift in ionic balance is harmful, activating damaging intracellular cascades including lipid peroxidation, proteolysis, free radical generation (161), and resulting in the activation of pro-apoptotic gene expression (157) and loss of dendritic spines.

Energy metabolism is also significantly affected by post-TBI ionic imbalance. As the sodium-potassium pump attempts to restore membrane potential, increasing amounts of ATP are required. However, ATP availability is limited by decreased oxygen and glucose, due to impaired cerebral blood flow (52). As calcium accumulation increases from extracellular sources, the failure of energy resources to correct ionic shifts initiates the release of calcium from intracellular stores (115; 151). This prolonged rise in intracellular calcium is regarded as a hallmark consequence of TBI (49; 50; 90; 149; 160).

Calcium accumulation is seen within hours of brain injury, and persists for several days (52). This overload can lead to several pathological processes, including the activation of calcium-dependent proteases (151; 160), disruption of structural elements such as neurofilaments and microtubules, and the activation of apoptotic genetic signals (52). Prolonged elevation of intracellular calcium also has a profound impact on mitochondria, with dramatic effects on structure, function, and most notably, oxidative stress (52; 151; 157; 160).

OXIDATIVE STRESS AND PROTEIN CARBONYLATION

As intracellular calcium concentration rises, it is sequestered into the mitochondrial matrix across the inner mitochondrial membrane (80; 151). In addition to interfering with ATP synthesis, this ionic accumulation causes the generation of reactive oxygen species (ROS) (80; 117). ROS generation is due to several possible effects of calcium overload-induced mitochondrial dysfunction, including impeded respiration, uncoupled electron transfer (110), and reduced populations of electron acceptors in the mitochondrial matrix (32). The main species of ROS generated by mitochondria is superoxide, a short-lived but highly reactive molecule. Superoxide may be converted to several other ROS, including hydrogen peroxide and hydroxyl radicals. Relative to superoxide and hydroxyl radicals, hydrogen peroxide is a poorly reactive molecule; however, unlike superoxide, it is able to cross cell membranes (15). In contrast, hydroxyl radicals are highly reactive and much more toxic than superoxide (15; 133). These ROS react with neural membrane lipids through peroxidation, generating reactive carbonyl species (RCS) (165) such as acrolein and 4-hydroxynonenal (135; 136) (see Fig. 1).

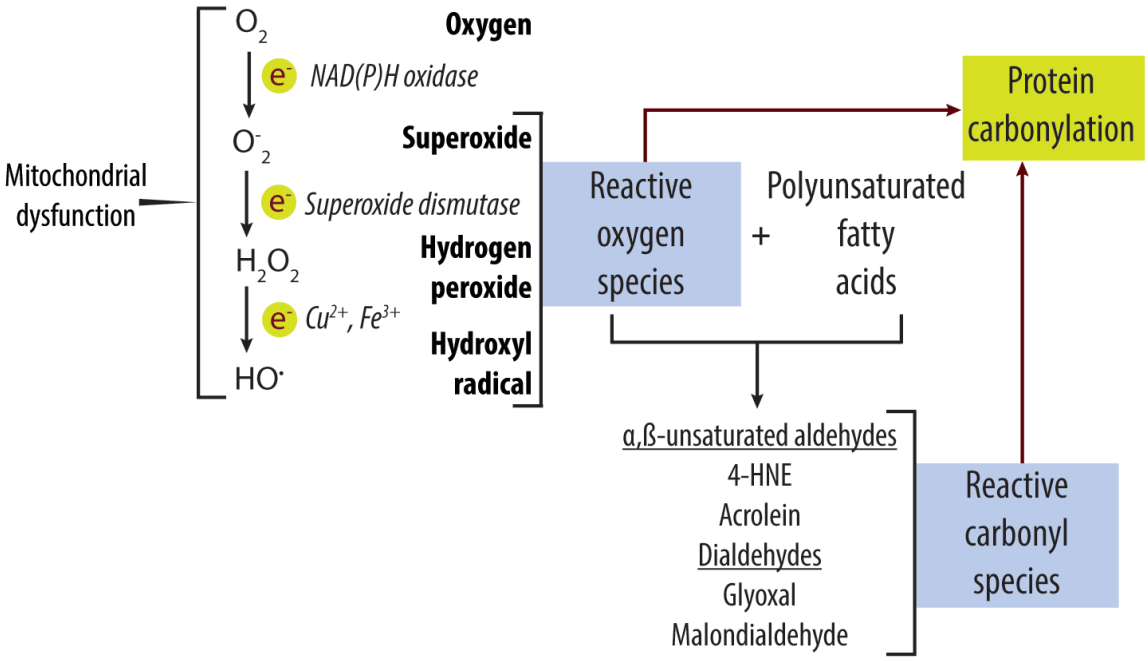

Figure 1. Mechanisms of protein carbonylation following mitochondrial dysfunction. In the wake of mitochondrial dysfunction driven by calcium overload, oxygen is reduced to hydroxyl radicals through a series of electron reductions catalyzed by enzymes such as NAD(P)H oxidase and superoxide dismutase. Hydroxyl radicals, as well as the intermediate molecules superoxide and hydrogen peroxide, are known as reactive oxygen species (ROS). ROS are highly reactive molecules that target polyunsaturated fatty acids, such as those in the lipid membranes of neural cells, forming breakdown products of lipid peroxidation. These products are categorized as reactive carbonyl species (RCS). Both ROS and RCS catalyze irreversible protein carbonylation.

ROS and RCS catalyze an important consequence of oxidative stress known as protein carbonylation. Carbonylation involves the modification of amino acids, including lysine, cysteine, or histidine, to carbonyl derivatives within proteins. A growing body of evidence indicates that protein carbonylation occurs in several neuropathologies, including Alzheimer's disease and Parkinson's disease (26). This modification disrupts both protein structure and function, thereby contributing to injury pathology (40). Recent work (162) has suggested that direct oxidation of proteins by ROS, but not indirect carbonylation by RCS lipid by-products, is a reversible process that may mediate cell

signaling. Specifically, carbonylation is promoted by endothelin-1 (ET-1) in pulmonary tissue; however, this is a transient process. Thiol reductants, including thioredoxin, may serve to decarbonylate proteins in cardiac tissue. Wong, et al. (2012) also suggested that carbonylated proteins may regulate cell signaling processes by influencing molecules involved in signal transduction. The potential role of this modification in regulatory functions, as well as evidence of the possible reversibility of carbonylation, suggest that this post-translational modification may have an important role in the modulation of cell signaling and intracellular processes.

A great deal of research has focused on the role of oxidative stress in the ongoing pathology of TBI (70). However, this research has mainly focused on the use of global carbonylation as a measure of overall oxidative stress in pathology, rather than identifying the specific neural regions, cell types, or proteins affected by this modification. Furthermore, while clinical findings have identified gender-based differences in TBI prognosis (53; 125), little work to date has addressed how gender affects the expression of protein carbonylation in neural tissue following TBI. These gaps in TBI research are significant, as protein carbonylation may underlie long-term changes following injury.

CALCIUM OVERLOAD AND PROTEIN CITRULLINATION

Elevated intracellular calcium also causes a less-studied protein modification known as citrullination. Under normal conditions, protein citrullination is essential for a number of basic physiological functions, including epidermal hydration (127), epigenetic regulation of gene expression (142), hair growth (127), and neural plasticity in stages of early brain development (60). However, in states of pathology, abnormal hyper-

citrullination of proteins may occur. The role of abnormal protein citrullination is best understood in the case of rheumatoid arthritis, an autoimmune disorder involving progressive inflammation of synovial joints (57). In this disorder, the citrullination of proteins prompts an autoimmune response due to the formation of antigenic epitopes. However, protein citrullination is also implicated in several neurodegenerative disorders with altered calcium homeostasis, including Alzheimer's disease (65), temporal lobe epilepsy (9), glaucoma (19), and multiple sclerosis (MS) (6).

Dramatically elevated intracellular calcium is an essential condition for the activation of peptidylarginine deiminases (PADs), the family of enzymes which catalyze the conversion of intra-peptide arginine residues to intra-peptide citrulline residues (64) (See Fig. 2). PAD enzymes exist as five isoforms: PAD1, PAD2, PAD3, PAD4, and PAD6 (159). Each of these isoforms has a physiological role within its expressed tissue: for example, PAD1 serves to regulate cornification within the epidermis, and is also expressed in the uterus. PAD3 is also expressed in the epidermis, as well as hair follicles, while PAD6 is associated with the ovary and testes, serving to regulate embryonic development (159). PAD2 and PAD4, however, are the only PAD enzymes found in neural tissue. PAD2 is localized to astrocytes (38; 68; 115) and oligodendrocytes (55), while PAD4 is exclusively expressed in neurons (2). PAD2 and PAD4 also exhibit the capacity to regulate gene activity through localization to the nucleus and histone citrullination (66; 77; 159).

As depicted in Fig. 2, increased free calcium associates with PAD to allosterically activate this enzyme's activity, which catalyzes the conversion of intra-peptidyl arginine to intra-peptidyl citrulline within other proteins. Disordered calcium homeostasis results

in an abnormal profile of protein citrullination, resulting in the formation of antigenic epitopes.

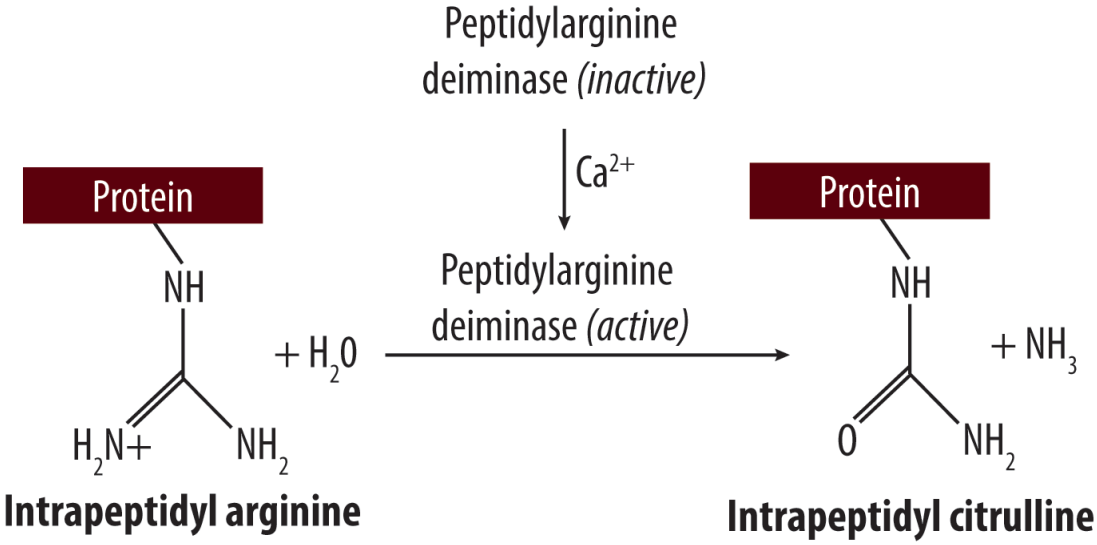

Figure 2. Mechanisms of protein citrullination following intracellular calcium overload. Peptidylarginine deiminase (PAD) enzymes are activated by high levels of intracellular calcium. Once activated, PAD enzymes catalyze the conversion of intrapeptidyl arginine residues to intrapeptidyl citrulline residues. Ammonia (NH_3) is released as a byproduct of this reaction. (Figure adapted from Tešija-Kuna & Žirović (2008)).

While elevated intracellular calcium concentration is a necessary prerequisite for PAD activation, little attention has been given to the possible presence of citrullinated proteins following TBI-induced calcium overload. As suggested by its role in other inflammatory and neurological diseases, citrullination may play a role in the long-term pathology that follows TBI, as this modification can lead to the development of several forms of dysfunction, including abnormal autoimmune responses.

PATHOLOGICAL EFFECTS OF CARBONYLATION AND CITRULLINATION

We propose that abnormalities in protein carbonylation and citrullination serve as possible mediators of chronic pathology following TBI. As such, these post-translational

modifications represent a potential *third*, enduring phase of dysfunction following primary and secondary phases.

The most common effect of protein carbonylation is inactivation of modified enzymes (56). However, carbonylation can also destabilize crucial cellular structure components (165) and promote protein aggregation due to tertiary structure modifications, which can reveal hydrophobic residues to aqueous environments and prompt misfolding (26). The relationship between carbonylation and protein degradation is complex: while carbonylation renders the affected protein more susceptible to breakdown, a high degree of environmental oxidative stress can lead to the carbonylation of proteasomal components themselves. This renders the proteasome dysfunctional, and effectively inhibits the degradation of carbonylated proteins (26). Thus, in the environment of extreme oxidation that can follow TBI, it is possible that carbonylated proteins are no longer targeted by the damaged proteasome for breakdown, and may rather accumulate as misfolded aggregates (26; 56). While several of the proteins that are carbonylated as a consequence of TBI have been identified (107), the functional effect of carbonylation in TBI pathology is not fully recognized, leaving a significant gap in the understanding of the long-term proteomic effects of oxidative stress following injury.

Citrullination also affects proteins in a number of ways. The addition of a citrulline residue in the place of arginine results in the loss of a positive charge, which can alter tertiary structure, proteolytic susceptibility, and protein-protein interactions (68; 76). In MS, the citrullination of myelin basic protein (MBP) limits the ability of this protein to appropriately associate with lipids (57), which in turn contributes to demyelination by destabilizing sheath structure (95). It has been proposed that the

dysfunctional effects of citrullination on myelin sheath structure play a major role in the development of MS (57). Furthermore, citrullinated proteins are also observed within the extracellular plaques seen in post-mortem brains affected by Alzheimer's disease, suggesting a functional role for this modification in neurodegenerative pathology.

Perhaps most importantly, in addition to altering both protein structure and function, citrullination has the potential to create "altered-self" epitopes that may be antigenic, prompting the adaptive immune system to launch autoimmune responses against previously benign proteins (33; 164). For example, the citrullination of MBP in MS leads not only to myelin degradation, but also results in the generation of autoantigenic MBP isomers, which are consequently targeted by T-cell lymphocytes (152). As noted above, the effects of citrullination are most significantly studied in the context of rheumatoid arthritis, where anti-citrullinated protein antibodies are utilized as diagnostic biomarkers due to the dramatic antigenicity of this modification in inflamed synovial joint spaces (57). Thus, citrullination has the capacity to prompt an adaptive immune response against selectively modified proteins. An investigation into protein citrullination following brain injury is merited, and may indicate an autoimmune component in the chronic pathology of TBI.

SUMMARY

Intracellular calcium overload is a well-documented pathological effect of TBI. Because protein carbonylation and citrullination are logical and plausible outcomes of oxidative stress and calcium excitotoxicity, it is important to investigate the expression of these damaging post-translational modifications following injury (Figure 3).

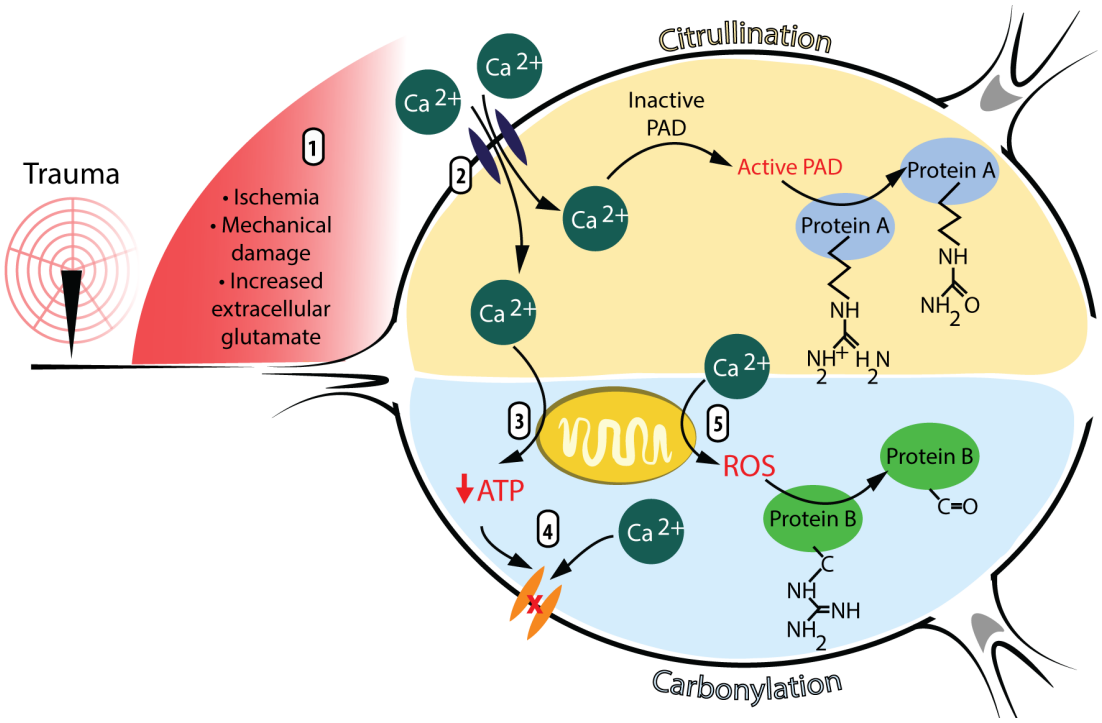

Figure 3. Proposed model of proteomic changes following TBI-induced calcium overload. After traumatic injury, ischemia and mechanical damage (tearing, shearing, and hemorrhage) lead to increased extracellular glutamate, an excitatory amino acid (1). This causes significant ionic imbalance, prompting a dramatic influx of calcium into cells (2). High intracellular levels of calcium impair mitochondrial function, causing decreased energy metabolism (3). ATP depletion prevents the efflux of calcium to restore ionic homeostasis (4). In addition, calcium-induced mitochondrial dysfunction leads to the production of reactive oxygen species (ROS) (5). Two post-translational modifications, citrullination and carbonylation, are driven by calcium overload. Citrullination, the conversion of intrapeptidyl arginine to intrapeptidyl citrulline residues, is catalyzed by peptidylarginine deiminase, which is a calcium-dependent enzyme (top panel). Carbonylation, the conversion of an intrapeptidyl amino acid (Lys, Cys, His) to a carbonyl group, is driven by the effects of ROS (bottom panel). Both citrullination and carbonylation are irreversible proteomic modifications with significant effects on protein structure and function.

This research investigates the expression of carbonylation and citrullination in a rodent model of TBI, controlled cortical impact (CCI), five days following injury. The first manuscript focuses on protein carbonylation, while the second manuscript examines protein citrullination. Both manuscripts identify specific proteins modified following

injury, and examine what regions and neural cell types are most susceptible to each modification. Furthermore, the impact of gender on the expression of these modifications is investigated, as clinical studies have documented that female patients exhibit reduced mortality and decreased complications after TBI as compared to males (17; 53; 125).

CHAPTER 2: Protein carbonylation after traumatic brain injury: cell specificity, regional susceptibility, and gender differences

Rachel C. Lazarus[a], John E. Buonora[a, 1], David M. Jacobowitz[a, b],

and Gregory P. Mueller[a, b, c, *]

[a] Program in Neuroscience

[b] Department of Anatomy, Physiology, and Genetics

[c] Center for Neuroscience and Regenerative Medicine

Uniformed Services University of the Health Sciences

4301 Jones Bridge Road

Bethesda, MD 20814, USA

* Corresponding Author

Gregory P. Mueller, Ph.D.

Department of Anatomy, Physiology, and Genetics

Uniformed Services University of the Health Sciences

4301 Jones Bridge Road

Bethesda, MD 20814, USA

Phone: (301) 295-3507

Email: Gregory.Mueller@usuhs.edu

ABSTRACT

Protein carbonylation is a well-documented and quantifiable consequence of oxidative stress in several neuropathologies, including multiple sclerosis, Alzheimer's disease, and Parkinson's disease. Although oxidative stress is a hallmark of traumatic brain injury (TBI), little work has explored the specific neural regions and cell types in which protein carbonylation occurs. Furthermore, the effect of gender on protein carbonylation after TBI has not been studied. The present investigation was designed to determine the regional and cell specificity of TBI-induced protein carbonylation and how this response to injury is affected by gender. Immunohistochemistry was used to visualize protein carbonylation in the brains of adult male and female Sprague–Dawley rats subjected to controlled cortical impact (CCI) as an injury model of TBI. Cell-specific markers were used to colocalize the presence of carbonylated proteins in specific cell types, including astrocytes, neurons, microglia, and oligodendrocytes. Results also indicated that the injury lesion site, ventral portion of the dorsal third ventricle, and ventricular lining above the median eminence showed dramatic increases in protein carbonylation after injury. Specifically, astrocytes and limited regions of ependymal cells adjacent to the dorsal third ventricle and the median eminence were most susceptible to postinjury protein carbonylation. However, these patterns of differential susceptibility to protein carbonylation were gender dependent, with males showing significantly greater protein carbonylation at sites distant from the lesion. Proteomic analyses were also conducted and determined that the proteins most affected by carbonylation in response to TBI include glial fibrillary acidic protein, dihydropyrimidase-related protein 2, fructose-bisphosphate aldolase C, and fructose-bisphosphate aldolase A. Many other proteins,

however, were not carbonylated by CCI. These findings indicate that there is both regional and protein specificity in protein carbonylation after TBI. The marked increase in carbonylation seen in ependymal layers distant from the lesion suggests a mechanism involving the transmission of a cerebral spinal fluid-borne factor to these sites. Furthermore, this process is affected by gender, suggesting that hormonal mechanisms may serve a protective role against oxidative stress.

Key words: Carbonylation; Reactive oxygen species; Reactive carbonyl species; Traumatic brain injury; Median eminence; Dorsal third ventricle; Astrocytes; Ependymal cells; Free radicals

INTRODUCTION

Traumatic brain injury (TBI) is a major public health issue affecting over 1.7 million Americans annually, with falls, collision incidents, and motor vehicle accidents being the leading causes of injury (48). The consequences of TBI can be complex and long lasting, resulting in serious disorders that involve progressive cognitive deficits, epilepsy, and profound behavioral alterations. Although the molecular and cellular disturbances involved in these longer-term responses are not well understood, one common element in the pathology seems to be the establishment of a chronic inflammatory state that can persist in brain for weeks, months, and perhaps even years after TBI (107; 114).

A hallmark of inflammation is oxidative stress, which can be caused by metabolic dysfunction with numerous potential causes (44; 132). At the tissue and cellular levels, the pro-oxidative forces of inflammation following an injury can outweigh the capacity of antioxidative, protective mechanisms such as superoxide dismutase and glutathione peroxidase. The resulting state drives the formation of reactive oxygen species (ROS) and reactive carbonyl species (RCS), products of lipid peroxidation by ROS. In TBI, this condition results from injury-induced ischemia/reperfusion, hypoxia, elevated intracranial pressure, glutamate excitotoxicity, and intracellular calcium overload (35; 153), all of which contribute to the breakdown of mitochondrial bioenergetics due, in part, to abnormally aggregated proteins (107).

An important modification of oxidative stress is protein carbonylation, which involves the introduction of carbonyl groups into protein-bound amino acids. Protein carbonylation may occur either through direct oxidation of amino acid targets by ROS or

via interaction with RCS, which are themselves the product of lipid peroxidation (165). By either mechanism, the resulting carbonyl modifications can disrupt protein function and thereby contribute to injury pathology (40). Carbonylation has long been utilized as a metric of oxidative stress levels in various neurodegenerative pathologies, including multiple sclerosis (20) and Alzheimer's disease (147). Although several studies in TBI have explored protein carbonylation, this work has been largely limited to the use of this modification as a measure of total oxidative stress (120). Here, we identify four proteins that are preferentially carbonylated in response to TBI, investigate the susceptibility of various brain regions to carbonylation, identify cell types within these regions that are most affected by this modification, and, furthermore, differentiate gender-based differences in carbonylation after TBI. The results of this work shed light onto into the differential susceptibility of specific brain regions and cell types to TBI-induced oxidative stress, providing insights into the mechanisms of TBI pathology.

MATERIALS AND METHODS

Controlled Cortical Impact (CCI)

Adult male and adult female Sprague–Dawley rats (8–9 weeks of age) were purchased from Charles River Laboratories (Morrisville, NC, USA). Rats were housed in a barrier facility for animals accredited by the Association for Assessment and Accreditation of Laboratory Animal Care International. Before experimental procedures, rats were anesthetized with isoflurane (Baxter Healthcare Corp., Deerfield, IL, USA) vaporized in medical-grade oxygen (100%, Roberts Oxygen Co. Inc., Rockville, MD, USA), placed in a digital cranial stereotactic device (Leica Microsystems, Buffalo Grove, IL, USA), and subjected to unilateral CCI injury over the left hemisphere. Briefly, the

rats underwent a free-hand craniotomy (–3.8 mm from bregma in males, –3.0 mm in females). CCI was administered through the ImpactOne stereotaxic impactor (Leica Microsystems), which delivered a 3-mm flat-tipped impactor at 20° to a depth of 2 mm at 5 m/s with a 500-ms dwell time. After CCI, the incision was closed and the rats received buprenorphine 0.05 mg/kg for postoperative analgesia. Throughout all procedures, rat body core temperature was maintained at 37±0.3°C. Naïve rats received no anesthesia, incision, or craniotomy. Animals were euthanized 5 days after injury under anesthesia (10% chloral hydrate solution, 0.4 ml/100 g). All animal handling procedures were performed in compliance with guidelines from the National Research Council for the ethical handling of laboratory animals and were approved by the Institutional Animal Care and Use Committee of USUHS (IACUC Protocol APG 12-827, Bethesda, MD, USA).

Immunoblotting: protein carbonylation detection and identification in brain tissue

Tissue collection and preparation

Brains were removed immediately after euthanization, frozen on powdered dry ice, and stored at −80°C until used. Brains were hand-dissected to produce blocks of penumbral structures enriched in carbonylated proteins as identified immunohistochemically (see below). The contralateral brain region and equivalent region from the naïve animals were similarly collected.

One-dimensional gel electrophoresis

Protein fractions were prepared by homogenization in 5 volumes/tissue weight extraction solution (8 M urea, 2% 3-[(3-cholamidopropyl)dimethylammonio]-1-propane sulfonate (Chaps), and 50 mM dithiothreitol (DTT; Sigma–Aldrich, St. Louis,

MO, USA) containing 0.8% ampholytes (pH 3–10; Invitrogen Life Technologies, Carlsbad, CA, USA) and 1× Complete protease inhibitor mix (Roche, Indianapolis, IN, USA)). After homogenization and subsequent centrifugation (20,000*g*, 10 min, 4°C), the resulting supernatant was stored at −80°C until used. The efficiency of tissue solubilization was > 95%, as judged by protein assay and Coomassie staining of one-dimensional gels.

Protein samples were prepared for gel electrophoresis by combining with an equal volume of 2× reducing loading buffer (Novex NuPAGE LDS sample buffer; Invitrogen; containing 50 mM DTT) and heating at 70°C for 10 min. Samples were then fractionated (25 μl/4.16 μg per lane) using NuPAGE 10% Bis–Tris gels (Novex–Invitrogen) and transferred to nitrocellulose blots using an iBlot transfer apparatus (Invitrogen).

Fluid-phase isoelectric focusing (IEF)

To reduce the complexity of tissue homogenates for subsequent proteomic analyses, samples were prefractionated by fluid-phase IEF before one-dimensional gel electrophoresis. Samples of injured and contralateral hemisphere, and the corresponding regions from control naïve animals (n = 8 for each region), were homogenized in 5 volumes (wt/vol) IEF denaturant consisting of 7.7 M urea, 2.2 M thiourea, and 4.4% Chaps containing 1× Complete protease inhibitor mix (Roche) and clarified by centrifugation (20,000*g*, 10 min, 4°C). Tissue region pools were prepared and 200-μl aliquots of each pool supernatant were further diluted to 2.865 ml having a final composition of IEF denaturant plus ampholytes (150 μl, pH 3–10; Invitrogen), DTT (50 μl, 2 M stock), and bromophenol blue (10 μl, 10 mg/ml stock). The resulting sample was loaded into the IEF fractionator and focused using the following conditions: 100 V,

1.2 mA, 0 W (15 min); 200 V, 2.0 mA, 0 W (1 h); 400 V, 2.0 mA, 1 W (1 h); 600 V, 1.5 mA, 1 W (1 h). This resulted in fractions of proteins within the following p*I* ranges: 3.0–4.6, 4.6–5.4, 5.4–6.2, 6.2–7, and 7–9.1. IEF-fractionated proteins were further fractionated by size by one-dimensional gel electrophoresis (see *One-dimensional gel electrophoresis*).

Postelectrophoretic detection of carbonylated proteins

Postelectrophoretic detection of carbonylated proteins was performed as described by Conrad et al. (36) with minor modifications. Briefly, nitrocellulose membranes were washed in 20% methanol/80% Tris-buffered saline/Tween 20 (TBS-T), equilibrated in 2 N hydrochloric acid (HCl), and then incubated with 0.5 mM 2,4-dinitrophenylhydrazine (DNPH; Sigma–Aldrich) in 2 N HCl (10 min, in the dark). The derivatized membranes were then washed three times with 2 N HCl (10 min per wash) followed by 50% methanol (five times, 10 min per wash). Membranes were then equilibrated in TBS-T, blocked with 5% fetal bovine serum/TBS-T, and probed overnight at 4°C with rabbit anti-DNP (Sigma–Aldrich; Catalog No. 9659, 1:1000 in TBS-T). Membranes were washed three times with TBS-T and probed with horseradish peroxidase-labeled, goat anti-rabbit IgG (Thermo Fisher Scientific, Waltham, MA, USA; Catalog No. 31460, 1:5000 in TBS-T, 3 h). Blots were washed (TBS-T) and visualized by enhanced chemiluminescence (Novex ECL HRP Chemiluminescent Substrate Reagent Kit; Invitrogen) using a FUJI LAS 3000 imager (Fujifilm, Minato, Tokyo, Japan). The images were analyzed using MultiGauge version 3.0 software (Fujifilm) and the intensity of protein bands was quantified with ImageJ software (W.S. Rasband, ImageJ, U.S. National Institutes of Health, Bethesda, MD, USA). Immunoreactive signals were

mapped to corresponding protein features of Coomassie-stained gels. These features were excised and processed for identification via peptide mass fingerprinting.

Protein identification by peptide mass fingerprinting

Coomassie-stained gel pieces were destained in 100 mM NH_4CO_3/50% acetonitrile at 37 °C for 90 min. Slices were dehydrated in 100% acetonitrile (5 min, at room temperature), followed by drying under vacuum. The dehydrated gel pieces were rehydrated in a minimal volume of a solution of 40 mM NH_4CO_3/50% acetonitrile containing 20 ng/μl trypsin (Trypsin Gold, Mass Spec Grade; Promega, Madison, WI, USA) and incubated overnight at 37°C. Peptide fragments were recovered from the gel slices by sequential washes with 75 μl 1% trifluoroacetic acid (TFA) (1 h) and 50 μl 5% TFA/50% acetonitrile (two washes, 1 h per wash). The washes were pooled, dried under vacuum, and then dissolved in 10 μl of 1% TFA. Tryptic digests were mixed 1:1 with α-cyanohydroxycinnamic acid matrix (10 mg/ml in 50% acetonitrile/0.1% TFA) containing bradykinin (1060.5692 Da) and adrenocorticotropic hormone fragment 18–29 (2465.1989 Da) (AnaSpec, San Jose, CA, USA) as internal standards and analyzed by matrix-assisted laser desorption ionization time-of-flight (MALDI-TOF) mass spectrometry, using a Voyager MALDI-TOF DE STR instrument (PE Biosystems). Peptide mass spectra data were analyzed via the Protein Prospector MS-Fit search engine (http://prospector.ucsf.edu/). Criteria for a positive identification were a MOWSE score greater than 1.00×10^7 and more than two times greater than any other identifications for the search, a coverage percentage greater than 25%, and a matched protein identifying with the appropriate molecular weight and p*I* for the fractionation procedure.

Immunohistochemistry

Tissue collection and preparation

Euthanized animals were perfused transcardially with 200 ml phosphate-buffered saline (PBS) followed by 200 ml 4% paraformaldehyde for fixation. Brains were stored in 4% paraformaldehyde overnight at 4°C and then equilibrated in a 30% sucrose solution (~48 h, 4°C). Coronal sections (20 μm thick) were collected from 2.5 mm rostral to 2.5 mm caudal to the CCI lesion site and mounted onto Colormark Plus adhesion slides (Thermo Fisher Scientific). Every tenth section was stained with thionine to create a reference library.

Detection of carbonylated proteins and cell-specific markers

Immunostaining for protein carbonyls was performed as described by Zheng and Bizzozero (165), with minor modifications. Each section was prepared by incubation with 100 μl DNPH (1 mg/ml in 2 N HCl) for 30 min at room temperature. Sections were then washed three times with 0.2% Triton X-100/PBS and blocked for 1 h at room temperature with 10% normal donkey serum. After three more washes with 0.2% Triton X-100/PBS, each tissue section was incubated at 4°C overnight with 100 μl of 1:1000 rabbit anti-DNP (Sigma–Aldrich; Catalog No. D9656) in 0.3% Triton X-100/PBS. Colocalization experiments were performed by co-incubating sections with cell-specific markers: mouse anti-NeuN (detects neurons; EMD Millipore, Billerica, MA, USA; Catalog No. MAB377; 1:1000), mouse anti-glial fibrillary acidic protein (GFAP; detects astrocytes; EMD Millipore; Catalog No. MAB360; 1:1000), goat anti-Iba1 (detects microglia and macrophages; Abcam, Cambridge, UK; Catalog No. ab5076; 1:100), and mouse anti-Olig2 (detects oligodendrocytes; EMD Millipore; Catalog No. MABN50,

1:100). Slides were washed three times with 0.2% Triton X-100/PBS and then incubated with 100 μl secondary antibody solution: 1:100 donkey anti-rabbit IgG (H+L), conjugated to green-fluorescent Alexa Fluor 488 dye (Invitrogen); 1:100 donkey anti-mouse or anti-goat IgG (H+L), conjugated to red-fluorescent Alexa Fluor 594 dye (Invitrogen; Catalog Nos. A-21203 and A-11058, respectively). After 3 h of incubation, this solution was replaced with 4′,6-diamidino-2-phenylindole (DAPI; Sigma–Aldrich; Catalog No. D32670, 0.01% in 0.2% Triton X-100/PBS, 5 min at room temperature) for nuclear staining. Sections were washed three times with 0.2% Triton X-100/PBS and one time with 1× PBS and then visualized with a Zeiss LSM 5 Pascal confocal microscope (Zeiss, Jena, Germany).

Preadsorption control

Specificity of the carbonylation immunohistochemistry was confirmed by immunoneutralizing the primary antibody with carbonylated protein standard. Briefly, β-casein protein was chemically carbonylated by incubation with ferric chloride ($FeCl_3$) (15 mg in 2 ml 37.5 mM 4-(2-hydroxyethyl)-1-piperazineethanesulfonic acid (Hepes), pH 7.2, containing 37.5 mM ascorbate and 0.15 mM $FeCl_3$; 5 h, 37°C). The reaction mixture was then dialyzed against 50 mM Hepes and 1 mM ethylenediaminetetraacetic acid (pH 7.2) overnight at room temperature. A control reaction was conducted similarly with the absence of $FeCl_3$. Derivatization of protein carbonyl groups was carried out by combining the protein dialysates with an equal volume of 12% sodium dodecyl sulfate and an equal volume of 10 mM DNPH prepared in 1 N HCl. Reactions proceeded in the dark for 15 min at room temperature and were then neutralized with the addition of 3.25 ml 2 M Tris–HCl. The derivatized proteins were dialyzed against H_2O overnight. The

carbonylation status of the two preparations was confirmed by Western blot using anti-DNP immunodetection. Preadsorption of the primary antibody was carried out by incubating anti-DNP IgG (~2 μg) with carbonylated, DNPH-derivatized β-casein (~100 μg protein) at 4°C, overnight. An additional control condition was established by similarly incubating anti-DNP antibody in the absence of modified β-casein protein.

Statistical analysis

Carbonylation immunohistochemistry was quantified according to region using a blinded scoring system, with 0 reflecting the lowest amount of carbonylation fluorescence intensity in a region and 3 reflecting the greatest amount across all sections evaluated. Regions scored were the cortical lesion site, dorsal third ventricle, and median eminence. Sixteen brain sections per animal were scored using sections located from bregma –2.12 mm to bregma –3.30 mm (control/CCI male rats n=7 and 9, respectively; control/CCI female rats n=9 and 7, respectively). Comparisons between groups were analyzed by ANOVA with a Tukey HSD post hoc test. $p<0.05$ was considered significant (MultiGauge version 3.0 software; Fujifilm).

RESULTS

CCI increases protein carbonylation in specific regions of the brain

An initial immunoblotting experiment was performed to confirm that the CCI model resulted in a reproducible pattern of protein carbonylation in brain. We investigated the profile of carbonylated proteins in whole-brain lysates. Injured brain lysates were compared to contralateral uninjured tissue lysates from the same animal using Coomassie staining and Western blotting for DNP in one-dimensional gels (Figure 4). Total carbonylation (based on total lane intensity) was increased approximately 10%

in samples from injured brain tissue compared to the signal observed in contralateral, uninjured brain tissue. Interestingly, carbonylation was enhanced for a small group of specific protein features (arrows) in response to CCI. These results confirmed that CCI causes the upregulation of carbonylation of specific proteins.

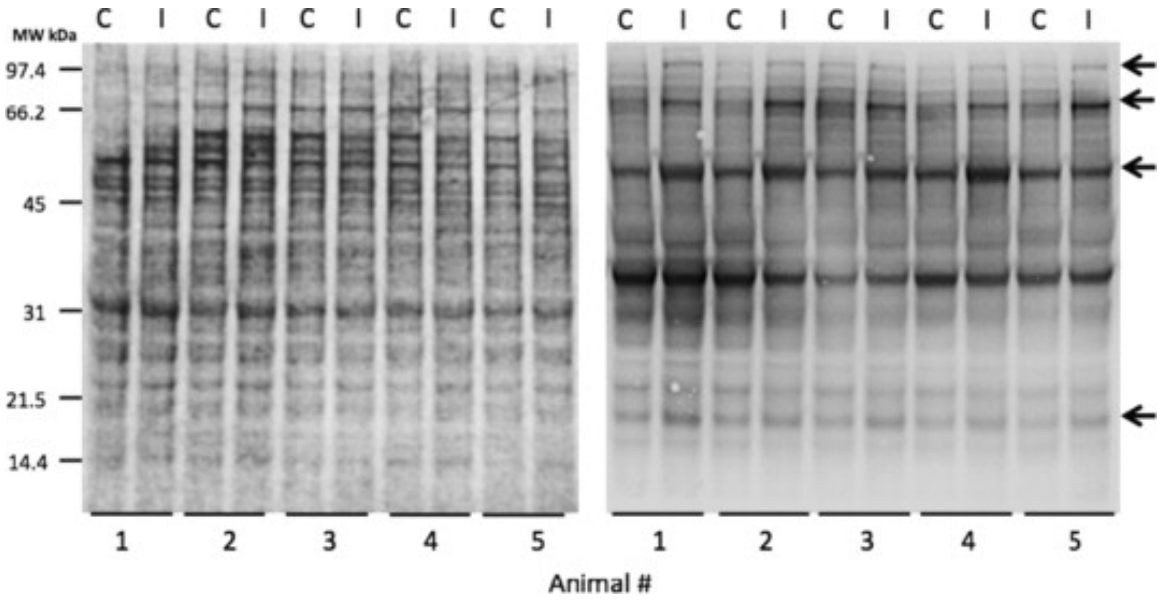

Figure 4. Effects of CCI on protein carbonylation in rat brain. Five days after experimentally administered CCI, extracts were obtained from dissected regions of brain containing the injury penumbra (I) and the corresponding contralateral control region (C). Lysates were analyzed (4.2 μ g/lane) for protein carbonylation by one-dimensional gel electrophoresis followed by Western blotting. Coomassie staining of the protein remaining in the transferred gel was used to confirm equal protein loading (left). DNP Western blotting was performed to detect protein carbonylation in CCI-injured brain samples versus uninjured contralateral brain samples (right). Arrows indicate protein bands for which carbonylation was most affected by CCI. Images are representative of three independent experiments. A total of *n*=5 CCI animals were examined.

Peptide mass fingerprinting was used to identify specific proteins carbonylated in response to CCI. Figure 5 presents a representative analysis in which proteins present in control and TBI extracts were fractionated by fluid-phase IEF, followed by one-dimensional gel electrophoresis. Proteins having enhanced carbonylation after injury

were visualized by Western blotting for DNP, mapped to corresponding features on Coomassie-stained gels, and identified as GFAP, dihydropyrimidase-related protein 2 (also known as collapsing response mediator protein 2, or CRMP2), fructose-bisphosphate aldolase C (ALDOC), and fructose-bisphosphate aldolase A (ALDOA).

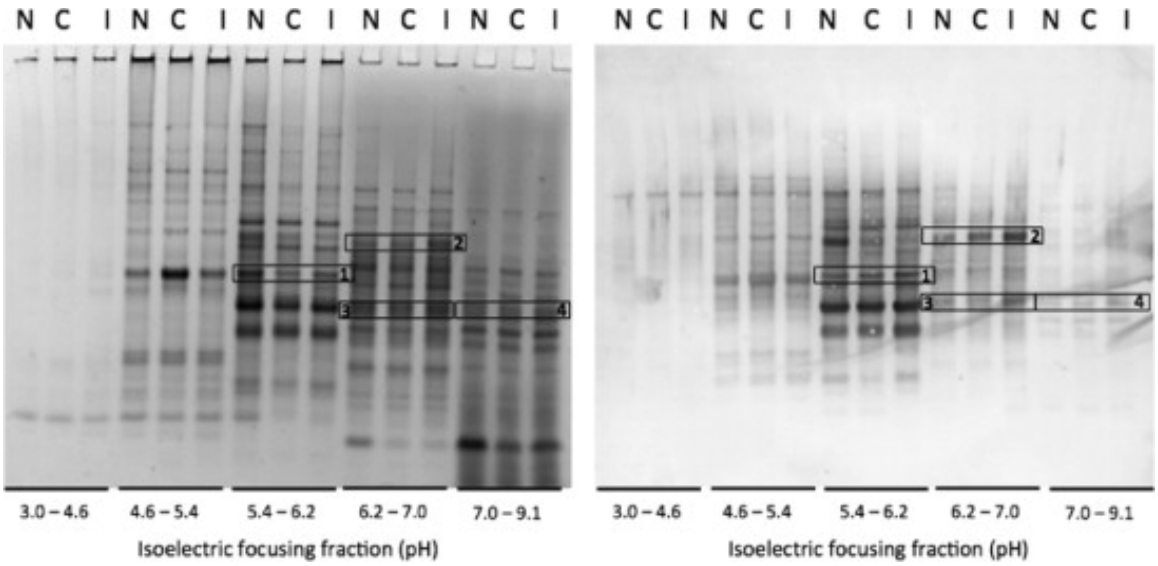

Figure 5. Identification of rat brain proteins carbonylated after CCI. Proteins present in extracts of naïve rat brain (N) and contralateral (C) and ipsilateral (I) regions of CCI-injured rats were fractionated by fluid-phase IEF (p*I* ranges listed at bottom) and one-dimensional gel electrophoresis. Proteins were transferred to nitrocellulose, derivatized, and probed with anti-DNP antibody (right). Proteins remaining in the gel were visualized by Coomassie staining (left). Features showing increased carbonylation in response to TBI (numbered boxes, right) were mapped to the corresponding Coomassie features (left) and identified by peptide mass fingerprinting as: (1) GFAP (49,957 Da; p*I* 5.4), (2) CRMP2 (62,278 Da; p*I* 6.0), (3) ALDOC (39,284 Da; p*I* 6.7), and (4) ALDOA (39,352 Da; p*I*8.3). Images are representative of three independent experiments. A total of *n*=8 CCI and *n*=8 naïve animals were examined.

To identify specific regions of the brain in which increased protein carbonylation occurred after TBI, we performed anti-DNP immunohistochemistry. Total brain DNP staining is displayed in Figure 6, with the site of CCI indicated in the upper left cortex.

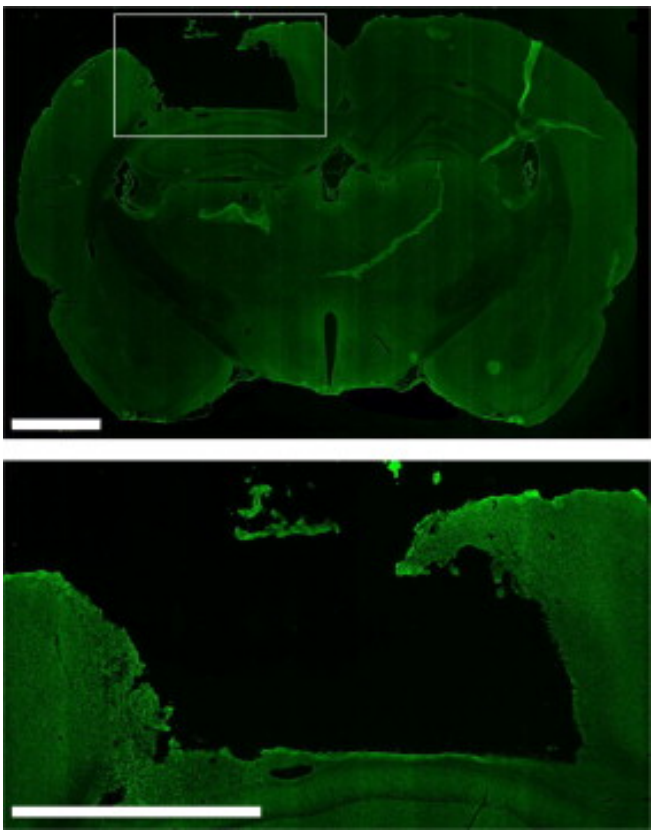

Figure 6. Effects of CCI on protein carbonylation immunohistochemistry in rat brain. Brain tissue was collected 5 days after CCI and evaluated by anti-DNP immunofluorescence. A whole-slice image (top, ×1 original magnification, scale bar indicates 2 mm) and an image of the lesion site (bottom, ×2.5 original magnification, scale bar indicates 2 mm) are shown. Images are representative of three independent experiments. A total of *n*=16 CCI animals and *n*=16 naïve animals were examined, with 16 slices per animal from bregma –2.12 mm to bregma –3.30 mm.

At higher magnification, the fluorescence intensity of anti-DNP labeling in the vicinity of the lesion was clearly distinguished from that observed in the uninjured contralateral cortex (Figure 7, panels A and B, respectively). The specificity of the immunolabeling was confirmed by immunoneutralization of the anti-DNP primary antibody. Preincubation of the antibody with a carbonylated control protein, β-casein, effectively eliminated anti-DNP labeling in injured brain tissue (Figure 7, panel C). No

reduction in signal was observed using anti-DNP antibody preincubated with unmodified β-casein (Figure 7, panel D).

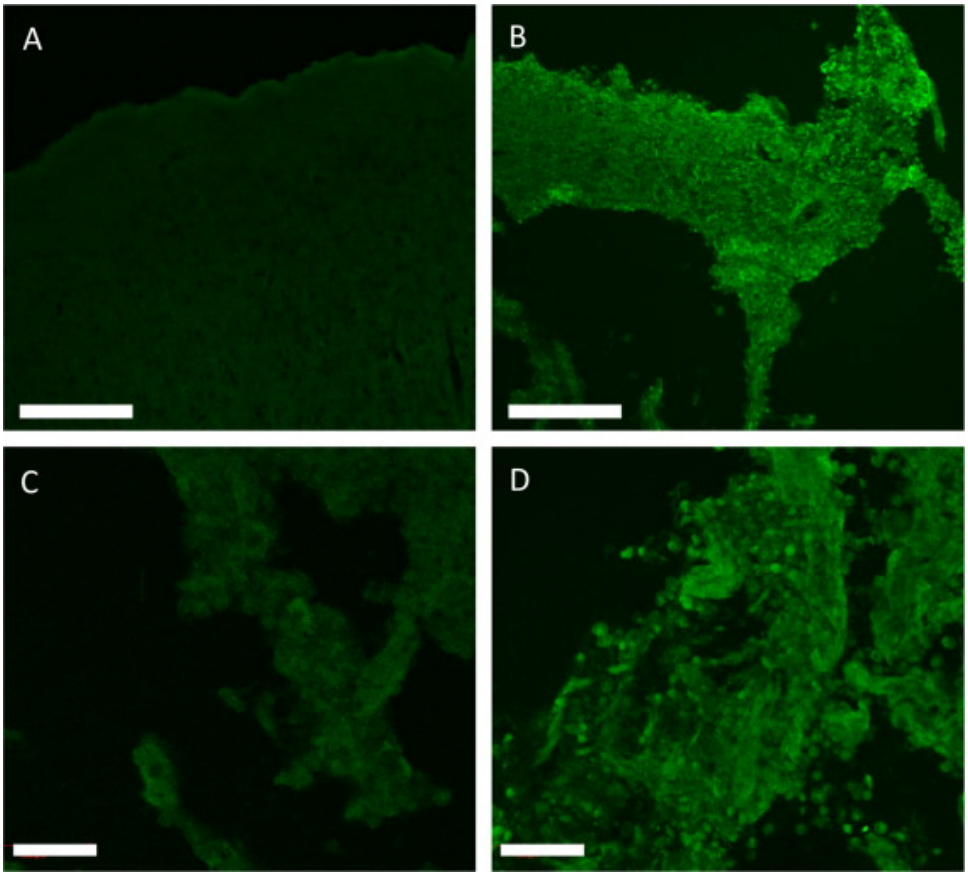

Figure 7. The CCI-induced increase in anti-DNP immunofluorescence is specific for protein carbonylation. Brain tissue was collected 5 days after CCI and evaluated by anti-DNP immunofluorescence. Anti-DNP immunofluorescence in the cerebral cortex contralateral to the injury and the CCI-injured cortex are depicted in (A) and (B), respectively (original magnification ×10, scale indicates 200 μm). Immunoneutralization of the anti-DNP antibody with (C) carbonylated and derivatized β-casein but not (D) unmodified β-casein resulted in reduced DNP immunohistochemical staining of the CCI-injured brain (original magnification ×20, scale bar, 100 μm). Images are representative of three independent experiments. A total of *n*=16 CCI animals and *n*=16 naïve animals were examined, with 16 slices per animal from bregma –2.12 mm to bregma –3.30 mm.

In addition to the immediate area of the lesion, CCI increased protein carbonylation in the region of the dorsal third ventricle (Figure 8, panels A and B) and

the median eminence (Figure 8, panels C and D) compared to these regions in naïve, control animals. Staining was especially pronounced in the ependymal cells lining the third ventricle of both regions. In comparison, basal levels of anti-DNP immunofluorescence in the equivalent regions of naïve control animals were very low. The most intense anti-DNP immunofluorescence after CCI was also observed in ependymal cells located adjacent to the paraventricular thalamic nuclei in the CCI-injured animals (Figure 8, panel B). Figure 5 also shows anti-DNP immunofluorescence in the median eminence region of control and CCI-lesioned rats (Figure 8, panels C and D, respectively). Immunolabeling was concentrated in the ependymal cells and processes lining the floor of the third ventricle at the median eminence of CCI animals (Figure 8, panel D). This pattern of intense labeling was not observed in comparable sections prepared from uninjured control animals (Figure 8, panel C). Together, these immunohistochemical findings indicate that discrete regions of the brain exhibit an upregulation of protein carbonylation after CCI. This response is most pronounced in the cortical area surrounding the area of injury and in the ependymal areas of the dorsal third ventricle/paraventricular region and the median eminence.

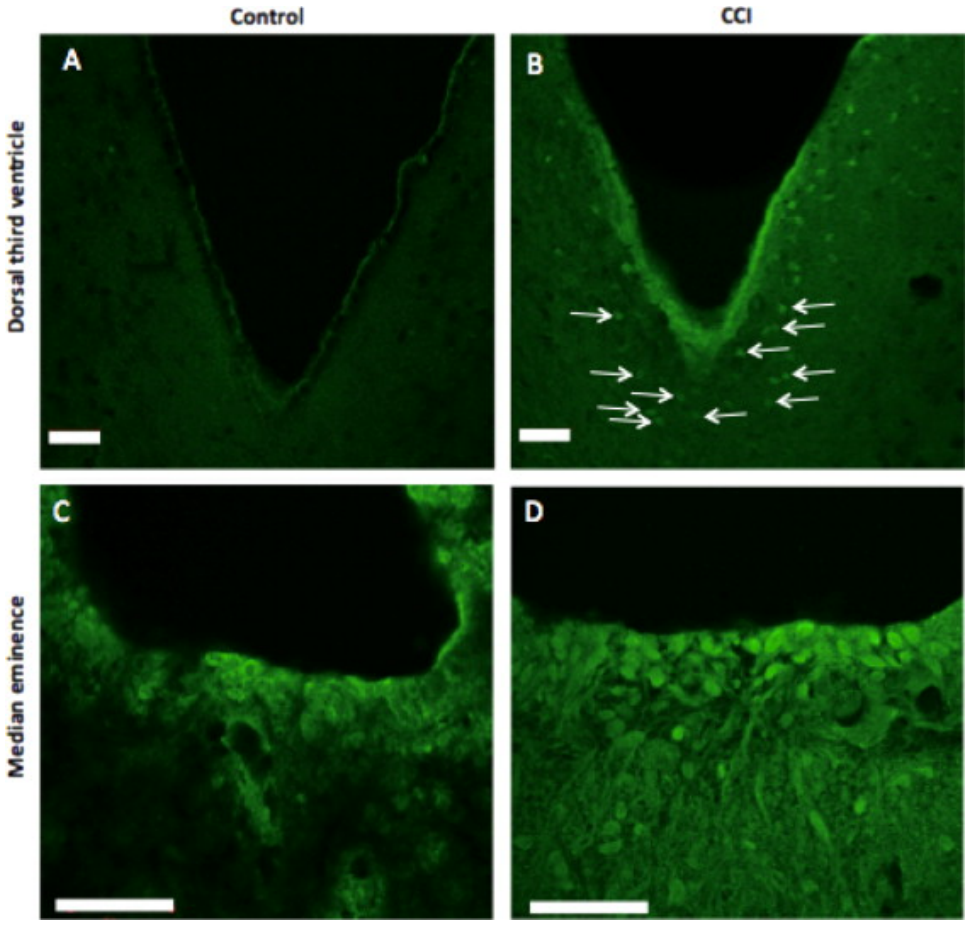

Figure 8. Effects of CCI on protein carbonylation in ependymal cells lining the dorsal third ventricle and median eminence. Brain tissue was collected 5 days after CCI and evaluated by anti-DNP immunofluorescence (A and C, naïve control; B and D, CCI). (A and B) Representatives of the dorsal third ventricle. (C and D) Representatives of the ventricle lining above the median eminence. After CCI, ependymal cells lining the dorsal third ventricle became highly immunoreactive, as did distinct cells located in the adjacent parenchyma of the paraventricular thalamic nucleus (B, arrows). Also after CCI, cells lining the ventricle of the median eminence showed an increase in protein carbonylation (D). (A and B) Original magnification ×20, scale 50 μm. (C and D) Original magnification ×40, scale 50 μm. Images are representative of three independent experiments. A total of *n*=16 CCI animals and *n*=16 naïve animals were examined, with 16 slices per animal from bregma –2.12 mm to bregma –3.30 mm.

Cell specificity of CCI-induced protein carbonylation

Experiments involving dual immunohistochemical staining were conducted to identify the cell types exhibiting increased protein carbonylation after CCI. The increase

in carbonylation observed in the brain tissue surrounding the lesion was most significantly associated with astrocytes (Figure 9, panels A–C). Anti-DNP labeling predominantly colocalized with that of anti-GFAP, a marker for astrocytes. Labeling by anti-DNP was observed within both astrocytes (Figure 9, panels A–C, white arrows) and enlarged, GFAP-negative cells undergoing apparent degeneration (Figure 9, panels A–C, red arrows). In some cases, astrocytic foot processes appeared to surround these enlarged cells. The vast majority (>90%) of astrocytes in the injury lesion expressing carbonylated proteins were reactive astrocytes, as judged by enhanced GFAP expression, cellular hypertrophy, and disruption of individual cellular domains (140).

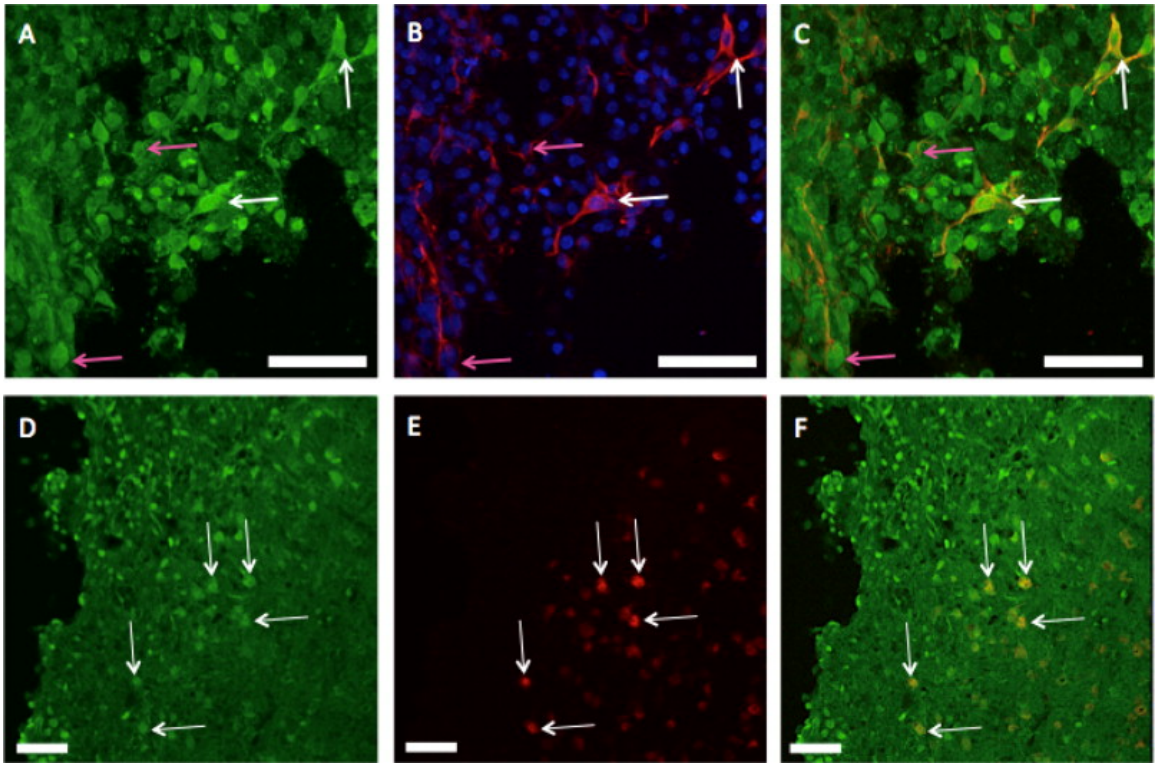

Figure 9. CCI-induced protein carbonylation is most significantly associated with astrocytes in the region of a CCI lesion. Brain tissue was collected 5 days after CCI and evaluated by coimmunofluorescence. (A–C) Representatives of the astrocyte and DNP detection at the injury site, (D–F) representatives of neuron and DNP detection at the injury site. Carbonylated proteins within the penumbra region were identified by anti-DNP immunohistochemistry (green, A and D). (B) and (E) represent anti-GFAP (astrocytes, red) and anti-NeuN (neurons, red)

detection, respectively, in the injury lesion. (B) also illustrates counterstaining with DAPI (blue) for the detection of nuclei. Merged images (C and F) indicate the detection of carbonylated proteins and their relation to astrocytes (C) and neurons (F). Astrocytes containing carbonylated proteins are shown in yellow (C). Astrocyte bodies and processes (red) contained carbonylated proteins (green, A), resulting in a yellow colocalization signal as indicated by white arrows (C). Astrocyte processes surrounding degenerating cells that contained carbonylated proteins are indicated by pink arrows (C). Neurons were identified using anti-NeuN (red, E), and protein carbonylation was identified using anti-DNP (green, D). The merged image indicates locations where both labels occur (yellow, F). Arrows indicate neurons that contained carbonylated proteins. (A–C) Original magnification ×40, scale 50 μm. (D–F) Original magnification ×20, scale 100 μm. Images are representative of three independent experiments. A total of *n*=3 CCI animals and *n*=3 naïve animals were examined, with four slices per animal from bregma –2.12 mm to bregma –3.30 mm.

Immunohistochemical labeling of carbonylated proteins in the penumbra region also appeared in neurons, as indicated by the colocalization of anti-DNP and anti-NeuN labeling (Figure 9, panels D–F, white arrows). However, this colabeling was limited to only a relatively small proportion of the total number of neurons visualized by NeuN, compared to the relatively greater amount of carbonylated proteins within astrocytes as visualized by GFAP. Data also indicated that protein carbonylation was not significantly associated with oligodendrocytes, microglia, or macrophages.

Gender influences regional patterns of protein carbonylation

A number of studies have indicated that gender plays a role in determining the consequences of oxidative injuries of the brain (14; 125). The present investigation sought to determine whether gender affects protein carbonylation after CCI. A scoring system was developed to quantitatively assess the effects of CCI on protein carbonylation and to investigate the influence of gender on the response. The scoring system was based on overall intensity and extent of anti-DNP immunofluorescence detected in each region.

Scores were developed on a 0–3 scale for each region examined. A score of 0 reflected the basal state of carbonylation observed in control animals and a score of 3 was assigned to the greatest signal observed for a given region, across all animals studied.

Representative images for scoring of each region of interest are presented in Figure 10.

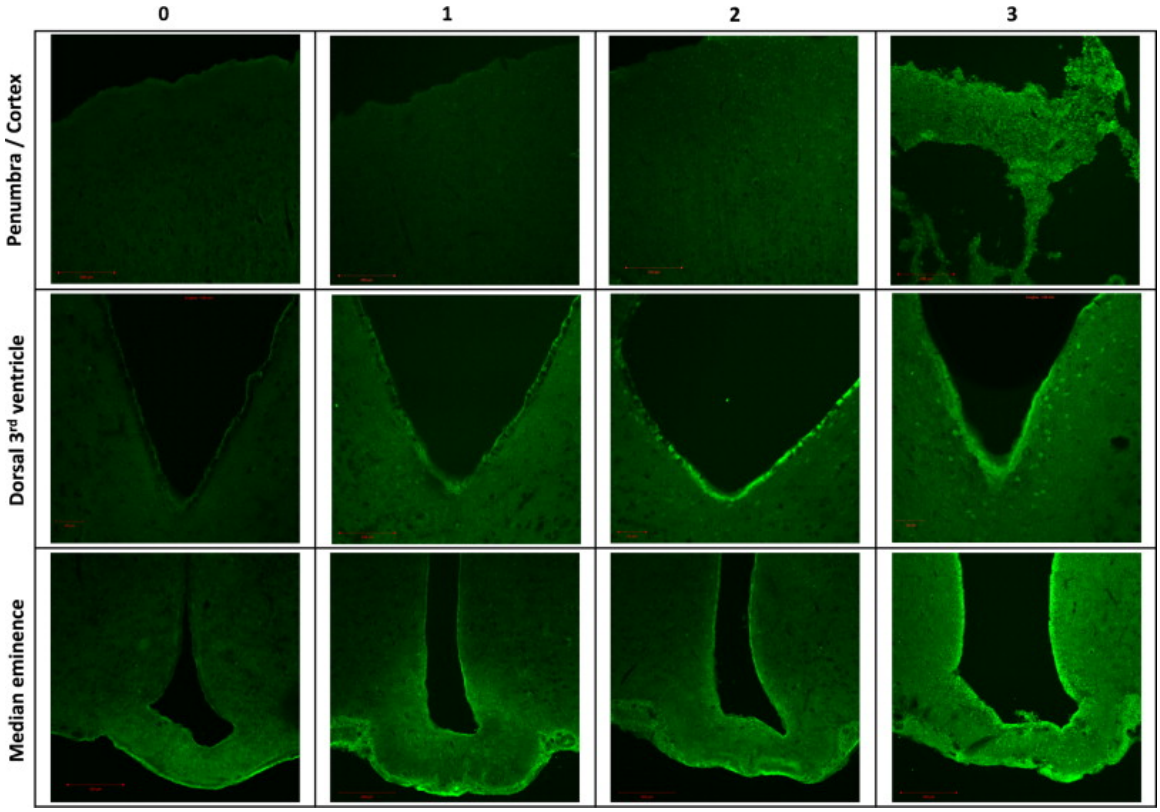

Figure 10. Representative images depicting the carbonylation scoring system. Brain tissue was collected 5 days after CCI and evaluated by anti-DNP immunofluorescence. Images show relative increments in anti-DNP immunofluorescence (0–3) observed in the penumbra/cortex, dorsal third ventricle, and median eminence regions. The distinguishing feature differentiating a score of 2 versus a score of 3 for the dorsal third ventricle was the anti-DNP labeling of peri-ependymal cells located in the parenchyma both lateral and ventral to the dorsal third ventricle. This observation reflected a stippled pattern of carbonylation-positive cells expanding approximately 10 to 50 μm into surrounding tissue from the ependymal lining of the ventricle. Penumbra/cortex and median eminence images, original magnification ×10; dorsal third ventricle images, original magnification ×20. Images are representative of three independent experiments. A total of *n*=16 CCI animals and *n*=16 naïve animals were examined, with 16 slices per animal from bregma –2.12 mm to bregma –3.30 mm.

As shown in Figure 11 and Figure 12, immunohistochemical and quantitative analysis indicated that the degree of protein carbonylation observed in the area of acute injury, 5 days after CCI, did not appreciably differ between male and female rats in that both genders had a maximal score of 3.

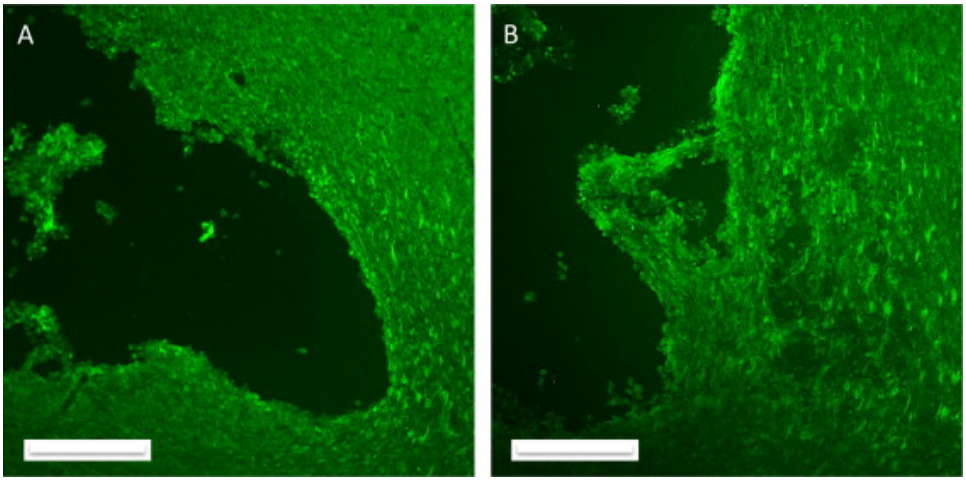

Figure 11. Gender did not affect the degree of protein carbonylation in the cerebral cortex of control and CCI-lesioned rats. Brain tissue was collected 5 days after CCI and evaluated by anti-DNP immunofluorescence. As shown qualitatively for a representative (A) male and (B) female, and quantitatively in Figure 13, the degree of protein carbonylation after CCI in the penumbra region was not significantly affected by gender. Original magnification ×20, scale 100 μm. Images are representative of three independent experiments. A total of *n*=16 CCI animals (7 female, 9 male) were examined, with 16 slices per animal from bregma –2.12 mm to bregma –3.30 mm.

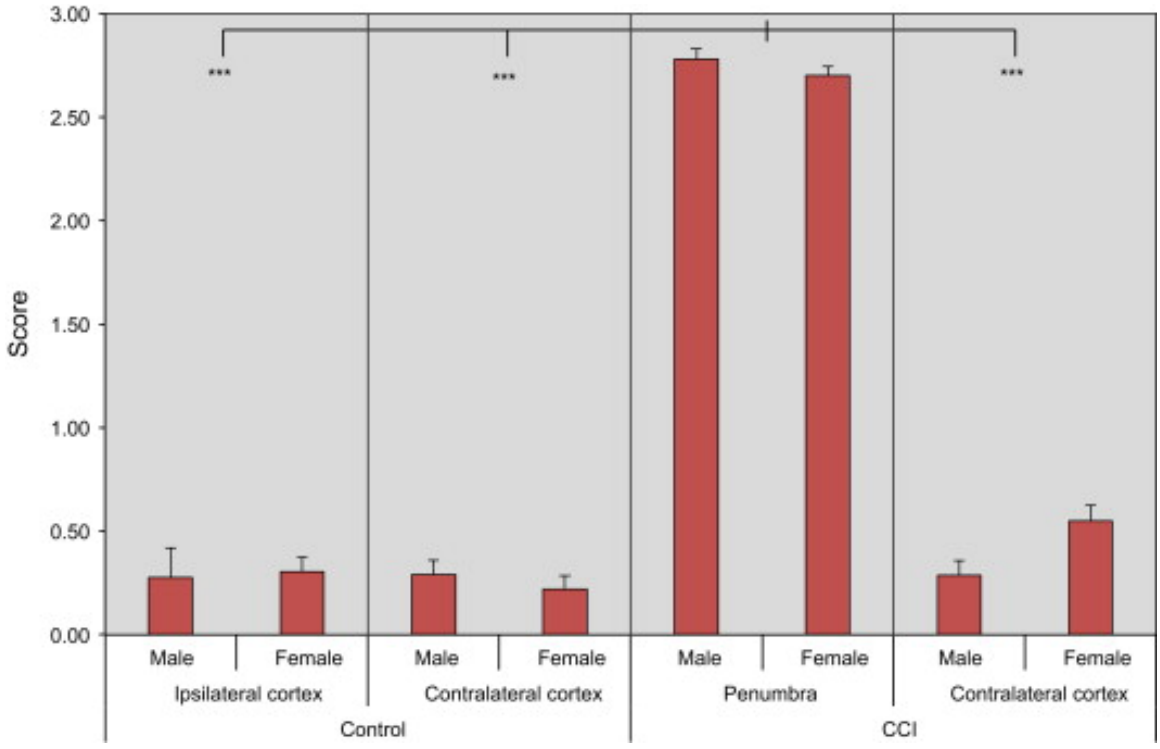

Figure 12. Effects of CCI on protein carbonylation in regions of the cerebral cortex of male and female rats. Brain tissue was collected 5 days after CCI and evaluated by anti-DNP immunofluorescence. Sections were scored for protein carbonylation as described under Material and methods. Data indicate means ± SEM. A post hoc Tukey HSD analysis indicated a statistically significant difference (***p<0.001) between the scores of the penumbra versus other cortical regions of the injured and naïve animals. Graph is representative of three independent experiments. A total of n=16 CCI animals (7 female and 9 male) and n=16 naïve animals (9 female and 7 male) were examined, with 16 slices per animal from bregma –2.12 mm to bregma –3.30 mm.

The response in the injury area was six-fold greater than that observed in regions of cerebral cortex distant from the lesion site (***p<0.0001). The carbonylation score for the contralateral cortex of injured animals was not different from the score observed in the naïve animal group. There were no gender differences observed across cortical regions compared here.

We next analyzed the effects of gender on CCI-induced protein carbonylation in the dorsal third ventricle and median eminence regions of brain. As shown in Figure 13,

carbonylation scores for median eminence of control animals were higher for males compared to females. This gender difference was further reflected in the response to CCI in that carbonylation scores were significantly elevated over control values in males but only tended to be so in females. A similar pattern was observed in the dorsal third ventricle, in which CCI-induced protein carbonylation was significantly greater in males compared to females. The carbonylation state of the dorsal third ventricle of control males tended to be higher than that of control females; however, this difference did not achieve statistical significance.

Figure 13. Gender differences in the effects of CCI on protein carbonylation in the median eminence and dorsal third ventricle. Brain tissue was collected 5 days after CCI and evaluated by anti-DNP immunofluorescence. Sections were scored for protein carbonylation as described under Material and methods. Data indicate means ± SEM. N.S., not statistically significant; $^{*}p<0.05$; $^{**}p<0.01$. Regarding the median eminence, a one-way ANOVA indicated significantly different levels of protein carbonylation between the animal gender and the injury conditions ($F(3,27) = 13.096$, $p=0.000$). A post hoc Tukey HSD analysis indicated a statistically significant difference between male naïve and male CCI protein carbonylation ($^{*}p<0.05$), a statistically significant difference between male naïve and female naïve protein carbonylation ($^{*}p<0.05$), and a statistically significant difference between male CCI and female CCI protein carbonylation ($^{**}p<0.01$). There was not a statistically significant difference between female naïve and female CCI protein carbonylation (N.S., $p=0.192$). Regarding the dorsal third ventricle, a one-way ANOVA indicated significantly different levels of protein carbonylation between the animal gender and the injury conditions ($F(3,28) = 11.874$, $p=0.000$). A post hoc Tukey HSD analysis indicated a statistically significant difference between male naïve and male CCI protein carbonylation ($^{*}p<0.05$) and a statistically significant difference between male CCI and female CCI protein carbonylation ($^{**}p<0.01$). There was not a statistically significant difference between male naïve and female naïve protein carbonylation (N.S., $p=0.311$) or between female naïve and female CCI protein carbonylation (N.S., $p=0.996$). Graph is representative of three independent experiments. A total of $n=16$ CCI animals (7 female and 9 male) and $n=16$ naïve animals (9 female and 7 male) were examined, with 16 slices per animal from bregma –2.12 mm to bregma –3.30 mm.

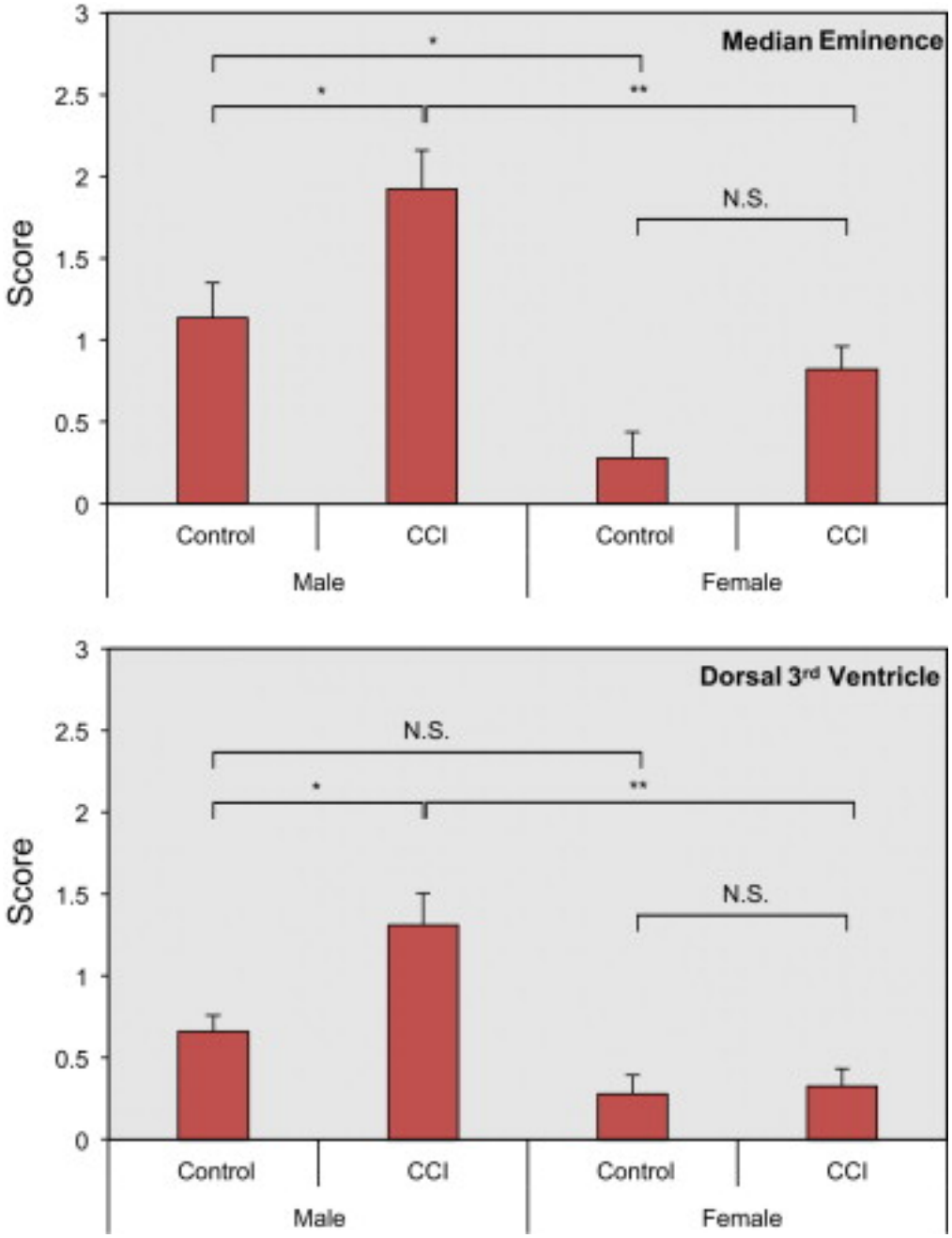

DISCUSSION

Protein carbonylation is a well-documented consequence and measureable indicator of oxidative stress in multiple neuropathologies, including Alzheimer's disease and Parkinson's disease (26). Recently, interest has focused on the role of oxidative stress in the pathology of TBI (70). To date, research has concentrated on measures of global

carbonylation within the central nervous system, whereas little work has explored the neural regions, cell types, and specific proteins affected by this modification. Furthermore, although significant research has identified gender-based differences in TBI prognosis (53; 125), few researchers have examined how gender affects the magnitude or regional distribution of protein carbonylation after TBI.

The pathophysiology of TBI is both complex and dynamic, involving physical injury, ischemia/reperfusion, hypoxia, glutamate excitotoxicity, intracellular calcium overload, and elevated intracranial pressure (35; 144; 153; 161). Collectively, these conditions establish an environment of mitochondrial dysfunction, marked by the generation of ROS, including superoxide and hydrogen peroxide. These molecules drive the formation of RCS, such as acrolein and 4-hydroxynonenal, which are by-products of lipid peroxidation (135; 136). RCS, in turn, catalyze the generation of intra-protein carbonyls, further compromising cellular functions and exacerbating injury pathology. The data from this investigation show that the astrocytes in the immediate area of the injury lesion site, along with the ependymal cells lining the dorsal third ventricle and the floor of the third ventricle above the median eminence, contain the highest levels of protein carbonylation at 5 days after CCI. A time point of 5 days post-injury was considered to be sufficiently removed from the injury event to gain insights into the longer-term processes involved in brain injury. Whereas both genders showed similar levels of protein carbonylation at the site of injury, males showed a greater increase in carbonylation in ependymal cells distant from the lesion.

Within the injury region, the vast majority of astrocytes rich in carbonylated proteins were reactive astroglia, as indicated by complex, overlapping processes and

hypertrophic cell bodies (140). Astrocytes have been proposed to be the first line of defense against oxidative stress after acute TBI (43; 102; 113). Astrocytes play a key role in balancing the oxidative load of the brain after injury, through their ability to scavenge ROS and thereby buffer the spread of oxidative stress (108). Whereas astrocytes have the capacity to combat oxidative stress to the benefit of other adjacent cells, they themselves are still vulnerable to the actions of ROS, which can cause mitochondrial damage, accelerated senescence, and cell death (31; 72). Our results support these conclusions by demonstrating that at the site of lesion, astrocytes are the dominant cell type showing increased protein carbonylation post-CCI. Whereas some neurons exhibited increased protein carbonylation after CCI, this response was minimal in comparison to astrocytes. The carbonylation status of oligodendrocytes and microglia and macrophages in the lesion area was essentially unaffected by CCI.

Our data indicate that CCI induces carbonylation in a subpopulation of cells distant from the region of the acute injury, specifically, in the ependymal lining of the dorsal third ventricle and median eminence. This unanticipated response was more pronounced in male rats compared to females. Ependymal cells form a barrier between cerebrospinal fluid (CSF) and neural tissue, acting as both a physical and a metabolic interface (42), The mechanism by which oxidative damage is transmitted to specific regions of the ependymal system is not fully understood, but may involve: (1) the transport of reactive molecules from the site of injury via the CSF and (2) a selective sensitivity of the ependymal lining of the dorsal third ventricle and median eminence to these mediators. Likely CSF-borne molecules include 4-hydroxynonenal, acrolein, and malondialdehyde, all of which are highly reactive aldehyde products of ROS-catalyzed

lipid peroxidation. Unlike ROS, however, these compounds are relatively long-lived and can withstand extracellular transport from their site of generation (27; 135). In this regard, elevated levels of 4-hydroxynonenal have been documented in the CSF of patients with neuropathologies, including amyotrophic lateral sclerosis (138) and Parkinson's disease (134). The selective sensitivity of specific ependymal zones lining the dorsal third ventricle and area above the median eminence may reflect unique functional characteristics of the cells involved. In support of this proposal, ependymal cells lining the ventricles of the brain have been shown to display a broad range of heterogeneity with respect to structure and function (13; 69), membrane protein expression (13), and vulnerability to CSF-borne toxins (69). Similarly, the ependymal lining at the base of the third ventricle, directly above the median eminence, is well known for its unique structure (112), neurogenic cell populations (79), and neuroendocrine regulation (119). Therefore, we propose that aldehyde by-products of lipid peroxidation are generated by ROS at the site of acute injury, are transported through the cerebroventricular system, and interact with susceptible, CSF-adjacent periventricular ependymal cells to propagate carbonylated protein species.

The significance of increased protein carbonylation in the ependymal regions is not yet fully understood. It is known that a subset of ependymal cells of both the median eminence and the dorsal third ventricle extend foot-like processes into the brain parenchyma and onto resident capillaries (103). Moreover, this subset exhibits endocytosis of macromolecules from the CSF (112), which could lead to a local accumulation of RCS, thus propagating protein carbonylation. Our present immunohistochemical findings are also consistent with the proposal that carbonylation-

containing ependymal cells may expand into the surrounding parenchyma, possibly serving as a mechanism for repair.

This investigation is the first to examine the effects of gender on the differential patterns of protein carbonylation after TBI. Basal levels of protein carbonylation were low but detectable in all brain regions investigated here. Interestingly, normal male rats exhibited a significantly greater degree of protein carbonylation in the ependymal zones of the dorsal third ventricle and median eminence compared to normal females. TBI produced dramatic and comparable increases in carbonylation in the acute injury region in both male and female rats. However, injured males showed a significantly greater increase in protein carbonylation than injured females in the ependymal zones of the dorsal third ventricle and median eminence, sites distant from the lesion. Accordingly, whereas male and female rats seem to respond similarly at the site of acute injury, females may be more resistant to secondary processes at sites distant to the injury. In this regard, clinical studies document that female patients exhibit reduced mortality and decreased complications after TBI (17; 53; 125). It has been proposed that the ovarian steroid hormone progesterone serves to regulate metabolic functions in the brain (63) and counteracts the excitotoxic effects of TBI (83; 145; 146), possibly by protecting against lipid peroxidation and the generation of RCS (126).

Although it is well recognized that oxidative stress drives many processes of secondary injury after brain injury, clinical trials involving antioxidant interventions have had limited success in preventing the sequelae of TBI (10; 71; 118; 129; 154). Our findings indicate that oxidative stress from TBI occurs within 5 days of injury, both locally at the site of acute impact and at sites distant from the site of impact. The lack of

efficacy from antioxidants may be due to post-injury delays such that the irreversible effects of protein carbonylation may have occurred well before antioxidants could be applied. TBI-induced protein carbonylation and other forms of oxidative stress occur rapidly and effects appear to persist for extended periods of time after injury (11; 18; 21; 84). Accordingly, timely administration of antioxidant therapy post-injury has been difficult to achieve clinically. Also, multiple mechanisms are involved in the processes of oxidative stress, suggesting that a single treatment strategy may be inadequate in targeting the full spectrum of oxidative processes requiring management.

The research here has identified the selective carbonylation of GFAP, CRMP2, ALDOA, and ALDOC in response to TBI. The identification of GFAP, a major component of astrocytes, is consistent with our immunohistochemical findings, showing that these cells are particularly susceptible to oxidative modification after injury. GFAP, CRMP2, and ALDOC have all been identified as being carbonylated in Alzheimer's disease (30; 147), indicating a potential role for this modification in long-term neuropathology. Recent work by Oikawa and associates (105) examining the effects of ischemia/reperfusion injury on the carbonylated proteome of the monkey hippocampus also showed enhanced carbonylation of CRMP2 and ALDOC. Additionally, GFAP is a major target for carbonylation in experimental autoimmune encephalitis, a murine model of multiple sclerosis (165). All four of the proteins identified in this work are also functionally grouped, as they all contribute to the maintenance of cellular structure (47; 62; 91; 116). In addition, CRMP2 functions in axonal guidance, serving an important role in neuronal regeneration after injury (150). Taken together, these findings suggest that carbonylation may provide a proteomic basis for mechanisms of sustained pathology

after TBI. Understanding the mechanisms, nature, localization, and timing of protein modifications after TBI may provide a guide for the development of more effective TBI therapies that target both oxidative stress and its downstream consequences.

CONCLUSION

In conclusion, this study demonstrates in rats that TBI induces carbonylation in specific brain regions, cell types, and proteins and that males are more susceptible to TBI-induced protein carbonylation than females. These results suggest that: (1) region-specific protein carbonylation may play an important role in the etiology of TBI pathology and (2) females are less susceptible to the ongoing pathological spread of protein modifications after injury. These gender-specific effects may point to possible approaches for intervention to address the secondary, pathological spread of protein modifications after TBI-induced oxidative stress.

ACKNOWLEDGMENTS

The authors thank Dr. Regina Day for her assistance in preparation of this publication. Support for this work included funding from the Uniformed Services University of the Health Services (T0702554 and R07028414) and TriService Nursing Research Program (N12-P12). The views expressed are the private views of the authors and do not necessary reflect the official policy or position of the Uniformed Services University of the Health Sciences, the Department of the Army, the Department of Defense, or the United States government.

CHAPTER 3: Protein citrullination: A proposed mechanism for long-term pathology in traumatic brain injury

Rachel C. Lazarus[a], John E. Buonora[b], Michael N. Flora[c], James G. Freedy[c], Gay R. Holstein[d], Giorgio P. Martinelli[d], David M. Jacobowitz[a,c], and Gregory P. Mueller [a,c,e *]

[a] Program in Neuroscience, Uniformed Services University of the Health Sciences, Bethesda, MD, USA

[b] US Army Graduate Program in Anesthesia Nursing, Ft. Sam Houston, TX, USA

[c] Department of Anatomy, Physiology, and Genetics, Uniformed Services University of the Health Sciences, Bethesda, MD, USA

[d] Department of Neurology, Icahn School of Medicine at Mount Sinai, New York, NY, USA

[e] Center for Neuroscience and Regenerative Medicine, Uniformed Services University of the Health Sciences, Bethesda, MD, USA

* Corresponding Author

Gregory P. Mueller, Ph.D.

Department of Anatomy, Physiology, and Genetics

Uniformed Services University of the Health Sciences

4301 Jones Bridge Road

Bethesda, MD 20814, USA

Phone: (301) 295-3507

Email: Gregory.Mueller@usuhs.edu

ABSTRACT

Protein citrullination is a calcium-driven post-translational modification proposed to play a causative role in the neurodegenerative disorders of Alzheimer's disease, multiple sclerosis (MS) and prion disease. Citrullination can result in the formation of antigenic epitopes that underlie pathogenic autoimmune responses. This phenomenon, which is best understood in rheumatoid arthritis, may play a role in the chronic dysfunction following traumatic brain injury (TBI). Despite substantial evidence of aberrations in calcium signaling following TBI, there is little understanding of how TBI alters citrullination in the brain. The present investigation addressed this gap by examining the effects of TBI on the distribution of protein citrullination and on the specific cell types involved. Immunofluorescence revealed that controlled cortical impact in rats profoundly up-regulated protein citrullination in the cerebral cortex, external capsule, and hippocampus. This response was exclusively seen in astrocytes; no such effects were observed on the status of protein citrullination in neurons, oligodendrocytes or microglia. Further, proteomic analyses demonstrated that the effects of TBI on citrullination were confined to a relatively small subset of neural proteins. Proteins most notably affected were those also reported to be citrullinated in other disorders including prion disease and MS. *In vivo* findings were extended in an *in vitro* model of simulated TBI employing normal human astrocytes. Pharmacologically-induced calcium excitotoxicity was shown to activate the citrullination and breakdown of glial fibrillary acidic protein, producing a novel candidate TBI biomarker and potential target for autoimmune recognition. In summary, these findings demonstrate that the effects of TBI on protein citrullination are selective with respect to brain region, cell type and proteins

modified, and may contribute to a role for autoimmune dysfunction in chronic pathology following TBI.

Key words: Traumatic brain injury, citrullination, astrocytes, calcium, glial fibrillary acidic protein.

INTRODUCTION

Traumatic brain injury (TBI) is a major cause of injury and death in the US, with over 1.7 million TBIs occurring annually and at least 5.3 million Americans currently living with ongoing disability (157). Traumatic brain injuries in civilians are largely due to automobile accidents, as well as falls, sports, and firearms (161). Military populations are at disproportionately elevated risk for blast-related TBI due to the devastating effects of improvised explosive devices (61). While there is a very large body of information on causes and global consequences of TBI, much less is known about the mechanisms underlying long-term pathology.

The long-term consequences of TBI can be complex, and often result in progressive cognitive and behavioral changes. Studies have indicated that anywhere from 10% – 50% of individuals with TBI suffer from persistent symptoms following injury (12), including attention deficits and short-term memory loss (157). This long-term dysfunction follows in the wake of two main injury phases: (1) the primary injury, caused by the immediate forces of the trauma (117; 161); and (2) the subsequent secondary injury, which presents as a constellation of dysfunctional molecular processes including impaired metabolism, free radical production, inflammation, and glutamate excitotoxicity (157). At present, it is not well understood how these various dysfunctional processes following acute injury can lead to progressive, chronic pathology after TBI.

A hallmark mechanism of secondary injury following TBI is prolonged imbalance in cellular calcium homeostasis, resulting in excitotoxic calcium overload (49; 90; 149). Following TBI, ischemia can lead to a dramatic loss of glucose and oxygen delivery to the central nervous system, thereby limiting the production of ATP. In the absence of

adequate energy, ionic homeostasis is lost and calcium toxicity ensues. The abnormally large increase in intracellular calcium originates from both the influx from the extracellular space across multiple calcium channels, and from the mobilization of intracellular calcium stores (151). The result is a pathologically prolonged state of elevated intracellular calcium (149).

The downstream effects of cellular calcium toxicity have been examined closely in regard to mitochondrial dysfunction and oxidative stress. However, little attention has been given to the role of TBI-induced calcium overload in the activation of peptidylarginine deiminase (PAD) enzymes. This family of calcium-dependent enzymes catalyzes the post-translational modification of citrullination, resulting in the conversion of intrapeptidyl arginine residues to citrulline residues. In addition to altering both the normal structure and function of proteins, citrullination generates "altered-self" epitopes that may be antigenic, prompting autoimmune responses against previously benign proteins (33; 164). Altered calcium homeostasis accompanied by protein citrullination has been implicated in several neurodegenerative disorders, including Alzheimer's disease (65), temporal lobe epilepsy (9), glaucoma (19), rheumatoid arthritis (82), and multiple sclerosis (6).

At present, understanding of the specific proteins modified by citrullination is very limited outside the field of immunology, where the antigenic properties of abnormal citrullination are studied largely within the context of rheumatoid arthritis. Additionally, there is no data available regarding the regional and cellular specificity of protein citrullination in neural tissue following TBI. Here, we identify the regions and cell types most susceptible to protein citrullination following TBI, and also identify a subset of

neural proteins that are preferentially citrullinated in response to injury. Furthermore, we present the development of an *in vitro* model for simulating TBI through astrocytic calcium excitotoxicity, and identify a citrullinated breakdown product of glial fibrillary acidic protein (GFAP). Until now, citrullination has been primarily associated with chronic, progressive autoimmune and neural disorders. The present findings indicate that protein citrullination is a feature of TBI that may contribute to the long-term pathogenic mechanisms following acute injury, including those that involve the adaptive immune system.

MATERIALS AND METHODS

Controlled Cortical Impact (CCI)

CCI was conducted as described in Lazarus et al. (2015). Briefly, adult male and female Sprague-Dawley rats (Charles River Laboratories, Morrisville, North Carolina, USA) were anesthetized, then subjected to unilateral CCI over the left hemisphere administered through a ImpactOne stereotaxic impactor (Leica Microsystems, Buffalo Grove, Illinois, USA), which delivered a 3 mm flat-tipped impactor at 20° to a depth of 2 mm at 5 m / s with a 500 ms dwell time at -3.8 mm bregma in males / - 3.0 mm bregma in females. Naïve animals received no anesthesia or CCI treatment. Animals were euthanized five days following injury. All animal handling procedures were performed in compliance with guidelines from the National Research Council for the ethical handling of laboratory animals, as approved by the Institutional Animal Care and Use Committee of USUHS (IACUC Protocol APG 12-827, Bethesda, Maryland, USA).

Immunohistochemistry

Tissue collection and preparation

Tissue was collected and prepared as described previously (78). Briefly, euthanized animals underwent transcardial perfusion (phosphate buffered saline (PBS) followed by 4% paraformaldehyde) after which brains were removed for storage overnight at 4°C in 4% paraformaldehyde and then equilibration in a 30% sucrose solution (2 days, 4°C). Brains were sectioned coronally (20 μm) across the breadth of the lesion site (2.5 mm rostral to 2.5 mm caudal) with a Leica CM1900 cryostat (Leica Microsystems), and sections were then mounted on slides and stored at -80°C. The following groups of gender / conditions were prepared for immunohistochemical analysis: n = 11 male rats, CCI; n = 8 male rats, naïve control; n = 10 female rats, CCI; n = 7 female rats, naïve control.

Detection of cell-specific citrullination

The region and cell-specific effects of CCI on protein citrullination were determined using a mouse monoclonal anti-citrulline antibody (mAb 6B3, IgG2b) (87). The antibody was purified from expression medium by Protein A affinity chromatography (HiTrap Protein A HP column (17-0403-01; GE Healthcare, Buckinghamshire, United Kingdom) on a GE ÄKTA FPLC fast protein liquid chromatography instrument (FPLC; 18-1900-26; GE Healthcare), aliquoted for single-use and stored at -80°C.

Immunodetection of citrullinated proteins was performed as follows. Brain sections were incubated at 4°C overnight with 125 μl of 1:1000 mouse anti-citrulline 6B3 antibody in 0.3% Triton X-100/PBS, with 1:100 normal donkey serum (NDS) as a

blocking agent (16 sections per animal). Co-localization experiments were performed by co-incubating these sections with mAb 6B3 and either: (1) goat anti-GFAP (1:1000; ab53554; Abcam, Cambridge, England) (astrocytes); (2) goat anti-ionized calcium-binding adapter molecule (Iba1; 1:500; ab5076; Abcam) (microglia); (3) rabbit anti-neuronal nuclei (NeuN; 1:500; ab104225; Abcam) (neurons); or (4) rabbit anti-myelin basic protein (MBP; 1:1000; ab40390; Abcam) (oligodendroglia). Slides were washed five times with 0.2% Triton X-100/PBS and then incubated for 30 min with 125 µl of secondary antibody solution: 1:100 donkey anti-mouse IgG (H+L), conjugated to green-fluorescent Alexa Fluor 488 dye (A-21202; Invitrogen, Waltham, Massachusetts, USA); and either 1:100 donkey anti-goat, conjugated to red-fluorescent Alexa Fluor 594 (A-11058, Invitrogen), or 1:100 donkey anti-rabbit, conjugated to red-fluorescent Alexa Fluor 594 (A-21207; Invitrogen). The sections were washed five times with 0.2% Triton X-100/PBS and one time with 1× PBS (5 m) and then visualized with an Olympus BX61 fluorescent motorized system microscope (Olympus, Shinjuku, Tokyo, Japan) using iVision-Mac software (BioVision Technologies, Exton, Pennsylvania, USA).

Preadsorption control

Specificity of the mAb 6B3 anti-citrulline antibody in immunofluorescence was confirmed through immunoneutralization using a mixture of citrullinated protein molecular weight standards (trypsinogen, glyceraldehyde 3-phosphate dehydrogenase, bovine albumin, trypsin inhibitor, alpha-lactalbumin, carbonic anhydrase, and egg albumin) prepared in-house via 10 hour incubation at 37°C with active PAD enzyme cocktail (0.5 µg / µl; P312-37C-25; SignalChem, Richmond, British Columbia, Canada) in Tris buffer (50 mM Tris HCl, pH 7.4); 5 mM $CaCl_2$; and 0.73 mM dithiothreitol (DTT;

Sigma–Aldrich, St. Louis, MO, USA)). Concurrently, a control sample was prepared in an identical manner, without the addition of the PAD enzyme cocktail.

Identification of citrullinated protein species in injured rat brain

Tissue collection and preparation

Brains were collected, snap-frozen with powdered dry ice, and stored at -80°C until use. Brains were thawed on wet ice and then hand-dissected to produce blocks of tissue encompassing the lesion site (penumbra region) and the surrounding tissue shown by immunohistochemistry to have increased protein citrullination following CCI. The equivalent region from naïve animals (control tissue) was similarly collected. Tissue blocks were homogenized in 5 volumes / tissue weight extraction solution, consisting of: 7.7 M urea; 2.2 M thiourea; and 4.4% CHAPS; also containing 1x Complete protease inhibitor mix (Roche). Samples were clarified by centrifugation (20,000 x g, 10 min, 4°C), and resulting supernatants were fractionated by 2-dimensional electrophoresis (2-DE).

Fluid-phase Isoelectric Focusing (F-IEF)

Treatment group pools (control and injury penumbra) were prepared (N = 4/pool) and fractionated by F-IEF. Briefly, 200 µl aliquots of each pool was diluted up to 2.865 ml in IEF running solution (7.7 M urea; 2.2 M thiourea; 4.4% CHAPS; ampholytes (150 µl, pH 3 – 10; ZM0021, Invitrogen); DTT (50 µl, 2 M); and bromophenol blue (10 µl, 10 mg/ml). Samples were loaded into the ZOOM IEF Fractionator (ZMF10002; Invitrogen) and focused according to the following conditions: (1) 100 V, 1.2 mA, 0 W (15 min); (2) 200 V, 2.0 mA, 0 W (1 h); (3) 400 V, 2.0 mA, 1 W (1 h); (4) 600 V, 1.5 mA, 1 W (1 h)

resulting in fractions of proteins within the following five pI ranges: 3.0 – 4.6; 4.6 – 5.4; 5.4 – 6.2; 6.2 – 7.0; and 7.0 – 9.1.

Molecular weight fractionation

Proteins in each of the F-IEF fractionations were further resolved by molecular weight fractionation using conventional one-dimensional gel electrophoresis. Samples were combined with an equal volume of 4x reducing loading buffer (Novex NuPAGE LDS sample buffer; 50 mM DTT; Invitrogen), heated at 70°C (20 min) and then fractionated (10 µl per well) using NuPAGE 4 - 12% Bis-Tris gels (Novex, Invitrogen). Proteins were transferred to nitrocellulose blots using an iBlot transfer apparatus & gel transfer stacks (Nitrocellulose Mini; 1B301002, Invitrogen).

Immunoblotting

Blots were blocked with 5% instant nonfat dry milk / Tris-buffered saline/Tween 20 (TBS-T) (1 h, room temperature) and then incubated with the 6B3 primary antibody (1:300 in TBS-T; mAb stock = 1.79 mg/mL) for 1 h at room temperature, then 4°C overnight. Following equilibration to room temperature (30 min), membranes were washed in TBS-T (5 times over 60 min), incubated with secondary antibody, horseradish peroxidase-labeled, goat anti-mouse IgG (1:2500 in 5% TBS-T; 31430, Thermo Scientific) for 2 h at room temperature and then visualized by enhanced chemiluminescence (ECL) (Novex ECL HRP Chemiluminescent Substrate Reagent Kit; WP20005, Invitrogen) using the FUJI LAS 3000 Imager (Fujifilm, Minato, Tokyo, Japan). Images collected were analyzed using MultiGauge software (v. 3.0, Fujifilm). In some cases, blots were reprobed with a second anti-protein citrulline antibody (1:500; MABN328EMD; Millipore; detection with horseradish peroxidase-labeled, goat anti-

mouse IgM; 1:2500 in TBS-T; 31440, Thermo Scientific), with final overnight washing, to confirm the 6B3 immunoreactive features and increase the sensitivity of detection. No new signals were revealed by this approach.

The specificity of mAb 6B3 for detecting citrullinated proteins on western blots was confirmed by immunoneutralization, similar to the approach used for immunohistochemistry (see above), but involving solid-phase preadsorption (versus fluid phase) to accurately replicate the conditions of western blotting. In this case, the 6B3 antibody was reacted with a strip of nitrocellulose (Protran® BA85, 0.45 μm pore size, binding capacity 80 μg/cm^2; Sigma-Aldrich; cut into 1.4 cm x 3 cm pieces) to which either the citrullinated or native forms of fibrinogen had been bound. The amount of protein absorbed to the strip was 200μl / 200μg of citrullinated human fibrinogen (400076, Cayman Chemical, Ann Arbor, Michigan, USA), or 200μl / 200μg human fibrinogen (16088, Cayman Chemical) in TBS-T. The duration of the antibody absorption was 16 h at 4°C.

Protein identifications

Immunoreactive signals of interest were mapped to corresponding features in Coomassie-stained gels. These features were excised and processed for identification through the ESMS-Basic Protein ID service using an Elite Orbitrap mass spectrometer (Thermo Scientific) by the W.M. Keck Mass Spectrometry & Proteomics Resource (W.M. Keck Foundation Biotechnology Resource Laboratory, New Haven, Connecticut, USA). Analyses results were received through and tracked within the Yale Protein Expression Database (YPED, Yale / NIDA Neuroproteomics Center, New Haven, Connecticut, USA). Criteria for a positive identification included: an expectation score

less than 1.0E-65, a percent coverage greater than 35.0%, and a pI and mw that were consistent with the fractionation data.

In vitro model of protein citrullination following TBI-induced excitotoxicity in astrocytes

An *in vitro* model of simulated TBI was established using normal human astrocytes (NHA CC-2565, Lonza, Allendale, New Jersey, USA) and treatment with the calcium ionophore, ionomycin (Free Acid, Streptomyces conglobatus, 407950, Calbiochem, Billerica, Massachusetts, USA), to simulate calcium excitotoxicity. Astrocytes were cultured to ~70% confluence in T-75 tissue culture flasks according to vendor instructions. Cells were washed with TBS (4 times) and then treated for 4 h (37°C, 95% O_2/5% CO_2) with either ionomycin (10 μM; 10 mL TBS) or dimethyl sulfoxide vehicle (DMSO; 10 μl/10 mL TBS). Following incubation, protease inhibitors were added to the flasks (final concentration of 1x; Complete protease inhibitor mix; 10269700, Roche) and cells were harvested by scraping and centrifugation (800 x g, 4°C, 10 min). Cells were extracted by vortexing into IEF denaturant (see section **2.3.2**) at a ratio of 1 part pellet to 4 parts buffer (v/v). Samples were clarified by centrifugation (15,000 x g, 4°C, 10 m). The resulting supernatent was processed by one-dimensional gel electrophoresis and immunoblotting as described above. Replicate immunoblots containing samples from three separate experiments each were probed with either anti-citrullinated protein (6B3) or anti-GFAP (1:3000, Z0334, DAKO, Carpinteria, California, USA). Each primary antibody was paired with an appropriate secondary antibody (6B3: horseradish peroxidase-labeled, goat anti-mouse IgG; 1:2500; 31430; Thermo Scientific; GFAP: horseradish peroxidase-labeled, goat anti-rabbit IgG; 1:3000; HAF008; R&D Systems) and blots were visualized by ECL.

RESULTS

Figure 14 presents the effects of CCI on the expression of citrullinated proteins in the rat cerebral cortex. Immunohistochemical analysis demonstrated that the basal level of protein citrullination as detected by labeling with mAB 6B3 was very low under control conditions. In contrast, CCI induced a marked increase in the immunolabeling of cells in the cortex. This up-regulation of protein citrullination was most pronounced in the vicinity of the lesion. The morphology of the affected cells was remarkably consistent, suggesting that the effects of CCI on protein citrullination were cell-specific.

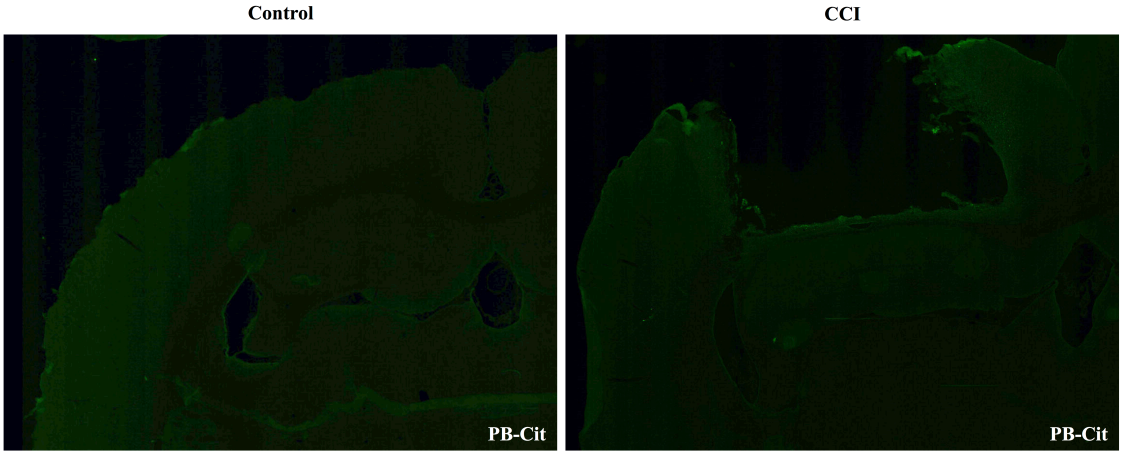

Figure 14. Injury upregulates the expression of citrullinated proteins in the cerebral cortex. Brain tissue was collected five days after CCI and evaluated for protein citrullination by anti-protein citrulline immunolabeling using mAB 6B3. The panels show immunolabeling in sections of control (left) and injured brain (right) (2X magnification). Data are representative of 15 control animals (8 males and 7 females) and 21 CCI animals (11 males and 10 females). No gender-based differences were observed. PB-cit: Protein-bound citrulline.

The specificity of mAb 6B3 labeling of citrullinated proteins in TBI brain was confirmed by immunoneutralization. As shown in Figure 15, preabsorption of the mAb 6B3 with citrullinated protein standard effectively eliminated the labeling of cells in the cerebral cortex and hippocampus of CCI brain. In this experiment, the active labeling

condition utilized mAb 6B3 that had been exposed to the identical absorption procedures as the neutralized mAb 6B3, except that the neutralizing proteins were not citrullinated under the control condition. Additionally, a secondary-only control was also conducted and further confirmed the specificity of the anti-citrullinated protein labeling.

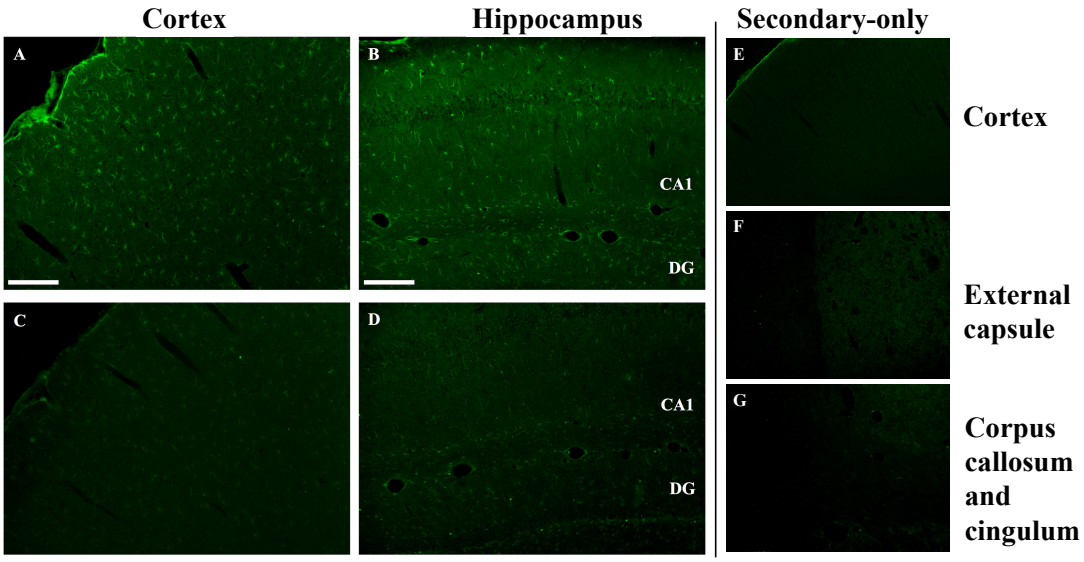

Figure 15. Specificity of anti-protein citrulline immunolabeling by mAb 6B3. Panels A and B show immunofluorescent signals from mAb 6B3 anti-protein citrulline labeling of the injured cerebral cortex (panel A) and ipsilateral hippocampus (panel B). Panels C and D show immunolableing of equivalent sections with mAb 6B3 that was preadsorbed with citrullinated protein standards. Panels E, F, and G show secondary-only control images of the cortex, external capsule, and corpus callosum / cingulum (20x magnification). The control and immunoneutralized preparations of mAb 6B3 were treated identically, with the exception of the presence or absence of neutralizing citrullinated proteins. Data are representative of two independent experiments. Scale bar: 200 μm.

The regional effects of CCI on protein citrullination are summarized in Figure 16. CCI produced a marked increase in protein citrullination throughout the injured cortex, extending from lateral to the lesion site to regions of the cortex not directly impacted by CCI (Figure 16, panel B). Similarly, immunolabeling of the injured ipsilateral hippocampal formation (Figure 16, panel E) and external capsule (Figure 16, panel H)

revealed a significant degree of protein citrullination in these regions. To a lesser extent, protein citrullination was also observed in fibers extending ventrally from the lesion site towards the midline corpus callosum (not shown). Other brain regions, including the amygdala and caudatoputamen, were completely negative for protein citrullination in these CCI animals. Furthermore, there was no gender difference observed in the regionalization or magnitude of protein citrullination following injury. In general, CCI appeared to have little effect on the status of protein citrullination in contralateral brain structures, with the exception of the dorsal hippocampus, where approximately 20% of injured animals (4 of 21) displayed an intense labeling of unusually large and rounded cells (Figure 16, panel F). Finally, 6B3 immunolabeling was uniformly low across all regions studied in control male and female animals (Figure 16, Panels A, D, and G).

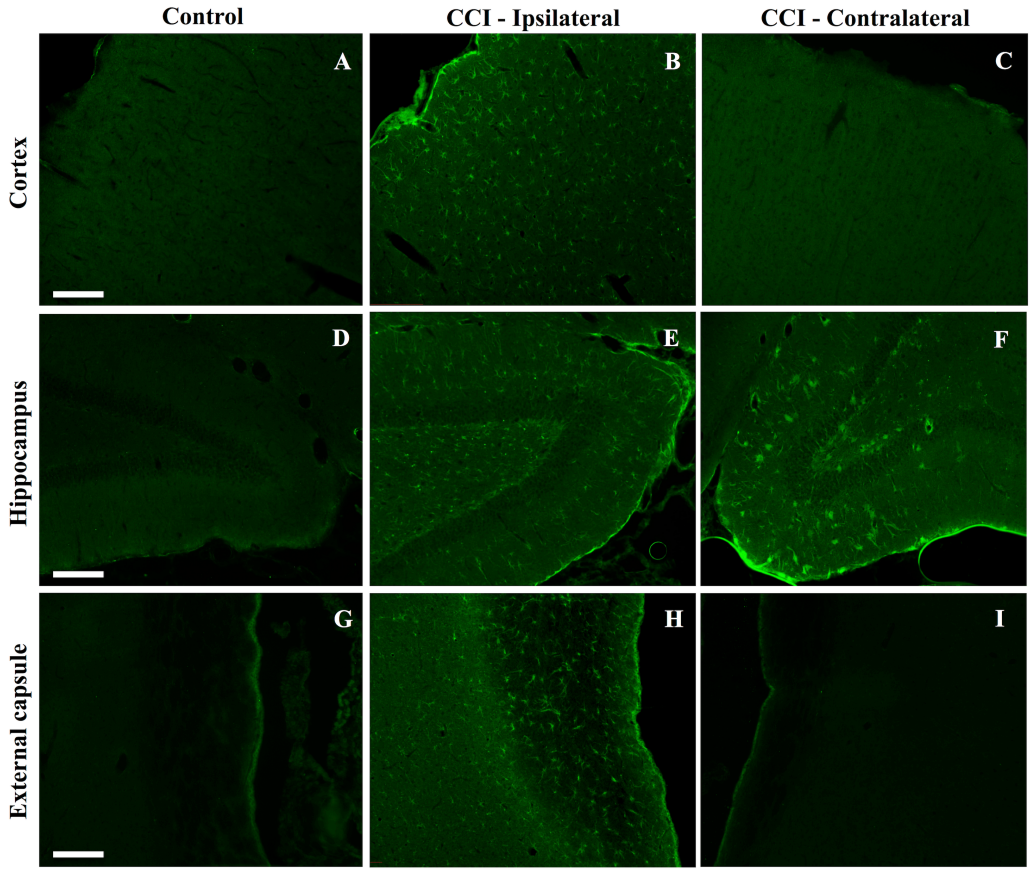

Figure 16. Increased protein citrullination in the cerebral cortex, hippocampus and external capsule following CCI. Anti-protein citrulline immunolabeling by mAb 6B3 is shown for the control brain regions (panels A, D, and G), regions ipsilateral to the lesion (panels B, E, H) and regions contralateral to the lesion (panels C, F, and G). Structures representated are the cerebral cortex (A-C), hippocampus (D-F), and external capsule (G-I). Data are representative of 15 control animals (8 males and 7 females) and 21 CCI animals (11 males and 10 females). No gender-based differences were observed. Scale bar: 200 μm.

Dual immunofluorescence revealed astrocytes to be the principal cell type in which protein citrullination was affected by CCI. Figure 17 shows that anti-citrulline labeling in the cortex and external capsule was predominantly colocalized with GFAP. Similar observations were made in other affected brain regions.

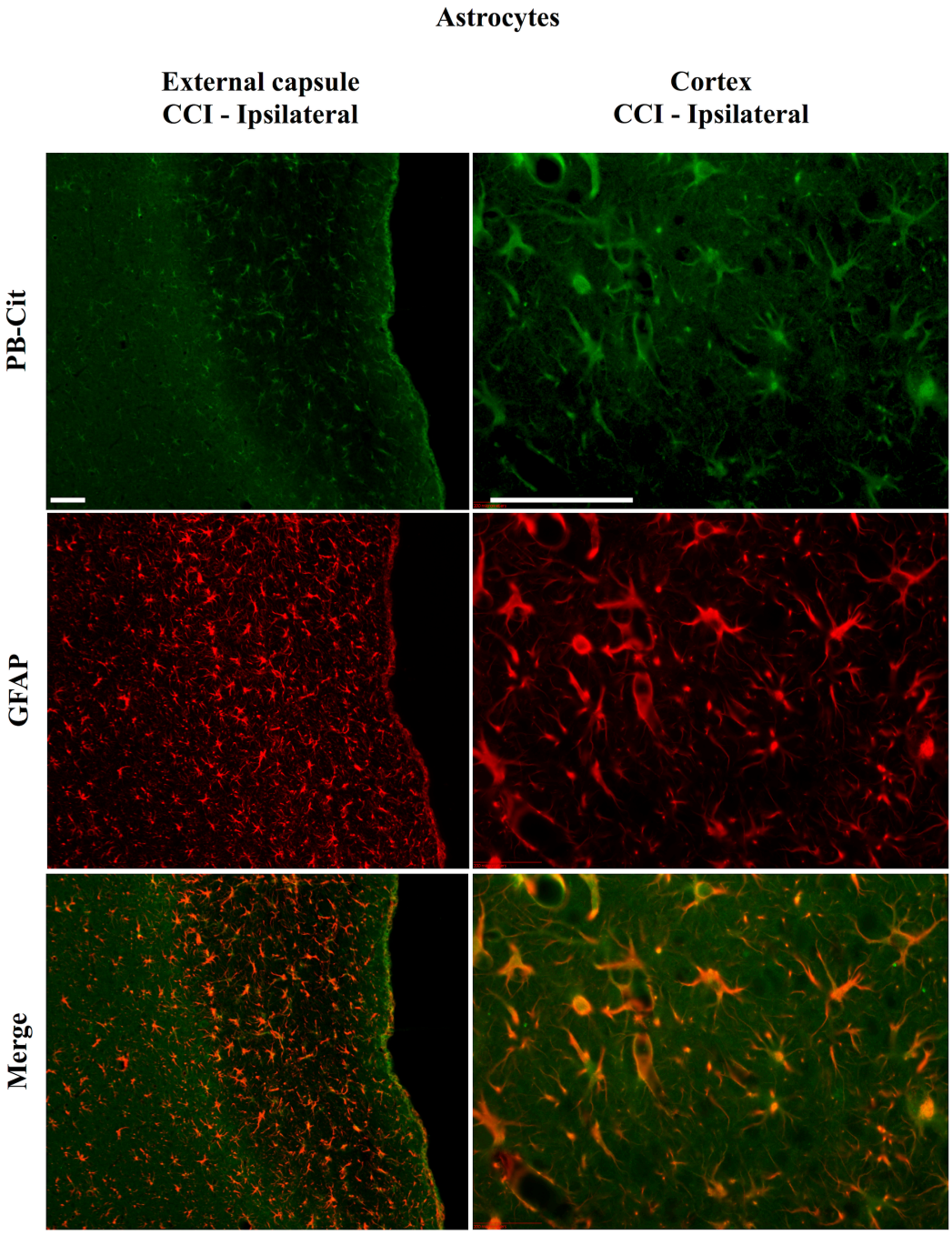

Figure 17. Localization of CCI-induced protein citrullination to astrocytes. Panels on the left show the colocalization of mAb 6B3 labeling with anti-GFAP labeling in the external capsule. Panels on the right show the colocalization of mAb 6B3 labeling with anti-GFAP labeling in the cerebral cortex. Data are representative of 15 control animals (8 males and 7 females) and 21 CCI animals (11 males and 10 females). No gender-based differences were observed. Scale bar: 200 μm. PB-cit: Protein-bound citrulline.

The findings presented in Figure 18 further confirm that CCI-induced protein citrullination was not significantly associated with neurons (NeuN), microglia / macrophages (Iba1), or oligodendrocytes (MBP) in the cortex. Citrullination was also not significantly associated with these cell types in any other brain regions investigated (not shown).

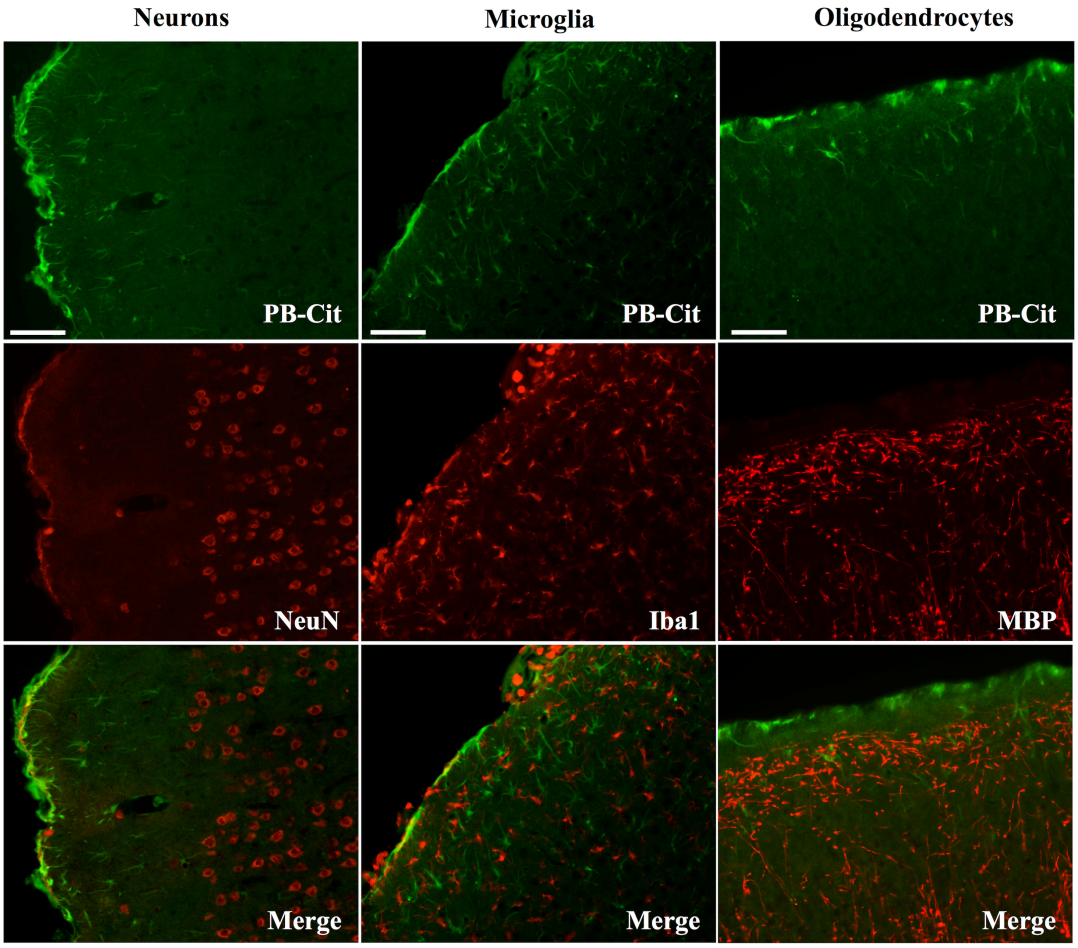

Figure 18. CCI did not affect the status of protein citrullination in neurons, microglia or oligodendrocytes. Sections of cerebral cortex ipsilateral to CCI were probed with mAb 6B3 to label protein bound citrulline (PB-Cit; upper panels) and either anti-NeuN, Iba1, or MBP to label neurons, microglia, or oligodendrocytes, respectively (middle panels). The merge of the two signals is presented in the lower panels. Data are representative of 8 separate experiments. Scale bar = 200 μm.

The distinctive profile of CCI-induced protein citrullination in the ipsilateral and contralateral hippocampus is shown in Figure 19. As noted above, increased anti-citrullinated protein labeling was clearly evident in the ipsilateral hippocampus of all animals studied (Figure 19, panel A), and this labeling colocalized with GFAP labeling (Figure 19, panels B and C). In addition, in ~20% of injured animals, the contralateral hippocampus also displayed intense 6B3 labeling (Figure 19, panel D) that colocalized with GFAP labeling. The co-labeled cells were morphologically distinct from traditional stellate astrocytes, displaying a rounded, branchless appearance consistent with that of a macrophage (Figure 19, panels E-G).

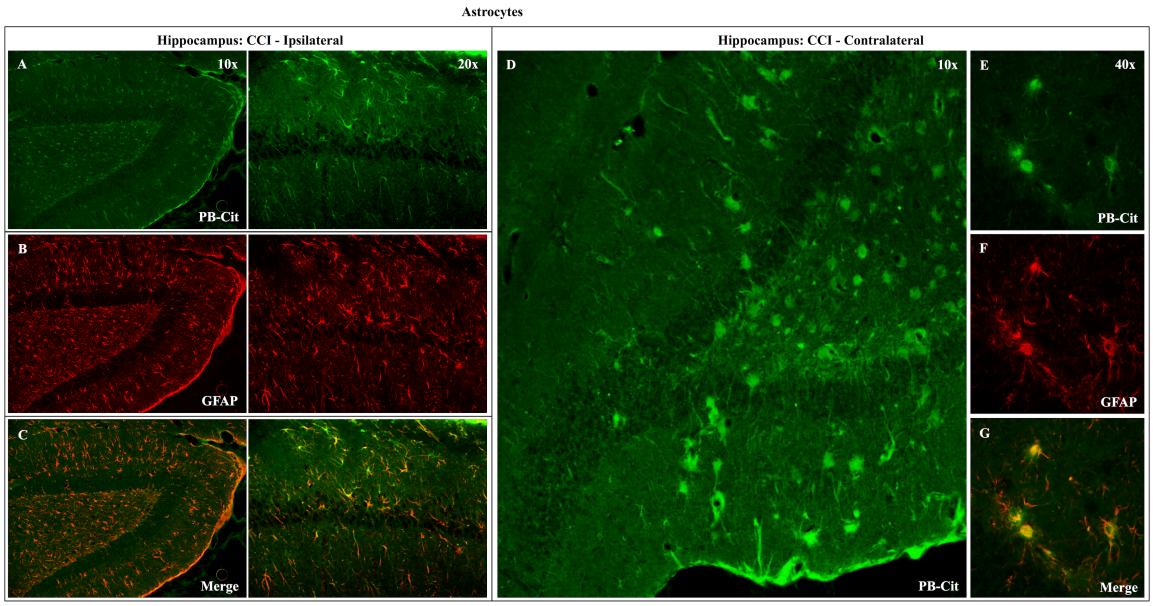

Figure 19. Effects of CCI on protein citrullination in GFAP-positive cells of the ipsilateral and contralateral hippocampus. Colocalization of anti-protein citrulline and anti-GFAP labeling in astrocytes of the ipsilateral hippocampus is depicted in the pairs of panels presented on the left (A-C). Panel D shows the distinctive anti-citrullinated protein immunolabeling of large, rounded cells observed in the contralateral hippocampus of approximately 20% of CCI animals (4 of 21). While these cells lacked the classical stellate morphology of astrocytes, the anti-citrullinated protein labeling colocalized with GFAP immunolabeling (panels E-G). PB-cit: Protein-bound citrulline.

Figure 20 demonstrates the specificity of the 6B3 antibody for detecting citrullinated proteins in a western blot format. Shown on the left is the Coomassie staining for human fibrinogen (Fib) and the same preparation of fibrinogen that was enzymatically citrullinated by reaction with PAD4 (C-Fib). The protein staining shows that the characteristic profile of purified human fibrinogen is modestly affected by reaction with PAD4. Presented on the right are immunoblots showing the reactivity of mAb 6B3 with the citrullinated fibrinogen preparation (Active/C-Fib) and the elimination of this reactivity by preabsorption of 6B3 with citrullinated fibrinogen prior to blotting (Neutralized/C-Fib). There was no reactivity of mAb 6B3 with fibrinogen that had not been citrullinated by PAD4 treatment (Active/Fib).

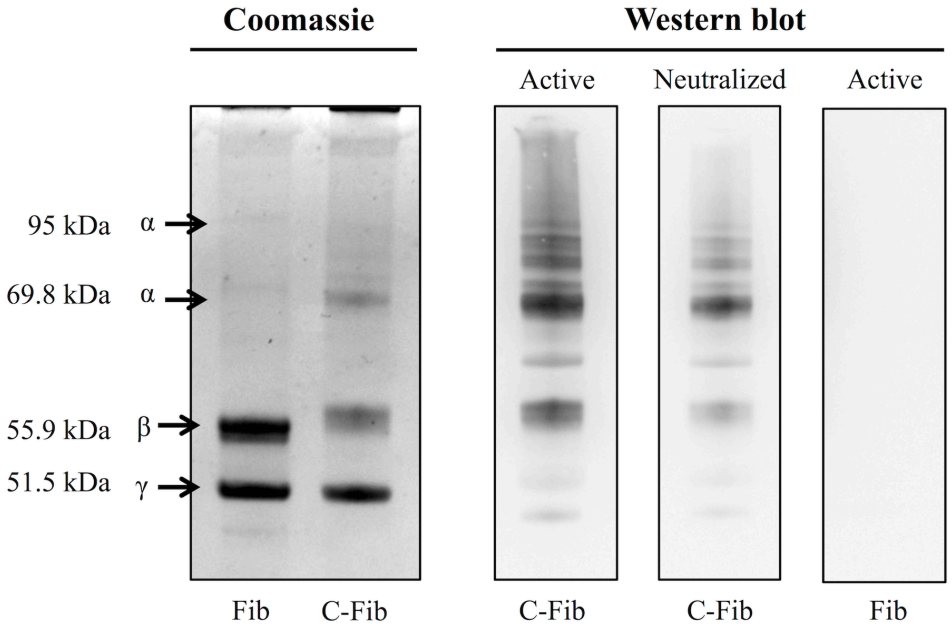

Figure 20. Specificity of anti-protein citrulline mAb 6B3 detection for western blotting. Displayed on the left are two Coomassie-stained profiles showing the protein composition of native fibrinogen (Fib) and citrullinated fibrinogen (C-Fib). The western blot (right) shows three immunoblots in which: citrullinated fibrinogen was probed with active mAb 6B3 (Active/C-Fib; left lane); citrullinated fibrinogen was probed with immunoneutralized mAb 6B3 (Neutralized/C-Fib; middle lane); and native fibrinogen was probed with active mAb 6B3 (Active/Fib; right lane).

Proteomic analysis revealed that the effects of CCI on protein citrullination were specific to a discrete subset of proteins making up the entire brain proteome, and further, that the proteins involved are primarily associated with cytoskeletal structure and metabolic processes (Figure 21). Shown in the upper left panel are the proteomes of control and injured cerebral cortex fractionated by fluid phase isoelectric focusing. Each pair of lanes, control (C) and CCI (I), show the proteins present in the four different pI partitions. As visualized by Commassie staining, CCI did not appreciably affect the general pattern of protein staining across the four pI fractions. In contrast, the pattern of protein citrullination was dramatically impacted by CCI (upper right panel). Consistent with immunohistochemistry findings (Figures 15 and 16), little protein citrullination was observed in control cortex (C), whereas CCI (I) resulted in the intense labeling of a distinctive subset of the fractionated proteins. The immunoreactive signals of the western blot were mapped to Commassie features of the protein gel, and proteins were identified by peptide mass fingerprinting and tandem mass spectrometry. The proteins identified are presented in the lower panel of Figure 21. These proteins are functionally grouped as cytoskeletal components (including dynamin-1, GFAP, and several forms of tubulin); those involved in metabolic processes (including peroxiredoxin-1, dihydropyrimidinase-related protein 2, and creatine kinase B-type); and proteins involved in cell-cell signaling and synaptic transmission (synapsin-2, syntaxin-binding protein 1, and amphyiphysin).

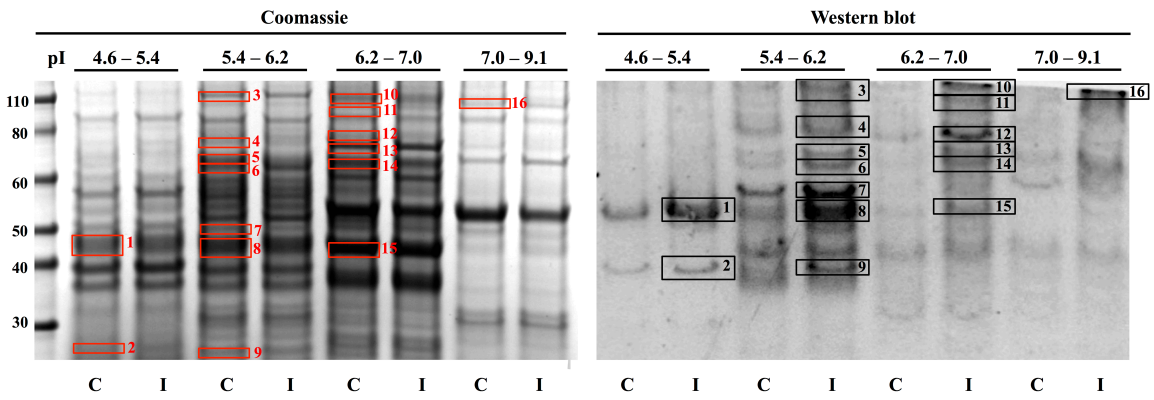

Sample	Score	Expectation	Protein ID	Protein name	MW	% Cov
1	3387	0	ALDOA_RAT	Fructose-bisphosphate aldolase A	39327	68.4
2	1223	3.70E-119	PRDX1_RAT	Peroxiredoxin-1	22095	60.3
	1083	3.90E-105	COF1_RAT	Cofilin-1	18521	83.7
	1059	1.10E-102	GSTP1_RAT	Glutathione S-transferase P	23424	52.9
	946	2.10E-91	TAGL_RAT	Transgelin	22588	62.7
3	7314	0	DYN1_RAT	Dynamin-1	97234	72.9
4	2547	0	SYN2_RAT	Synapsin-2	63417	65
	1448	0	MOES_RAT	Moesin	67697	54.9
	1241	0	SEPT9_RAT	Septin-9	63752	45.9
	735	0	ANXA6_RAT	Annexin A6	75706	44.9
5	1317	0	STIP1_RAT	Stress-induced-phosphoprotein 1	62530	43.3
	1170	8.00E-114	STXB1_RAT	Syntaxin-binding protein 1	67526	46.6
6	3296	0	DPYL2_RAT	Dihydropyrimidinase-related protein 2	62239	71.7
7	4618	0	ENOA_RAT	Alpha-enolase	47098	77.6
	886	2.00E-85	ENOG_RAT	Gamma-enolase	47111	36.4
	701	6.60E-67	GFAP_RAT	Glial fibrillary acidic protein	49927	35.8
8	1776	0	ALDOC_RAT	Fructose-bisphosphate aldolase C	39259	59.2
	960	8.30E-93	SEPT3_RAT	Neuronal-specific septin-3	40572	39.7
9	1516	0	TAGL3_RAT	Transgelin-3	22486	85.4
	698	1.20E-66	MBP_RAT	Myelin basic protein	21489	54.9
10	2399	0	HSP74_RAT	Heat shock 70 kDa protein 4	93997	52.1
	1830	0	GRAP1_RAT	GRIP1-associated protein 1	96015	49.7
11	3751	0	TERA_RAT	Transitional endoplasmic reticulum ATPase	89293	55.5
12	3017	0	NDUS1_RAT	NADH-ubiquinone oxidoreductase 75 kDa subunit, mitochondrial	79362	59
	1883	0	NSF_RAT	Vesicle-fusing ATPase	82600	43.5
	1837	0	GRP78_RAT	78 kDa glucose-regulated protein	72302	43.1
13	7555	0	HSP7C_RAT	Heat shock cognate 71 kDa protein	70827	82.2
	1953	0	ANXA6_RAT	Annexin A6	75706	57.9
14	1212	5.10E-118	STXB1_RAT	Syntaxin-binding protein 1	67526	42.1
15	3440	0	ACTB_RAT	Actin, cytoplasmic 1	41710	61.1
	1943	0	KCRB_RAT	Creatine kinase B-type	42698	54.9
	1488	0	TBB2B_RAT	Tubulin beta-2B chain	49921	47.4
	1433	0	TBB2A_RAT	Tubulin beta-2A chain	49875	47.4
	1237	1.60E-120	TBB4B_RAT	Tubulin beta-4B chain	49769	46.5
	1073	4.30E-104	TBB5_RAT	Tubulin beta-5 chain	49639	42.8
	932	5.20E-90	TBB3_RAT	Tubulin beta-3 chain	50386	35.3
16	2677	0	AMPH_RAT	Amphiphysin	74832	73.5
	1801	0	DREB_RAT	Drebrin	77424	43.3

Figure 21. Identification of proteins that are citrullinated in response to CCI. Extracts of control (C) and injured (I) cerebral cortex were fractionated by fluid-phase isoelectric focusing into defined pH ranges (shown at top) and then further resolved according to molecular weight using one-dimensional gel electrophoresis. Proteins were then transferred to nitrocellulose membranes and probed for protein-bound citrulline (see Methods) (right panel, "Western blot"). Gels run in parallel were visualized with Coomassie (left panel). Sixteen features showing increased citrullination in response to CCI (black numbered boxes, right panel) were mapped to corresponding Coomassie features (red numbered boxes, left panel) and identified by peptide mass finger printing and tandem mass spectrometry. Proteins identified are listed in the lower panel. Images are representative of six independent experiments. A total of n = 4 CCI and n = 4 control animals were examined.

To further investigate the cellular mechanisms of injury-induced protein citrullination, a model of simulated TBI was established. In this model, normal human astrocytes (obtained commercially) were incubated in control medium or in medium containing the calcium ionophore, ionomycin, to induce calcium excitotoxicity. Figure 22 shows the results of 3 separate experiments investigating the effects of ionomycin treatment on the proteolytic processing of GFAP (left panel) and the generation of citrullinated proteins (right panel). The data show that treatment with ionomycin consistently activated the proteolytic processing of intact GFAP (left panel; blue arrows) to produce a distinctive pattern of breakdown products. Probing with mAb 6B3 indicated that one of the GFAP breakdown products is preferentially citrullinated (right panel; orange arrow) in response to simulated TBI. In addition, several other protein features appeared to be heavily citrullinated in response to ionomycin treatment. The identity of these signals remains to be determined.

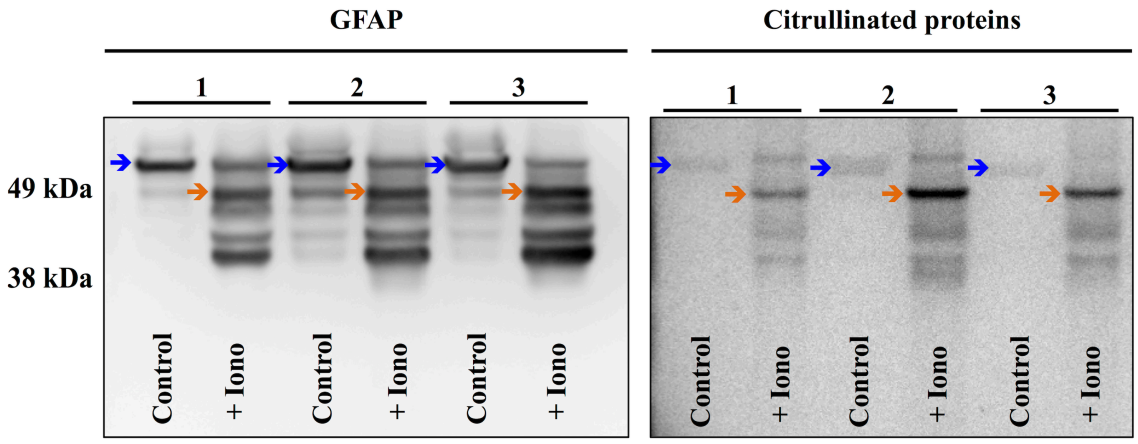

Figure 22. Simulated brain injury in normal human astrocytes reveals a spectrum of GFAP breakdown products and the hyper-citrullination of one GFAP species. Normal human astrocytes were treated with ionomycin (10 μM; 4h) and analyzed for GFAP (left panel) and protein-bound citrulline immunoreactivity (right panel) by western blot. The results of three independent experiments (A, B, and C) are presented, showing the immunoreactivity in extracts prepared from untreated control cells (Control) and cells treated with ionomycin (+ Iono).

The blue arrows indicate intact GFAP, while the orange arrows indicate the hyper-citrullinated GFAP breakdown product.

DISCUSSION

Protein citrullination is a calcium-dependent protein modification that has been largely studied in the context of autoimmune disorders, particularly rheumatoid arthritis. Abnormal protein citrullination in rheumatoid arthritis results in the generation of antigenic epitopes that become targeted by the adaptive immune system (57; 73). Protein citrullination is also found to be abnormal in several neurodegenerative disorders, including multiple sclerosis (MS) and Alzheimer's disease, suggesting that citrullinated proteins may also serve as antigenic targets in these conditions and thereby contribute to long-term pathogenesis. To date, however, little research has examined the effects of TBI on protein citrullination, where an acute mechanical injury can lead to progressive and sustained neuropathology. Currently, there are no data regarding the identity of specific proteins affected by citrullination following TBI, or information on the susceptibility of different brain regions or cell types to this modification following injury.

The constellation of dysfunctions resulting from TBI is often complex and dynamic, involving pathology caused by acute tissue damage and interactions amongst the ongoing changes caused by ischemia, hypoxia, excitotoxicity, and elevated intracranial pressure (157). A hallmark of acute TBI pathophysiology, however, is intracellular calcium overload (50). This shift in ionic balance is excitotoxic, activating a number of damaging intracellular cascades, including lipid peroxidation, proteolysis, free radical generation (161), and the activation of pro-apoptotic genes (157) with the loss of dendritic spines. Elevated intracellular calcium is an essential condition for the activation

of peptidylarginine deiminase (PAD) enzymes, which catalyze the conversion of intrapeptidyl arginine residues to citrulline residues (64).

PAD enzymes exist as several isoforms, two of which are found in neural tissue: PAD2 (38; 68; 115) and PAD4 (2). In humans, PAD2 is largely localized to astrocytes, while PAD4 is exclusively expressed in neurons (2). Moreover, PAD2 is localized to reactive astrocytes in the brains of mice affected by a prion disorder, scrapie, where its enzymatic activity is nearly double that of healthy mice (68). Research on the etiology of MS has suggested that PAD2 contributes to the pathology of demyelination, where its activity is thought to destabilize myelin sheath structure (95).

The present investigation in rats shows that TBI-induced protein citrullination is selectively localized to astrocytes. This finding is consistent with the understanding that following ischemia, astrocytes exhibit a dramatic rise in intracellular calcium due to a rapid influx of extracellular calcium through dysfunctional membrane channels, as well as the release of calcium from intracellular stores (50). While influxes in intracellular calcium are also found in neurons following mechanical injury, this rise is far less profound than that observed in astrocytes (128). Furthermore, astrocytes selectively display long-term defects in calcium signaling following TBI (128) and ultimately, astrocytic death precedes that of neurons in rat models of TBI (50). Related findings involving hypoxia confirm that astroglial injury is due to massive calcium influxes and resulting excitotoxicity (64). Models of TBI illuminate the biologic importance of astrocytes in brain injury, serving a protective role by shielding neurons from damage due to oxygen deprivation (155), glutamate neurotoxicity, and calcium excitotoxicity (89). It has been proposed that the intracellular rise of calcium within astrocytes is directly linked

to their neuroprotective effects on neurons, most likely due to their ability to sequester large amounts of calcium and thus stabilize the ionic environment for neurons (45). Our finding that protein citrullination is limited to astrocytes is consistent with this proposal.

Present results indicate that the up-regulation of protein citrullination induced by TBI occurs in astrocytes that are located in the cerebral cortex, external capsule, and hippocampus. In contrast, the status of protein citrullination in other brain regions (such as the amygdala and caudate putamen) and cell types was not appreciably altered by TBI. The mechanistic basis for this observation may relate to the up-regulation of voltage-gated, class C L-type Ca^{2+} channels that are selectively expressed in astrocytes and are particularly sensitive to activation by injury in the regions reported here (34). The finding that nimodipine, an L-type calcium channel blocker, protects against excitotoxic damage in cultured astrocytes supports this proposal (59). These findings correspond to a model of calcium excitotoxicity-induced citrullination. The selective citrullination of astrocytes in these particular regions may correspond to long-term dysfunctions associated with TBI, including learning and memory deficits associated with progressive hippocampal atrophy (157).

Our investigation showed that patterns of protein citrullination following TBI were similar between male and female rats. This finding is in contrast to our previous observations concerning the effects of TBI on protein carbonylation. Following injury, male rats showed far greater response in protein carbonylation as compared to female rats (78). Protein carbonylation is a reflection of oxidative stress (41), whereas citrullination is a marker of calcium influx (74; 156). Accordingly, the gender difference observed in carbonylation may be due to the protective antioxidant effects of ovarian steroids (124),

whereas a similar mechanism does not appear to exist in the case of citrullination. The extent to which these protein modifications contribute to gender differences in TBI complications and mortality (16; 17; 54) remains to be determined. It should be noted that the present experimental design focused on only one time-point post-TBI (five days), and as such, it is possible that gender differences in post-injury citrullination may be evident at other time-points.

The present investigation has identified 37 proteins as a very small subset of the entire brain proteome that is citrullinated in response to TBI. This selectivity in protein citrullination indicates that the mechanism involved maintains a high degree of specificity. Furthermore, several of the proteins identified here are reported to be citrullinated in neurodegenerative diseases, and thus may play causative roles in neuropathology. Specifically, citrullinated GFAP is a characteristic feature in MS and Alzheimer's disease (25; 57; 65; 100), and myelin basic protein (MBP), a major component of myelin sheath structure, is profoundly over-citrullinated in MS (25; 152). Similarly, GFAP, tubulin, peroxiredoxin 1, cofilin-1 and alpha/gamma enolase are selectively citrullinated in prion disease (68). Therefore, the link between abnormal protein citrullination and neurological disease appears strong. It should be noted that the 37 proteins identified as targets for TBI-induced citrullination were derived from the analysis of only 16 gel features. Accordingly, not all of the proteins identified in a single feature are necessarily citrullinated, and may have resulted from the analysis due to their co-purification with another citrullinated species. Nevertheless, the high correlation that exists between the specific proteins identified here and their reported citrullination in

various disease states is consistent with the proposal that these proteins are indeed targets for citrullination following TBI.

A potential mechanism by which abnormal protein citrullination contributes to neurological disease could involve the adaptive immune system. A significant proportion of the proteins identified here are also recognized as autoantigens, in both neurological and autoimmune-related disorders. For example, MBP is the signature citrullinated autoantigen of MS (24; 152). Autoantibodies targeting amphiphysin are associated with several neurological disorders, including sensory neuronopathy and encephalopathy (94). Additionally, dihydropyrimidinase-related protein 2 (CRMP2) is autoantigenic in autoimmune retinopathy (3). Finally, alpha enolase has been identified as a citrullinated autoantigen in rheumatoid arthritis (74), while citrullinated 78 kDa glucose-regulated protein is an autoantigen within the pancreatic beta-cells in Type 1 diabetes (122). Collectively, these findings support the proposal that injury-induced protein citrullination may generate immunological epitopes that become targets of the adaptive immune system. This process may serve as an underlying basis for chronic and progressive neurological disorders.

Finally, this report presents the development of an *in vitro* model for simulating TBI in a controlled and cell-specific manner. Shown here in normal human astrocytes are the effects of calcium excitotoxicity, a hallmark condition of TBI, on the hyper-citrullination of GFAP. Moreover, the findings confirm the proteolytic processing of GFAP to a series of breakdown products that are consistent with those reported by others using *in vitro* models of TBI (106; 166). Interestingly, our investigation showed that one of these breakdown products is heavily citrullinated, and thus may serve as the antigen

for the development of the anti-GFAP autoantibodies recently reported in TBI (163). Accordingly, the application to this and other models for simulated TBI may provide novel insights into consequences and mechanisms of TBI, and also identify informative biomarkers for assessing brain injury.

In conclusion, the present findings show that TBI dramatically up-regulates protein citrullination within astrocytes in specific brain regions. Additionally, this modification affects only a subset of the neural proteome, primarily affecting proteins involved in cytoskeletal structure, metabolic processes, and cell-cell signaling. A large proportion of these proteins have been identified as citrullinated in other pathologies, including MS, Alzheimer's disease, and rheumatoid arthritis, indicating a potential role for this protein modification in ongoing pathological processes. Interestingly, gender does not affect the degree or distribution of this modification in neural tissue, in contrast to previous observations involving TBI-induced protein carbonylation. Accordingly, gender differences in the CNS response to TBI may not involve differential responses in protein citrullination. In summary, this research indicates that abnormal protein citrullination is a feature of TBI that could contribute to ongoing pathological mechanisms following acute injury, possibly including aspects of autoimmune dysfunction.

ACKNOWLEDGMENTS

The authors would like to acknowledge the expert technical assistance of Ms. Tinghua Chen. Support for this work included a grant from the Defense Medical Research and Development Program (D61_I_10_J6_152), Department of Defense in the Center for Neuroscience and Regenerative Medicine (G1703D), as well as funding from the Uniformed Services University of the Health Services (T0702554 and R07028414).

All authors were involved in drafting the manuscript or revising it critically for important intellectual content to include the final approval of this version for publication. RL and GP Mueller substantially contributed to the conception and design of the work, analysis and interpretation of the data. JB, MF, JF, GH, GP Martinelli and DJ substantially contributed to the acquisition of the data. All agree to be accountable for all aspects of the work in ensuring that questions related to the accuracy or integrity of any part of the work are appropriately investigated and resolved.

CHAPTER 4: Discussion

The purpose of this work is to investigate the effects of TBI on two important post-translational protein modifications, carbonylation and citrullination. To date, little research has examined the specific regions, cell types, and proteins affected by these modifications following injury. Furthermore, while significant research has demonstrated gender-based differences in prognosis following TBI (53; 125), little work has investigated how gender impacts the distribution of these protein modifications after injury. Characterization of the selective impacts of carbonylation and citrullination allows insight into pathological pathways and ongoing dysfunction following TBI. Figure 23 presents these proposed pathways of long-term injury caused by TBI-induced carbonylation and citrullination.

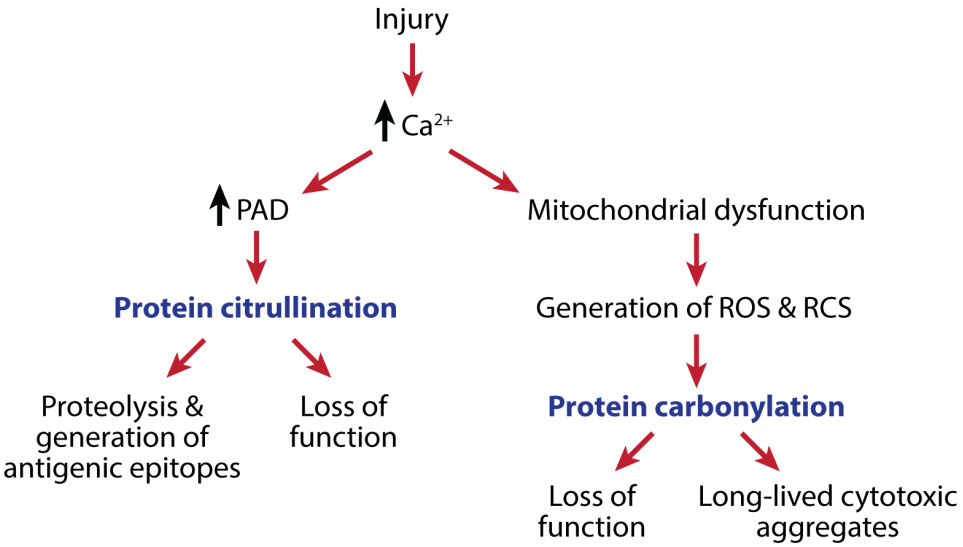

Figure 23. Potential ongoing effects of protein carbonylation and citrullination in TBI pathology. Injury may induce long-term dysfunction through the calcium-mediated proteomic modifications, carbonylation and citrullination. These modifications can elicit a number of pathological outcomes, including the generation of antigenic epitopes (citrullination) and formation of cytotoxic aggregates (carbonylation).

Following TBI, a number of progressive and pathological secondary injury mechanisms take place. One of these injury pathways involves dramatic ionic imbalance, leading to a damaging overload of intracellular calcium. This calcium excitotoxicity is a hallmark effect of TBI (49; 50; 90; 149; 160), and persists for several days following injury (52). Through this cascade, a series of cellular pathways become interrupted. Energy homeostasis is disturbed, as decreased cerebral blood flow limits oxygen and glucose availability (52). As intracellular calcium pathologically increases, the consequences of this accumulation may lead to dysfunctional protein carbonylation and protein citrullination.

Calcium overload can prompt carbonylation through the generation of reactive oxygen species (ROS) (80; 117) due to several possible pathways, including damaged respiration pathways, uncoupled electron transfer (110), and a decreased number of electron acceptors in the mitochondrial matrix (32). Reactive oxygen species can catalyze carbonylation through either direct interaction with proteins, or through the reaction of proteins with reactive carbonyl species, which are formed by the reaction of reactive oxygen species with polyunsaturated fatty acids (135; 136; 165).

Protein citrullination, in contrast, is not dependent on the presence of reactive oxygen species or reactive carbonyl species, but rather on the action of peptidylarginine deiminase (PAD). This family of enzymes is calcium-dependent: as calcium binds to PAD, a conformational change in the protein takes places, moving a catalytic residue into the enzyme's active site to act on arginine residues within other proteins (127). The reaction of PAD with arginine residues converts this amino acid to citrulline. Outside of the central nervous system, both carbonylation and citrullination are associated with

reperfusion / ischemia injuries, which can cause dysfunctional intracellular calcium regulation and oxidative stress in both the heart (130) and kidney (85). These tissues also express citrullinated proteins following reperfusion / ischemia trauma (8; 58), demonstrating that the calcium-associated modifications investigated here are both associated with damaged organ systems besides the CNS. In the brain, both carbonylation and citrullination can disrupt normal cellular physiology through a number of changes, including enzymatic inactivation (56), protein aggregation (26), and proteasomal inhibition (26).

Research presented within these manuscripts shows that carbonylation and citrullination impact separate brain regions five days following injury in a rodent model of TBI. While carbonylation was dramatically up-regulated at the site of the lesion and selective periventricular regions, including the area of the dorsal third ventricle and the median eminence, citrullination was increased in the cortex, external capsule, and hippocampus. Protein carbonylation and citrullination were both localized to astrocytes; however, carbonylation was also found in the ependymal cells of the dorsal third ventricle and median eminence. Furthermore, gender did not impact the magnitude or distribution of citrullination at five days following injury. In contrast, carbonylation was significantly affected by gender, in that male rats showed greater susceptibility to carbonylation at sites distant from the lesion site. Finally, proteomic analyses identified several proteins that were carbonylated following TBI, specifically GFAP, ALDOA, ALDOC and CRMP2. All four of these proteins, along with 33 others, were identified as expressing increased citrullination after TBI. The following sections will address the

significance of these findings and the implication of these data for understanding the long-term dysfunctions seen after TBI.

REGION AND CELL-SPECIFIC EFFECTS OF TBI ON PROTEIN CARBONYLATION AND CITRULLINATION

Five days following TBI in a rodent model of CCI, protein carbonylation and citrullination were expressed in specific cell types. Protein carbonylation was selectively expressed in astrocytes and ependymal cells, while protein citrullination was enhanced only in astrocytes. Further investigation revealed that neither of these post-translational modifications was significantly associated with neurons, oligodendrocytes, or microglia / macrophages, as indicated by co-localization with antibodies targeting NeuN, MBP and Iba1, respectively. As discussed in Chapter 3, our *in vitro* model of simulated TBI utilized the calcium ionophore, ionomycin, to induce excitotoxic calcium overload in normal human astrocytes. This series of experiments revealed that calcium overload induced the proteolytic processing of GFAP to a series of breakdown products, one of which is preferentially hyper-citrullinated. However, when this experimental protocol was repeated with neurons (SH-SY5Y), no citrullinated species were found in these cells prior to or following treatment with ionomycin (data not shown). These data suggest that astrocytes are distinctively susceptible to both protein carbonylation and citrullination at five days following TBI. In contrast, ependymal cells are selectively prone to carbonylation, but not citrullination.

TBI induces protein carbonylation in ependymal cells of the dorsal third ventricle and median eminence

Ependyma are specialized cells forming the barrier between cerebrospinal fluid and neural tissue, acting as both a metabolic and physical interface between these two

spaces (42). Interestingly, only certain populations of ependymal cells expressed increased protein carbonylation following TBI. This may reflect the broad heterogeneity of this cell type, as regards structure and function (13; 69), expression of membrane proteins (13), and differential vulnerability to CSF-borne toxins (69). The populations of affected ependyma lined the dorsal third ventricle and above the median eminence, at sites directly adjacent to CSF-filled cavities. While the ependymal cells near the dorsal third ventricle are not well characterized, the region at the base of the third ventricle just above the median eminence is well-known for its neurogenic cell populations (79) and involvement in neuroendocrine regulation (119).

It is possible that the unique exposure of ependyma to the CSF, and thus exposure to the reactive molecules transported within its mileu, prompt carbonylation within these cells. While reactive oxygen species have a limited capacity for diffusion across tissue following TBI, reactive carbonyl species are able to travel over longer distances (92). These lipid peroxidation products include the highly reactive aldehyde molecules 4-hydroxynonenal and malondialdehyde. Lipid peroxidation occurs as a very early event following TBI, with levels of peroxidation by-products elevated in neural tissue just thirty minutes following injury (7). Furthermore, these reactive molecules are rapidly increased in the CSF following TBI. As little as three hours following head trauma, levels of malondialdehyde are increased in the CSF, as compared to both uninjured controls and non-cerebral injured patients (2). Additionally, increased levels of 4-hydroxynonenal have been found in the CSF of patients with neurodegenerative disorders, including Parkinson's disease (134) and amyotrophic lateral sclerosis (138), suggesting a role for these aldehydes as indicators and mediators of pathology. Evidence has also suggested

that reactive carbonyl species are responsible for increased permeability of the blood-brain barrier following injury (1; 139). The specific regions of ependymal cells investigated here may be selectively susceptible to aldehyde-induced permeability, increasing their relative vulnerability to protein carbonylation through interaction with reactive carbonyl species transported through the CSF. Because 4-hydroxynonenal, malondialdehyde, and other reactive carbonyl species are relatively long-lived and can withstand extracellular transport from their site of generation (27; 135), it is conceivable that oxidative damage is transmitted to these selective regions of ependymal cells through the transport of reactive molecules from the site of injury via the ventricular system. The unique sensitivity of these particular ependymal regions may reflect unique functional characteristics of the cells involved, such as membrane permeability properties or membrane receptor protein heterogeneity. The lack of protein citrullination in ependymal cells is not surprising, given the limited distribution of citrullination-catalyzing PAD enzyme isoforms to mainly astrocytes (PAD2) (64) and neurons (PAD4) (2).

Region-specific protein carbonylation and citrullination within astrocytes following TBI

The greatest increases in protein carbonylation and citrullination following TBI were observed in astrocytes. To our knowledge, the work presented here is the first to show that astrocytes are acutely susceptible to these post-translational modifications following TBI. Five days after TBI, protein carbonylation is expressed in astrocytes of the lesion site (see Chapter 2). In contrast, protein citrullination is expressed only mildly in the lesion site, with the largest increase in this modification seen in astrocytes of the cerebral cortex, external capsule, and hippocampus (see Chapter 3).

One likely mechanism underlying astrocyte vulnerability to carbonylation and citrullination involves the complex interaction between these cells and calcium. Following TBI, a decrease in cerebral blood flow limits the amount of oxygen and glucose delivered to the brain, resulting in hypoxia and lack of metabolic support. During these post-injury conditions, astrocytes experience large elevations in intracellular calcium (45), to a much greater degree than the calcium influxes observed in neurons (128). Following ischemia, the disruption of cell membranes and mechanical stretching of cellular components leads to a rush of extracellular calcium into astrocytes. Additionally, mechanisms that normally offset the effects of extracellular glutamate are impaired (157). The glutamate-rich extracellular environment causes the activation of NMDA receptors (52), allowing a massive influx of calcium into cells. This influx further exacerbates the dramatically increased intracellular concentration of calcium due to direct injury (117; 157), causing a failure in energy metabolism (52) and the release of sequestered intracellular calcium from internal stores, including the endoplasmic reticulum and mitochondria (115; 151). While the precise response of astrocytes to calcium excitotoxicity is not fully defined, research has shown that astrocytes may exert a protective effect on neuronal viability by insulating these terminally differentiated cells from the effects of excessive extracellular glutamate (50), such that the accumulation of calcium by astrocytes serves to reduce extracellular calcium, and thus its damaging effects on neurons (45).

It is proposed that mitochondria are central to the effects of calcium overload on the expression of both carbonylated and citrullinated proteins in astrocytes. Large increases in intracellular calcium can lead to mitochondrial dysfunction through

interference with calcium sequestration in this organelle and uncoupling normal processes of energy metabolism. Impaired mitochondrial function leads to the enhanced generation of reactive oxygen species that are unchecked due to depleted stores of antioxidants, including glutathione (143). These reactive oxygen species generate carbonylation in two major ways. First, reactive oxygen species can directly carbonylate proteins by oxidizing carbon atoms within amino acids, including histidine, lysine, and cysteine, to form carbonyl groups. Second, reactive oxygen species generate aldehyde by-products through lipid peroxidation, and these reactive carbonyl species can introduce carbonyl groups into proteins. Citrullination is also catalyzed by astrocytic calcium overload. While homeostatic intracellular levels of calcium are in the range of the sub-micromolar, the optimal calcium concentration for PAD activation is in the high micromolar to millimolar range (131). Thus, the activation of PAD within astrocytes following TBI confirms proposals of astrocyte susceptibility to calcium overload in citrullination-inducing ischemic conditions.

Significant protein carbonylation was noted in the astrocytes of the lesion site (Chapter 2). It is probable that this observation reflects the acute, extreme oxidative stress at the most proximal site of tissue damage. Following impact, the lesion site is particularly prone to glutamate excitotoxicity, and thus calcium overload, as the mechanical shearing of cerebral blood vessels in the injured parenchyma leads to the increased release of this excitatory neurotransmitter (96). In contrast to carbonylation, protein citrullination in the lesion site was relatively less affected. This unexpected observation may be time-dependent. Because our experimental model necessarily examined tissue at only five days following injury, a more rapid time course for protein

citrullination at the lesion site might occur. In this manner, citrullinated proteins may clear from the injury site sooner than carbonylated proteins. A rapid clearance of citrullinated proteins could be due to at least two possible mechanisms. First, citrullination is known to alter tertiary structure to a more "open" conformation, and thereby could increase protein susceptibility to proteolytic degradation (93). Alternatively, protein citrullination may prompt cellular apoptosis (88), resulting in few citrullinated protein-containing cells remaining by day five after TBI. This possibility assumes that there is a degree of cell specificity in these citrullination and carbonylation responses.

Injury most predominantly affected protein citrullination in astrocytes of the cerebral cortex, external capsule, and hippocampus (Chapter 3). The molecular basis for this observation may relate to the up-regulation of a specific calcium channel in these three regions. Voltage-gated, class C L-type Ca^{2+} channels are uniquely expressed in astrocytes in response to ischemia, and are particularly sensitive to injury-mediated activation in the cortex, external capsule, and hippocampus (34). Nimodipine, an L-type calcium channel blocker, protects against astrocyte damage in conditions of calcium overload (59). It is possible, therefore, that these three regions are particularly susceptible to protein citrullination due to their unique activation of these calcium channels, which mediate calcium influx into astrocytes following hypoxia and ischemia (34). Protein carbonylation was not expressed in these regions at five days following injury, suggesting that oxidative stress in these regions is relatively low as compared to the proximal lesion site. This could be due to regional variations in cellular physiology including: variable antioxidant capacities; relative metabolic needs of each region; and differing levels of

reactive metal ions, including copper and iron, which can drive metal-catalyzed protein carbonylation.

Neurons and oligodendrocytes do not express protein citrullination after TBI

While past investigations have documented the presence of PAD2 in neurons, our work in both an *in vivo* CCI animal model and an *in vitro* model of simulated TBI calcium excitotoxicity failed to show protein citrullination in neurons following injury. Nevertheless, citrullinated proteins are reported to accumulate in neurons in both Alzheimer's pathology (2), and Parkinson's disease (98). Our findings showed that acute calcium toxicity, as induced in both of our models of injury, prompted astrocyte protein citrullination but not neuronal protein citrullination. This difference may be explained by cell-specific PAD isoforms. As noted earlier, astrocytes and neurons contain two separate isoforms of PAD: while astrocytes express PAD2, neurons express PAD4. Our data suggest that calcium overload may be necessary and sufficient for PAD2 activation, while necessary but *insufficient* for PAD4 activation. Considering the neurodegenerative nature of Alzheimer's and Parkinson's diseases, it is possible that PAD4 activation reflects a chronic rather than acute mechanism, including prolonged calcium imbalance, or perhaps other signaling pathways that have not yet been elucidated. Further investigation should reveal the precise molecular pathways that catalyze the activation of these specific isozymes, as this will reveal the detailed pathological progression of citrullination in damaged neural tissue.

It is of particular note that oligodendrocytes did not express citrullinated proteins, with consideration to the fact that proteomic analyses identified MBP as a citrullinated protein following TBI. MBP is a major structural component on the cytoplasmic side of

myelin sheaths, which are produced by oligodendrocytes, and this protein is considered to constitute a cell-specific marker for oligodendrocytes. There are several possible reasons that MBP was identified as a citrullinated protein by our proteomic studies, but did not colocalize with immunohistochemical probing. First, citrullinated MBP is highly susceptible to proteolysis (25), and these characteristic breakdown products may not be identified by anti-MBP immunohistochemical probing due to mismatched epitope detection by the antibody. Second, it is possible that the subcellular location of citrullinated MBP disallows for its identification by immunohistochemical techniques using anti-MBP antibodies. The predominant form of MBP in oligodendrocytes is membrane-associated, and it is possible that citrullination causes breakdown MBP products to relocate to separate intracellular domains. To investigate the possible presence of citrullinated proteins in oligodendrocytes, future work could utilize an *in vitro* model for oligodendrocytes similar to the astrocyte excitotoxicity methods detailed in this research. Furthermore, immunohistochemical studies may make use of anti-MBP reagents targeting separate, unique epitopes in order to detect citrullinated breakdown products. These reagents may also have greater efficacy in detecting intracellular populations of citrullinated MBP.

GENDER MODULATES PROTEIN CARBONYLATION FOLLOWING INJURY

This investigation has demonstrated that protein carbonylation, but not citrullination, is affected by gender. While the magnitude and distribution of protein citrullination following TBI was not observed to be different between males and females following injury, the degree of protein carbonylation was significantly influenced by gender. Specifically, protein carbonylation in uninjured male rats was significantly

greater than that observed in uninjured female rats, indicating a gender difference in the status of protein carbonylation in healthy animals. While male and female rats expressed a comparable degree of protein carbonylation in the lesion site, regions distant from the lesion site, specifically the ependymal zones of the dorsal third ventricle and the median eminence, were profoundly affected in males as compared to females.

As discussed above, it is possible that the carbonylation of proteins in ependymal cells reflects the effects of soluble reactive carbonyl species, in the form of reactive oxygen species-driven lipid peroxidation products. It has been proposed that the ovarian steroid progesterone may protect against the formation of reactive carbonyl species by preventing lipid peroxidation (124). It is therefore possible that female hormones serve a protective role against the formation of CSF-borne reactive carbonyl species. The observation that both male and female rats displayed similar degrees of protein carbonylation in the lesion site itself may be due to the fact that protein carbonylation in the site of direct injury reflects the acute action of transient reactive oxygen species rather than reactive carbonyl species.

Under current conditions, ovarian steroids may protect against the generation of reactive oxygen species and reactive carbonyl species. In support of this proposal is that females recover better following TBI as compared to males (17; 53; 125). The absence of gender effects in TBI-induced protein citrullination predicts that males and females are affected equally; however, this is not the case. Rather, in chronic autoimmune disorders involving abnormal citrullination, most notably multiple sclerosis (37) and rheumatoid arthritis (39), females are more profoundly affected than males. This suggests that factors in addition to gender contribute to the chronic pathology of these two conditions.

Alternatively, the present experimental design may have investigated a time point that simply was not informative for gender differences in long-term pathology caused by abnormal citrullination.

SELECTIVE MODIFICATION OF PROTEINS FOLLOWING TBI

The proteomic analyses reported here provide the first insights into the carbonylation and citrullination proteomes of TBI. As noted in Chapter 2, four proteins were identified as having enhanced carbonylation following injury: (1) GFAP; (2) CRMP2; (3) ALDOC; and (4) ALDOA. These proteins have also been identified as being carbonylated in other neurodegenerative disorders, including Alzheimer's disease (GFAP, CRMP, ALDOC) (30; 147), ischemic/reperfusion injury (CRMP2, ALDOC) (105), and multiple sclerosis (GFAP) (165).

Our work investigating protein citrullination (Chapter 3) revealed 37 separate protein species citrullinated in response to injury. In addition to identifying several cytoskeletal and metabolically-related proteins, this investigation showed that GFAP, CRMP2, ALDOA and ALDOC are also citrullinated in addition to being carbonylated. Furthermore, a large proportion of these 37 proteins have been identified as being citrullinated in other pathologies, including multiple sclerosis, Alzheimer's disease, prion disease, and rheumatoid arthritis (25; 57; 65; 68; 74; 99; 152).

The modified proteins identified here have essential roles in cellular repair, structure, metabolism, and signaling. For example, CRMP2 functions in axonal guidance, serving an important role in neuronal regeneration after injury (150), while GFAP is a major structural component of astrocytes. In addition to GFAP, several other structural proteins were found to be citrullinated following injury, including dynamin-1 and several

forms of beta-tubulin. Another functional group of modified proteins are those involved in metabolic processes, including peroxiredoxin-1 and creatine kinase b. Furthermore, several of the citrullinated proteins identified have established roles in cell-cell signaling, including synapsin-2, syntaxin-binding protein 1, and amphiphysin.

Interestingly, our findings are concordant with the results of other proteomic investigations on protein citrullination in rheumatoid arthritis and multiple sclerosis. Both diseases are associated with increased citrullination of key structural proteins and enzymes involved in cellular metabolic processes (73). Furthermore, several of the citrullinated proteins identified here, including ALDOA, ALDOC, and myelin basic protein have been shown to be citrullinated in other neural pathologies (23; 67). Proteomic analyses have also indicated that carbonylated proteins identified in this investigation are also found in other neurodegenerative pathologies. For example, carbonylated forms of both CRMP2 and GFAP characterize Alzheimer's disease (22; 29; 147) and aging rodent brain tissue (111; 163). GFAP has also exhibited increased carbonylation in these pathologies. Table 1 presents modified proteins identified by this investigation, along with a review of literature showing evidence that these proteins are carbonylated and / or citrullinated in other pathologies.

These findings suggest that particular proteins are selectively susceptible to either carbonylation or citrullination across multiple pathologies. Furthermore, four of the proteins identified here are altered by both modifications following TBI. The "double" modification of the proteins CRMP2, ALDOA, ALDOC, and GFAP may be due to at least two possible mechanisms. First, it is possible that an initial protein modification may yield a protein species that is more susceptible to a subsequent modification. For

example, it is known that protein citrullination alters the tertiary structure of myelin basic protein, reshaping this protein into a more open conformation (93). While this alteration is shown to increase the protein's susceptibility to protease degradation (93), it may also allow access of reactive oxygen species and reactive carbonyl species to previously inaccessible amino acids which may now be carbonylated. A second possibility is that the "double" identification of proteins actually reflects two separate pools of modified proteins. For instance, rather than a single pool of CRMP2 that is both carbonylated and citrullinated, it is possible that we have identified two individual groups, one carbonylated and the other citrullinated. If this is the case, then these separate post-translational groups may reflect the distinct regions affected by each modification, as revealed by our immunohistochemical investigations. Future research should investigate whether these proteins are present in neural regions as a single "double modification" pool, two separate pools of modified proteins, or all three. This may be accomplished through a number of experimental approaches, including: (1) dual immunohistochemical probing for citrullination and carbonylation, co-localized with a specific protein probe (for example, GFAP); (2) immunoprecipitation for a specific citrullinated or carbonylated protein, followed by immobilization on a membrane and immunoblotting for the second modification; and (3) investigation of specific proteins using collision-induced dissociation tandem mass spectrometry to identify specific sites of carbonylation and citrullination on peptide fragments.

			CARB	CIT	CARB	CIT	CARB	CIT	CARB	CIT	CARB	CIT
			ALZHEIMER'S DISEASE		PRION DISEASE		MULTIPLE SCLEROSIS/EAE		AGING BRAIN		OTHER	
CARBONYLATED		CRMP2	(22; 29)						(111)			
		ALDOA				(67; 68)			(111)			
		ALDOC	(148)			(68)			(111)			
		GFAP	(22; 148)	(57; 65)		(67; 68)	(165)	(23; 57)				
	CITRULLINATED	PRDX1				(68)			(158)			
		COF1				(68)			(158)			
		SYN2							(111)			
		ENOA	(29)			(67; 68)						Rheum. arthritis: (75)*
		ENOG				(68)						
		MBP		(57)		(67; 68)		(23; 57)*				
		HSP74					(165)		(111)			
		NSF							(111)			
		GRP78										Type 1 Diabetes: (123)*
		HSP7C	(29; 148)						(111)			
		STXB1	(22)									
		ACTB	(4)				(165)		(141)			
		KCRB	(4; 28)						(111)			
		TUBULIN-BETA	(4)			(68)	(165)		(141)			

Table 1. Increased expression of selective protein carbonylation and citrullination in multiple neurodegenerative pathologies. Proteomic analyses in this investigation revealed several proteins carbonylated and citrullinated following TBI (blue column). Many of these proteins are modified in other pathological neural disorders, including Alzheimer's disease, prion disease, multiple sclerosis/EAE (experimental autoimmune encephalomyelitis), and aging brain tissue. Asterisk (*) indicates evidence of modification-induced autoantigenicity.

POTENTIAL LONG-TERM EFFECTS OF PROTEIN CARBONYLATION AND CITRULLINATION ON TBI PATHOLOGY

Protein susceptibility to carbonylation is selective, but there is no clear explanation as to the underlying mechanism of this specificity. Research has suggested that this vulnerability may be due to the presence of specialized binding sites, unique protein conformation, or the relative frequency of amino acids that are targeted by oxidation, including lysine, histidine, and cysteine (40).

The effects of protein carbonylation have been extensively investigated in the context of neurodegenerative disorders. Through alteration of protein structure, carbonylation impacts cellular physiology by alteration or inactivation of essential processes. For example, the carbonylation of tubulin in neuroblastoma cells can inhibit neurite outgrowth, which is essential for neural plasticity and regeneration (97). In this manner, oxidative stress can lead to a chronic, functional shift in injury recovery through proteomic modification. Furthermore, excessive carbonylation in environments of extreme oxidative stress can inhibit pathways for protein degradation. While mild levels of carbonylation increase a protein's susceptibility to breakdown, an acute degree of carbonylation can inhibit degradation due to the protein's inability to fit into the catalytic sites of the proeasomal complex (97). As a result, aggregation of carbonylated proteins can occur, forming cytotoxic accumulates that are associated with disorders including Alzheimer's and Parkinson's diseases (104).

While citrullination is less studied in the context of neurological pathologies, this modification is known to have significant effects on protein antigenicity. Specifically, in addition to changing structure, citrullination also changes the charge and cleavage sites of affected proteins, leading to the presentation of novel, potentially antigenic epitopes

(156). This phenomenon is observed in multiple sclerosis, where the citrullination of myelin basic protein prompts myelin degeneration due to a loosened aggregation of lipids in the sheath structure (95). Citrullination of myelin basic protein also increases its susceptibility to degradation by proteinases, including cathespin D, leading to the formation and release of antigenic, citrulline-containing peptides which are presented to peripheral T cells (24). In healthy neural tissue, a small fraction of total myelin basic protein contains citrullinated residues; however, this amount increases three-fold in multiple sclerosis, inducing a targeted T cell response (5; 152). Citrullinated epitopes are the hallmark of the adaptive immune response in rheumatoid arthritis. Citrullination in this disorder elicits a dramatic production of targeted autoantibodies, to such a significant degree that anti-citrullinated protein antibodies serve as a diagnostic biomarker for this disease (60). Interestingly, two other proteins identified in this investigation are targeted as antigens in separate pathological conditions. Glucose-regulated protein 78 was identified in this research as citrullinated following TBI. Previous work has shown that the citrullinated form of this protein is an autoantigen in Type 1 Diabetes, where modified glucose-regulated protein 78 is secreted by pancreatic beta cells and prompts the production of autoantibodies (122). The current investigation also identified the protein amphiphysin as citrullinated following TBI. To our knowledge, this protein has not been noted as citrullinated in other disorders. However, interestingly, several neurological disorders, including encephalopathy and myelopathy, show increased expression of autoantibodies targeting amphiphysin. It is possible that this immune response is triggered by citrullinated epitopes as of yet unrevealed. Future research is required to determine whether citrullination is the mechanism underlying the antigenic

nature of amphiphysin in neural pathologies. Furthermore, while this immune response in neural tissue can cause significant tissue damage, the brain may also benefit from immune responses following injury. This benefit stems from the regulation of localized inflammation and re-building of the blood-brain barrier by the immune-modulating "glial scar," a post-injury collection of astrocytes, microglia, macrophages and extracellular matrix molecules (121). Future research should address the possible detriments and benefits of a citrullination-mediated immune response in neural tissue following injury, including aspects of localized inflammation and immune clearance.

SUMMARY AND CONCLUSIONS

The work presented here describes the distribution and selective proteomic effects of carbonylation and citrullination that occur five days following TBI. This investigation has shown that protein carbonylation and citrullination affect distinct neural regions, but are both dramatically expressed in astrocytes following injury. While gender influences the magnitude and regionalization of protein carbonylation, there is no such influence on protein citrullination after TBI. Furthermore, we have identified four proteins that are selectively carbonylated after injury. These four proteins, along with 33 others, are also citrullinated at five days following TBI.

This work has identified many proteins that are similarly carbonylated or citrullinated in neurodegenerative disorders, including Alzheimer's disease, prion disease, and multiple sclerosis. It is conceivable that shared modifications across disorders are indicative of shared pathological pathways. For example, our findings indicate that myelin basic protein is citrullinated following TBI, just as this protein is citrullinated in multiple sclerosis. Research has shown that myelin basic protein

undergoes proteolysis at specific cleavage sites following controlled cortical impact, reflecting similar processes in multiple sclerosis, as described earlier (81). The chronic demyelination noted in both multiple sclerosis and following TBI could reflect this shared protein modification, which would suggest a mechanistic link between acute, TBI-driven protein modification and chronic structural changes. The carbonylation of CRMP2 following TBI also represents a possible link for shared symptomatology. This protein, which is essential for axonal growth and neural regeneration, is carbonylated in the hippocampus in Alzheimer's disease (30), indicating a possible mechanistic role for CRMP2 carbonylation in the memory deficits seen in both this disorder and following TBI.

Currently, it is not well understood how the acute, mechanical impact of TBI leads to chronic pathology that can last anywhere from months to years. Protein modifications shared between TBI and neurodegenerative disorders may suggest a mechanistic link between physical injury and sustained dysfunction. Specific changes in protein structure and function, seen as early at five days following TBI, could lead to the pathological symptomatology mirrored in diseases such as Alzheimer's and multiple sclerosis. Revealing the specific proteomic effects of carbonylation and citrullination provides mechanistic insight into how acute injury translates into a chronic neurodegenerative disease. Future work addressing the time-course of these modifications, from days to weeks to years following TBI, will add significant understanding of how aberrant post-translational modifications translate into pathology. Further proteomic analyses of specific regions, including the hippocampus and cerebral cortex, could reveal biological correlates of region-related cognitive deficits, including

memory dysfunction and loss of executive function. We propose, therefore, that protein carbonylation and citrullination represent critical mechanistic links between acute physical injury and long-term pathology. Further investigations of these proteomic shifts following TBI will lend insight into the biological mechanisms of this injury and may also point to preventative measures to counteract long-term pathogenesis.

REFERENCES

1. Abdul-Muneer P, Chandra N, Haorah J. 2014. Interactions of Oxidative Stress and Neurovascular Inflammation in the Pathogenesis of Traumatic Brain Injury. *Mol Neuobiol* [Epub ahead of print]

2. Acharya N, Nagele E, Han M, Coretti N, DeMarshall C, et al. 2012. Neuronal PAD4 expression and protein citrullination: Possible role in production of autoantibodies associated with neurodegenerative disease. *Journal of Autoimmunity* 38:369 - 80

3. Adamus G, Bonnah R, Brown L, David L. 2013. Detection of autoantibodies against heat shock proteins and collapsin response mediator proteins in autoimmune retinopathy. *BMC Ophthalmol* 13

4. Aksenov M, Aksenova M, Butterfield D, Geddes J, Markesbery W. 2001. Protein Oxidation in the Brain in Alzheimer's Disease. *Neuroscience* 103:373 - 83

5. Anderton S. 2004. Post-translational modifications of self antigens: implications for autoimmunity. *Current Opinion in Immunology* 16:753 - 8

6. Anzilotti C, Pratesi F, Tommasi C, Migliorini P. 2010. Peptidylarginine deiminase 4 and citrullination in health and disease. *Autoimmunity Reviews* 9:158 - 60

7. Arent M, de Souza L, Dafre A. 2014. Perspectives on Molecular Biomarkers of Oxidative Stress and Antioxidant Strategies in Traumatic Brain Injury. *BioMed Research International* 2014:1-18

8. AS S, JI B, K M, al. e. 2014. VWF-mediated leukocyte recruitment with chromatin decondensation by PAD4 increases myocardial ischemia/reperfusion injury in mice. *Blood* 123:141 - 8

9. Asaga H, Ishigami A. 2001. Protein deimination in the rat brain after kainate administration: Citrulline-containing proteins as a novel marker of neurodegeneration. *Neuroscience Letters* 299:5 - 8

10. Ates O, Cayli S, Altinoz E, Gurses I, Yucel N, et al. 2006. Neuroprotection by resveratrol against traumatic brain injury in rats. *Molecular and Cellular Biology* 294:137 - 44

11. Azimzadeh O, Scherthan H, Sarioglu H, Barjaktarovic Z, Conrad M, et al. 2011. Rapid proteomic remodeling of cardiac tissue caused by total body ionizing radiation. *Proteomics* 11:3299 - 311

12. Bales J, Wagner A, Kline A, Dixon C. 2009. Persistent cognitive dysfunction after traumatic brain injury: A dopamine hypothesis. *Neurosci Biobehav Rev* 33:981 - 1003

13. Barrett P, Ivanova E, Graham ES, Ross AW, Wilson D, et al. 2006. Photoperiodic regulation of cellular retinoic acid-binding protein 1, GPR50 and nestin in tanycytes of the third ventricle ependymal layer of the Siberian hamster. *Journal of Endocrinology* 191:687 - 98

14. Bayir H, Marion DW, Puccio AM, Wisniewski SR, Janesko KL, et al. 2004. Marked gender effect on lipid peroxidation after severe traumatic brain injury in adult patients. *Journal of Neurotrauma* 21:1 - 8

15. Bayr H. 2005. Reactive Oxygen Species. *Critical Care Medicine* 33:S498 - S501

16. Berry C, Ley E, Tillou A, Cryer G, Marguilies D, Salim A. 2009. The effect of gender on patients with moderate to severe head injuries. *J Trauma: Inj., Infect., Crit Care* 67:950 - 3

17. Berry C, Ley EJ, Tillou A, Cryer G, Marguilies DR, Salim A. 2009. The effect of gender on patients with moderate to severe head injuries. *Journal of Trauma – Injury, Infection & Critical Care* 67:950 - 3

18. Beschorner R, Adjodah D, Schwab JM, Mittelbronn M, Pedal I, et al. 2000. Long-term expression of heme oxygenase-1 (HO-1, HSP-32) following focal cerebral infarctions and traumatic brain injury in humans. *Acta Neuropathologica* 100:377 - 84

19. Bhattacharya S, Crabb J, Bonilha V, Gu X, Takahara H, Crabb J. 2006. Proteomics Implicates Peptidyl Arginine Deiminase 2 and Optic Nerve Citrullination in Glaucoma Pathogenesis. *Invest. Ophthalmol. Vis. Sci.* 47:2508 - 14

20. Bizzozero OA, DeJesus G, Callahan K, Paruszyn A. 2005. Elevated protein carbonylation in the brain white matter and gray matter of patients with multiple sclerosis. *Journal of Neuroscience Research* 81:687 - 95

21. Bosken JM, Wang JA, Hall ED, eds. 2012. *Assessments of Oxidative Damage and Lipid Peroxidation After Traumatic Brain Injury and Spinal Cord Injury*, Vols. II: Springer Protocols Handbooks.

22. Boyd-Kimball D, Castegna A, Sultana R, Poon H, Petroze R, et al. 2005. Proteomic identification of proteins oxidized by Ah(1–42) in synaptosomes: Implications for Alzheimer's disease. *Brain Research* 1044:206 - 15

23. Bradford C, Cross A, Haddock G, Woodroofe N, Sharrack B. 2011. Citrullination of CNS proteins in the pathogenesis of multiple sclerosis. *Future Neurology* 6:521

24. Bradford C, Nicholas A, Woodroofe N, Cross A. 2002. Chapter 10: Deimination in Multiple Sclerosis and Experimental Autoimmune Encephalomyelitis. In *Protein Deimination in Human Health and Disease* ed. A Nicholas, S Bhattacharya:165 - 85: Springer. Number of 165 - 85 pp.

25. Bradford C, Ramos I, Cross A, Haddock A, McQuaid S, et al. 2014. Localisation of citrullinated proteins in normal appearing white matter and lesions in the central nervous system in multiple sclerosis. *Journal of Neuroimmunology* 273:85 - 95

26. Butterfield DA, Perluigi M, Reed T, Muharib T, Hughes CP, et al. 2012. Redox proteomics in selected neurodegenerative disorders: From its infancy to future applications. *Antioxidants and Redox Signaling* 17:1610 - 55

27. Carini M, Orioli M. 2010. Mass spectrometric strategies for identification and characterization of carbonylated peptides and proteins. In *Biomarkers for Antioxidant Defense and Oxidative Damage: Principles and Practical Applications*, ed. G Aldini, KJ Yeum, E Niki, RM Russell:173 - 97: Wiley-Blackwell. Number of 173 - 97 pp.

28. Castegna A, Aksenov M, Aksenova M, Thongboonkerd V, Klein J, et al. 2002. Proteomic identification of oxidatively modified proteins in Alzheimer's disease brain. Part I: creatine kinase BB, glutamine synthase, and ubiquitin carboxy-terminal hydrolase L-1. *Free Radical Biology and Medicine* 33:562 - 71

29. Castegna A, Aksenov M, Thongboonkerd V, Klein J, Pierce W, et al. 2002. Proteomic identification of oxidatively modified proteins in Alzheimer's disease brain. Part II: dihydropyrimidinase-related-protein 2, a-enolase and heat shock cognate 71. *Journal of Neurochemistry* 82:1524 - 32

30. Castegna A, Aksenov M, Thongboonkerd V, Klein JB, Pierce WM, et al. 2002. Proteomic identification of oxidatively modified proteins in Alzheimer's disease brain. Part II: dihydropyrimidinase-related protein 2, α-enolase and heat shock cognate 71. *Journal of Neurochemistry* 82:1524 - 32

31. Chen Y, Swanson RA. 2003. Astrocytes and Brain Injury. *Journal of Cerebral Blood Flow & Metabolism* 23:137 - 49

32. Chinopoulos C, Adam-Vizi V. 2006. Calcium, mitochondria and oxidative stress in neuronalpathology: Novel aspects of an enduring theme. *FEBS Journal* 273:433 - 50

33. Chirivi R, van Rosmalen J, Jenniskens G, Pruijn G, Raats J. 2013. Citrullination: A Target for Disease Intervention in Multiple Sclerosis and other Inflammatory Diseases? *J Clin Cell Immunol* 4

34. Chung Y, Shin C, Kim M, Cha C. 2001. Enhanced expression of L-type Ca2+ channels in reactive astrocytes after ischemic injury in rats. *Neuroscience Letters* 302:93 - 6

35. Clausen F. 2004. *Delayed cell death after traumatic brain injury: Role of Reactive Oxygen Species*. Uppsala University, Uppsala. 77 pp.

36. Conrad CC, Talent JM, Malakowsky CA, Gracy RW. 1999. Post-electrophoretic identification of oxidized proteins. *Biological Procedures Online* 2:39 - 45

37. Coyle P, Christie S, Fodor P, Fuchs K, Giesser B, et al. 2004. Multiple sclerosis gender issues: clinical practices of women neurologists. *Multiple Sclerosis* 10:582 - 8

38. Curis E, Nicolis I, Moinard C, Osowska S, Zerrouk N, et al. 2005. Almost all about citrulline in mammals. *Amino Acids* 29:177 - 205

39. Da Silva J, Hall G. 1992. The effects of gender and sex hormones on outcome in rheumatoid arthritis. *Baillere's Clinical Rheumatology* 6:193 - 219

40. Dalle-Donne I, Aldini G, Carini M, Colombo R, Rossi R, Milzani A. 2006. Protein carbonylation, cellular dysfunction, and disease progression. *Journal of Cellular and Molecular Medicine* 10:389 - 406

41. Dalle-Donne I, Giustarini D, Colombo R, Rossi R, Milzani A. 2003. Protein carbonylation in human diseases. *Trends in Molecular Medicine* 9:169 - 76

42. Del Bigio MR. 2010. Ependymal cells: biology and pathology. *Acta Neuropathologica* 119:55 - 73

43. Desagher S, Glowinski J, Premont J. 1996. Astrocytes protect neurons from hydrogen peroxide toxicity. *The Journal of Neuroscience* 16:2553 - 62

44. Devi L, Prabhu BM, Galati DF, Avadhani NG, Anandatheerthavarada HK. 2006. Accumulation of Amyloid Precursor Protein in the Mitochondrial Import Channels of Human Alzheimer's Disease Brain Is Associated with Mitochondrial Dysfunction. *Neuroscience* 26:9057 - 68

45. Duffy S, MacVicar B. 1996. In Vitro lschemia Promotes Calcium Influx and Intracellular Calcium Release in Hippocampal Astrocytes. *The Journal of Neuroscience* 16:71 - 81

46. Elder G, Cristian A. 2009. Blast-Related Mild Traumatic Brain Injury: Mechanisms of Injury and Impact on Clinical Care. *Mount Sinai Journal of Medicine* 76:111 - 8

47. Eng LF. 1985. Glial fibrillary acidic protein (GFAP): The major protein of glial intermediate filaments in differentiated astrocytes. *J Neuroimmunol* 8:203 - 14

48. Faul M, Xu L, Wald MM, Coronado V, Dellinger AM. 2010. Traumatic brain injury in the United States: National estimates of prevalence and incidence, 2002–2006. *Injury Prevention* 16

49. Fineman I, Hovda D, Smith M, Yoshino A, Becker D. 1993. Concussive brain injury is associated with a prolonged accumulation of calcium: A 45Ca autoradiographic study. *Brain Research* 624:94 - 102

50. Floyd C, Gorin F, Lyeth B. 2005. Mechanical strain injury increases intracellular sodium and reverses Na+/Ca2+ exchange in cortical astrocytes. *Glia* 51:35 - 46

51. Ghajar J. 2000. Traumatic brain injury. *The Lancet* 356:923 - 9

52. Giza C, Hovda D. 2001. The Neurometabolic Cascade of Concussion. *Journal of Athletic Training* 36:228 - 35

53. Goswasser Z, Cohen M, Keren O. 1998. Female TBI patients recover better than males. *Brain Injury* 12:805 - 8

54. Goswasser Z, Cohen M, Keren O. 1998. Female TBI patients recover better than males. *Brain Inj* 12:805 - 8

55. Gould R, Freund C, Palmer F, Feinstein D. 2000. Messenger RNAs Located in Myelin Sheath Assembly Sites. *Journal of Neurochemistry* 75:1834 - 44

56. Grimsrud P, Xie H, Griffin T, Bernlohr D. 2008. Oxidative Stress and Covalent Modification of Protein with Bioactive Aldehydes. *The Journal of Biological Chemistry* 283:21837-41

57. György B, Tóth E, Tarcsa E, Falus A, Buzás E. 2006. Citrullination: A posttranslational modification in health and disease. *Int J Biochem Cell Biol* 38:1662 - 77

58. Ham A, Rabadi M, Kim M, Brown K, Ma Z, et al. 2014. Peptidyl arginine deiminase-4 activation exacerbates kidney ischemia-reperfusion injury. *American Journal of Physiology - Renal Physiology* 307:F1052-F62

59. Haun S, Murphy E, Bates C, Horrocks L. 1992. Extracellular calcium is a mediator of astroglial injury during combined glucose-oxygen deprivation. *Brain Research* 593:45 - 50

60. Hensvold A, Reynisdottir G, Catrin A. 2002. Chapter 2: From Citrullination to Specific Immunity and Disease in Rheumatoid Arthritis. In *Protein Deimination in Human Health and Disease*, ed. A Nicholas, S Bhattacharya:25 - 40. New York: Springer. Number of 25 - 40 pp.

61. Hoge C, McGurk D, Thomas J, Cox A, Engel C, Castro C. 2008. Mild Traumatic Brain Injury in U.S. Soldiers Returning from Iraq. *The New England Journal of Medicine* 358:453 - 63

62. Ikegami K, Setou M. 2010. Unique Post-Translational Modifications in Specialized Microtubule Architecture. *Cell Structure and Function* 35:15 - 22

63. Irwin RW, Yao J, Hamilton RT, Cadenas E, Brinton RD, Nilsen J. 2008. Progesterone and estrogen regulate oxidative metabolism in brain mitochondria. *Endocrinology* 149:3167 - 75

64. Ishigami A, Maruyama N. 2010. Importance of research on peptidylarginine deiminase and citrullinated proteins in age-related disease. *Geriatr Gerontol Int*. 10 S53 - 8

65. Ishigami A, Ohsawa T, Hiratsuka M, Taguchi H, Kobayashi S, et al. 2005. Abnormal accumulation of citrullinated proteins catalyzed by peptidylarginine deiminase in hippocampal extracts from patients with Alzheimer's disease. *J Neurosci Res* 80:120 - 8

66. Jang B, Shin HY, Choi JK, Nguyen du PT, Jeong BH, et al. 2011. Subcellular localization of peptidylarginine deiminase 2 and citrullinated proteins in brains of scrapie-infected mice: nuclear localization of PAD2 and membrane fraction-enriched citrullinated proteins. *J Neuropathol Exp Neurol*. 70:116 - 24

67. Jang B, Jin J, Jeon Y, Cho H, Ishigami A, et al. 2010. Involvement of peptidylarginine deiminase-mediated post-translational citrullination in pathogenesis of sporadic Creutzfeldt-Jakob disease. *Acta Neuropathologica* 119:199 - 210

68. Jang B, Kim E, Choi J, Jin J, Kim J, et al. 2008. Accumulation of Citrullinated Proteins by Up-Regulated Peptidylarginine Deiminase 2 in Brains of Scrapie-Infected Mice. *The American Journal of Pathology* 173:1129 - 42

69. Johanson C, Stopa E, McMillan P, Roth D, Funk J, Krinke G. 2011. The distributional nexus of choroid plexus to cerebrospinal fluid, ependyma and brain: Toxicologic / pathologic phenomena, periventricular destabilization, and lesion spread. *Toxicologic Pathology* 39:186 - 212

70. Kavakli HS, Erel O, Karakayali O, Neceluoglu S, Tanriverdi F, et al. 2010. Oxidative stress in isolated blunt traumatic brain injury. *Scientific Research and Essays* 5:2832 - 6

71. Kent T, Tour J. 2009. Mission Connect Mild TBI Translational Research Consortium, Baylor College of Medicine, Houston, Texas

72. Kernt M, Arend N, Buerger A, Mann T, Haritoglou C, et al. 2013. Idebenone prevents human optic nerve head astrocytes from oxidative stress, apoptosis, and senescence by stabilizing BAX/Bcl-2 ratio. *Journal of Glaucoma* 22:404 - 12

73. Kidd B, Ho P, Sharpe O, Zhao X, Tomooka B, et al. 2008. Epitope spreading to citrullinated antigens in mouse models of autoimmune arthritis and demyelination. *Arthritis Research & Therapy* 10

74. Kinloch A, Tatzer V, Wait R, Peston D, Lundberg K, et al. 2005. Identification of citrullinated α-enolase as a candidate autoantigen in rheumatoid arthritis. *Arthritis Research & Therapy* 7:R1421 - R9

75. Kinloch A, Tatzer V, Wait R, Peston D, Lundberg K, et al. 2005. Identification of citrullinated α-enolase as a candidate autoantigen in rheumatoid arthritis. *Arthritis Research & Therapy* 7:R1421-R9

76. Lam G. 2006. *Round 4: Citrullinated Proteins, Peptidylarginine Deiminase (PAD), and Rheumatoid Arthritis*.

77. Lange S, Rocha-Ferreira E, Thei L, Mawjee P, Bennett K, et al. 2014. Peptidylarginine deiminases: novel drug targets for prevention of neuronal damage following hypoxic ischemic insult (HI) in neonates. *J Neurochem* 130:555 - 62

78. Lazarus R, Buonora J, Jacobowitz D, Mueller G. 2015. Protein carbonylation after traumatic brain injury: Cell specificity, regional susceptibility, and gender differences. *Free Radical Biology and Medicine* 78:89 - 100

79. Lee DA, Bedont JL, Pak T, Wang H, Song J, et al. 2012. Tanycytes of the hypothalamic median eminence for a diet-responsive neurogenic niche. *Nature Neuroscience* 15:700 - 2

80. Lifshitz J, Sullivan P, Hovda D, Wieloch T, McIntosh T. 2004. Mitochondrial damage and dysfunction in traumatic brain injury. *Mitochondrion* 4:705 - 13

81. Liu M, Akle V, Zheng W, Kitlen J, O'Steen B, et al. 2006. Extensive degradation of muelin basic protein isoforms by calpain following traumatic brain injury. *Journal of Neurochemistry* 98:700 - 12

82. Luban S, Li Z. 2010. Citrullinated peptide and its relevance to rheumatoid arthritis: An update. *Int J Rheum Dis* 13:284 - 7

83. Luoma JI, Kelley BG, Mermelstein PG. 2011. Progesterone inhibition of voltage-gated calcium channels is a potential neuroprotective mechanism against excitotoxicity. *Steroids* 76:845 – 55

84. Mackay GM, Forrest CM, Stoy N, Christofides J, Egerton M, et al. 2006. Tryptophan metabolism and oxidative stress in patients with chronic brain injury. *European Journal of Neurology* 13:30 – 42

85. Malis C, Bonventre J. 1986. Mechanism of Calcium Potentiation of Oxygen Free Radical Injury to Renal Mitochondria *THE JOURNAL OF BIOLOGICAL CHEMISTRY* 261:14201 - 8

86. Maloney-Wilensky E, Gracias V, Itkin A, Hoffman K, Bloom S, et al. 2009. Brain tissue oxygen and outcome after severe traumatic brain injury: A systematic review. *Crit Care Med* 37:2057 - 63

87. Martinelli G, Friedrich Jr. V, Holstien G. 2002. L-Citrulline immunostaining identifies nitric oxide production sites within neurons. *Neuroscience* 114:111 - 22

88. Mastronardi F, Wood D, Mei J, Raijmakers R, Tseveleki V, et al. 2006. Increased Citrullination of Histone H3 in Multiple Sclerosis Brain and Animal Models of Demyelination: A Role for Tumor Necrosis Factor-Induced Peptidylarginine Deiminase 4 Translocation. *Neurobiology of Disease* 26:11387 - 96

89. Mattson M, Rychlik B. 1990. Glia protect hippocampal neurons against excitatory amino acid-induced degeneration: Involvement of fibroblast growth factor. *Int J Dev Neurosci* 8:399 - 415

90. McIntosh T, Saatman K, Raghupathi R. 1997. Calcium and the Pathogenesis of Traumatic CNS Injury: Cellular and Molecular Mechanisms. *Neuroscientist* 3:169 - 75

91. Merkulova M, Hurtado-Lorenzo A, Hosokawa H, Zhuang Z, Brown D, et al. 2011. Aldolase directly interacts with ARNO and modulates cell morphology and acidic vesicle distribution. *Am J Physiol Cell Physiol*. 300:C1442–C55

92. Mertsch K, Blasig I, Grune T. 2001. 4-Hydroxynonenal impairs the permeability of an in vitro rat blood brain barrier. *Neuroscience Letters* 314:135 - 8

93. Moscarello M, Mastronardi F, Wood D. 2007. The Role of Citrullinated Proteins Suggests a Novel Mechanism in the Pathogenesis of Multiple Sclerosis. *Neurochemical Research* 32:251- 6

94. Murinson B, Guarnaccia J. 2008. Stiff-person syndrome with amphiphysin antibodies: Distinctive features of a rare disease. *Neurology* 71:1955 - 8

95. Musse A, Li Z, Ackerly C, Bienzle D, Lei H, et al. 2008. Peptidylarginine deiminase 2 (PAD2) overexpression in transgenic mice leads to myelin loss in the central nervous system. *Disease Models & Mechanisms* 1:229 - 40

96. Mustafa A, Al-Shboul O. 2013. Pathophysiology of traumatic brain injury. *Neurosciences* 8:221 - 34

97. Neely M, Sidell K, Graham D, Montine T. 1999. The Lipid Peroxidation Product 4-Hydroxynonenal Inhibits Neurite Outgrowth, Disrupts Neuronal Microtubules, and Modifies Cellular Tubulin. *J Neurochem* 72:2323 - 33

98. Nicholas A. 2010. Dual immunofluorescence study of citrullinated proteins in Parkinson diseased substantia nigra. *Neuroscience Letters* 495:26 - 9

99. Nicholas A, Sambandam T, Echols J, Barnum S. 2005. Expression of Citrullinated Proteins in Murine Experimental Autoimmune Encephalomyelitis. *The Journal of Comparative Neurology* 486:254 - 66

100. Nicholas A, Sambandam T, Echols J, Tourtellotte W. 2004. Increased citrullinated glial fibrillary acidic protein in secondary progressive multiple sclerosis. *J Comp Neurol* 473:128 - 36

101. Nilsson P, Laursen H, Hillered L, Hansen A. 1996. Calcium Movements in Traumatic Brain Injury: The Role of Glutamate Receptor-Operated Ion Channels. *Journal of Cerebral Blood Flow & Metabolism* 16:262 - 70

102. Noble PG, Antel JP, Yong VW. 1994. Astrocytes and catalase prevent the toxicity of catecholamines to oligodendrocytes. *Brain Research* 1-2:83 - 90

103. Novarro A, Tolivia J, Alvarez-Uria M. 1995. Ultrastructural study of a special type of ependymal cell at paraventricular level of the golden hamster third ventricle. *Histology and Histopathology* 10:861 – 8

104. Nystom T. 2005. Role of oxidative carbonylation in protein quality control and senescence. *EMBO* 24:1311 - 7

105. Oikawa S, Kobayashi H, Kitamura Y, Zhu H, Obata K, et al. 2014. Proteomic analysis of carbonylated proteins in the monkey substantia nigra after ischemia-reperfusion. *Free Radical Research* 48:694 - 705

106. Okonkwo D, Yue J, Puccio A, Panczykowski D, Inoue T, et al. 2013. GFAP-BDP as an Acute Diagnostic Marker in Traumatic Brain Injury: Results from the Prospective Transforming Research and Clinical Knowledge in Traumatic Brain Injury Study. *J Neurotrauma* 30:1490 - 7

107. Opii WO, Nukal VN, Sultana R, Pandya JD, Day KM, et al. 2007. Proteomic identification of oxidized mitochondrial proteins following experimental traumatic brain injury. *Journal of Neurotrauma* 24:772 - 89

108. Papadopoulos MC, Koumenis IL, Yuan TY, Giffard RG. 1998. Increased vulnerability of astrocytes to oxidative injury with age despite constant antioxidant defenses. *Neuroscience* 82:915 - 25

109. Park E, Bell J, Baker A. 2008. Traumatic brain injury: Can the consequences be stopped? *CMAJ* 178:1163 - 70

110. Peng T, Jou M. 2010. Oxidative stress caused by mitochondrial calcium overload. *Annals of the New York Academy of Sciences* 1201:183 - 8

111. Perluigi M, Di Domenico F, Giorgi A, Schinina M, Coccia R, et al. 2010. Redox Proteomics in Aging Rat Brain: Involvement of Mitochondrial Reduced

Glutathione Status and Mitochondrial Protein Oxidation in the Aging Process. *Journal Neurosci Res* 88:3498 - 507

112. Peruzzo B, Pastor FE, Blazquez JL, Amat P, Rodrigues EM. 2004. Polarized endocytosis and transcytosis in the hypothalamic tanycytes of the rat. *Cell Tissue Research* 317:147 - 64

113. Peuchen S, Bolanos JP, Heales SJR, Almeida A, Duchen MR, Clark JB. 1997. Interrelationships between astrocyte function, oxidative stress and antioxidant status within the central nervous system. *Progress in Neurobiology* 52:261 - 81

114. Piao CS, Stoica BA, Wu J, Sabirzhanov B, Zhao Z, et al. 2013. Combined inhibition of cell death induced by apoptosis inducing factor and caspases provides additive neuroprotection in experimental traumatic brain injury. *Neurobiology of Disease* 46:745 - 58

115. Raijmakers R, Vogelzangs J, Croxford J, Wesseling P, van Venrooij W, Pruijn G. 2005. Citrullination of central nervous system proteins during the development of experimental autoimmune encephalomyelitis. *J Comp Neurol* 486:243 - 53

116. Rangarajan ES, Park H, Fortin E, Sygusch J, Izard T. 2010. Mechanism of Aldolase Control of Sorting Nexin 9 Function in Endocytosis *The Journal of Biological Chemistry* 285:11983 - 90

117. Ray S, Dixon C, Banik N. 2002. Molecular mechanisms in the pathogenesis of traumatic brain injury. *Histology and Histopathology* 17:1137 - 52

118. Readnower RD, Chavko M, Adeeb S, Conroy MD, Pauly JR, et al. 2010. Increase in Blood Brain Barrier Permeability, Oxidative Stress, and Activated Microglia in a Rat Model of Blast Induced Traumatic Brain Injury. *Journal Neurosci Res* 88:3530 - 9

119. Rodrigues EM, Blazquez JL, Pastor FE, Pelaez B, Pena P, et al. 2005. Hypothalamic tanycytes: A key component of brain-endocrine interaction. *International Review of Cytology* 247:89 - 164

120. Rodríguez-Rodríguez A, Egea-Guerrero JJ, Murillo-Cabezas F, Carrillo-Vico A. 2014. Oxidative stress in traumatic brain injury. *Current Medicinal Chemistry* 21:1201 - 11

121. Rolls A, Shechter R, Schwartz M. 2009. The bright side of the glial scar in CNS repair. *Nature Reviews Neuroscience* 10:235-41

122. Rondas D, Crèvecoeur I, D'Hertog W, Ferreira G, Staes A, et al. 2014. Citrullinated glucose-regulated protein 78 is an autoantigen in type 1 diabetes. *Diabetes* 64:573 - 86

123. Rondas D, Crèvecoeur I, D'Hertog W, Ferreira G, Staes A, et al. 2015. Citrullinated glucose-regulated protein 78 is an autoantigen in type 1 diabetes. *Diabetes* 64:573 - 86

124. Roof R, Hoffman S, Stein D. 1997. Progesterone protects against lipid peroxidation following traumatic brain injury in rats. *Mol. Clin. Neuropathol.* 31:1 - 11

125. Roof RL, Hall ED. 2000. Estrogen-related gender difference in survival rate and cortical blood flow after impact-acceleration head injury in rats. *Journal of Neurotrauma* 17:1155 - 69

126. Roof RL, Hoffamn SW, Stein DG. 1997. Progesterone protects against lipid peroxidation following traumatic brain injury in rats. *Molecular and Clinical Neuropathology* 31:1 - 11

127. Rorhbach A, Arandjelovic S, Mowen K. 2002. Physiological Pathways of PAD Activation and Citrullinated Epitope Generation. In *Protein Deimination in Human Health and Disease*, ed. A Nicholas, S Bhattacharya:1 - 24: Springer. Number of 1 - 24 pp.

128. Rzigalinski B, Weber J, Willoughby K, Ellis E. 1998. Intracellular Free Calcium Dynamics in Stretch-Injured Astrocytes. *Journal of Neurochemistry* 70:2377 - 85

129. Rzigalinski BA, Meehan K, Whiting MD, Dillon CE, Hockey K, Brewer M. 2011. Antioxidant Nanoparticles. In *Nanomedicine in Health and Disease*, ed. RJ Hunter, Preedy, V. R. :100 - 21. St. Helier, Jerset, British Channel Islands: Science Publishers. Number of 100 - 21 pp.

130. Saini H, Dhalla N. 2005. Defective calcium handling in cardiomyocytes isolated from hearts subjected to ischemia-reperfusion. *American Journal of Physiology - Heart and Circulatory Physiology* 288:H2260-H70

131. Sambandam T, Belousova M, Accaviti-Loper M, Blanquicett C, Guercello V, et al. 2004. Increased peptidylarginine deminiase type II in hypoxic astrocytes. *Biochemical and Biophysical Research Communications* 325:1324 - 9

132. Schindler AF, Olson EC, Spitzer NC, Montal M. 1996. Mitochondrial Dysfunction Is a Primary Event in Glutamate Neurotoxicity. *The Journal of Neuroscience* 16:6125 - 33

133. Schmidley J. 1990. Free Radicals in Central Nervous System Ischemia. *Current Concepts of Cerebrovascular Disease and Stroke* 25:7 - 12

134. Selley MS. 1998. (E)-4-hydroxy-2-nonenal may be involved in the pathogenesis of Parkinson's disease. *Free Radical Biology & Medicine* 25:169 - 74

135. Semchyshyn HM, Luschchak VL. 2012. Interplay between oxidative and carbonyl stresses: Molecular mechanisms, biological effects and therapeutic strategies of protection. In *Oxidative Stress - Molecular Mechanisms and Biological Effects*, ed. HM Semchyshyn, VL Luschchak. Vassyl Stefanuk Precarapathian National Universiy, Ukraine. Number of.

136. Shao TX, Roberts KN, Markesbery WR, Scheff SW, Lovell MA. 2006. Oxidative stress in head trauma in aging. *Free Radical Biology & Medicine* 41:77 - 85

137. Sidaros A, Engberg A, Sidaros K, Liptrot M, Herning M, et al. 2007. Diffusion tensor imaging during recovery from severe traumatic brain injury and relation to clinical outcome: A longitudinal study. *Brain* 131:559 - 72

138. Simpson EP, Henry YK, Henkel JS, Smith RG, Appel SH. 2004. Increased lipid peroxidation in sera of ALS patients: A potential biomarker of disease burden. *Neurology* 62:1758 - 65

139. Smith S, Andrus P, Zhang J, Hall E. 1994. Direct Measurement of Hydroxyl Radicals, Lipid Peroxidation, and Blood-Brain Barrier Disruption Following Unilateral Cortical Impact Head Injury in the Rat. *Journal of Neurotrauma* 11:393 - 404

140. Sofroniew MV, Vinters HV. 2010. Astrocytes: Biology and pathology. *Acta Neuropathologica* 119:7 - 35

141. Soreghan B, Yang F, Thomas S, Hsu J, Yang A. 2003. High-Throughput Proteomic-Based Identification of Oxidatively Induced Protein Carbonylation in Mouse Brain. *Pharmaceutical Research* 20:1713 - 20

142. Spengler J, Schell-Toellner D. 2014. Neutrophils and their contributions to autoimmunity in rheumatoid arthritis. In *Protein Deimination in Human Health and Disease*, ed. A Nicholas, S Bhattacharya:97 - 111: Springer. Number of 97 - 111 pp.

143. Starkov A, Chinopoulos C, Fiskum G. 2004. Mitochondrial calcium and oxidative stress as mediators of ischemic brain injury. *Cell Calcium* 36:257 - 64

144. Starkov AA, Chinopulos C, Fiskum G. 2004. Mitochondrial calcium and oxidative stress as mediators of ischemic brain injury. *Cell Calcium* 36:257 - 64

145. Stein DG, Wright DW, Kellermann AL. 2008. Does progesterone have neuroprotective properties? *Annals of Emergency Medicine* 51:164 - 72

146. Sugino N, Shimamura T, Tamura H, Ono M, Nakamura Y, et al. 1996. Progesterone inhibits superoxide radical production by mononuclear phagocytes in psuedopregnant rats. *Endocrinology* 137:749 - 54

147. Sultana R, Butterfield DA. 2010. Role of oxidative stress in the progression of Alzheimer's disease. *Journal of Alzheimer's Disease* 19:341 - 53

148. Sultana R, Perluigi M, Newman S, Pierce W, Cini C, et al. 2010. Redox Proteomic Analysis of Carbonylated Brain Proteins in Mild Cognitive Impairment and Early Alzheimer's Disease. *Antioxid Redox Signal* 12:327 - 36

149. Sun D, Deshpande L, Sombati S, Baranova A, Wilson M, et al. 2008. Traumatic brain injury causes a long-lasting calcium (Ca2+)-plateau of elevated intracellular Ca levels and altered Ca2+ homeostatic mechanisms in hippocampal neurons surviving brain injury. *Eur J Neurosci* 27:1659 - 72

150. Suzuki Y, Nakagomi S, Namikawa K, Kiryu-Seo S, Inagaki N, et al. 2003. Collapsin response mediator protein-2 accelerates axon regeneration of nerve-injured motor neurons of rat. *Journal of Neurochemistry* 86:1042–50

151. Szydlowskaa K, Tymianskia M. 2010. Calcium, ischemia and excitotoxicity. *Cell Calcium* 47:122 - 9

152. Tranquill L, Cao L, Ling N, Kalbacher H, Martin R, Whitaker J. 2000. Enhanced T cell responsiveness to citrulline-containing myelin basic protein in multiple sclerosis patients. *Multiple Sclerosis* 6:220 - 5

153. Tyurin VA, Tyurina YY, Borisenko GG, Sokolova TV, Ritov VB, et al. 2000. Oxidative stress following traumatic brain injury in rats: Quantitation of biomarkers and detection of free radical intermediates. *Journal of Neurochemistry* 75:2178 - 89

154. Van Den Heuvel C, Vink R. 2004. Recent advances in the development of multifactorial therapies for the treatment of traumatic brain injury. *Expert Opinion on Investigational Drugs* 13:1263 - 74

155. Vibulsreth S, Hefti F, Ginsberg M, Dietrich W, Busto R. 1987. Astrocytes protect cultured neurons from degeneration induced by anoxia. *Brain Research* 422:303 - 11

156. Vossenaar E, Radstake T, van der Heijden A, van Mansum M, Dieteren C, et al. 2004. Expression and activity of citrullinating peptidylarginine deiminase enzymes in monocytes and macrophages. *Ann Rheum Dis* 63:373 - 81

157. Walker K, Tesco G. 2013. Molecular mechanisms of cognitive dysfunction following traumatic brain injury. *Front Aging Neurosci*. 5

158. Wang Q, Zhao X, He S, Liu Y, An M, Ji J. 2010. Differential Proteomics Analysis of Specific Carbonylated Proteins in the Temporal Cortex of Aged Rats: The Deterioration of Antioxidant Systems. *Neurochem Res* 35:13 - 21

159. Wang S, Wang Y. 2013. Peptidylarginine deiminases in citrullination, gene regulation, health and pathogenesis. *Biochimica et Biophysica Acta* 1829:1126 - 35

160. Weber J. 2012. Altered Calcium Signaling Following Traumatic Brain Injury. *Frontiers in Pharmacology* 3:1 - 16

161. Werner C, Engelhard K. 2007. Pathophysiology of traumatic brain injury. *British Journal of Anaesthesia* 99:4 - 9

162. Wong CM, Bansal G, Marcocci L, YJ S. 2012. Proposed role of primary protein carbonylation in cell signaling. *Redox Rep*. 17:90 - 4

163. Zhang Z, Zoltewicz J, Mondello S, Newsom K, Yang Z, et al. 2014. Human Traumatic Brain Injury Induces Autoantibody Response against Glial Fibrillary Acidic Protein and Its Breakdown Products. *PLoS One* 9:e92698

164. Zhao Y, Tian X, Li Z. 2010. Impact of citrullination upon antigenicity of fibrinogen. *Zhonghua Yi Xue Za Zhi* 90:628 - 32

165. Zheng J, Bizzozero OA. 2010. Accumulation of protein carbonyls within cerebellar astrocytes in murine experimental autoimmune encephalomyelitis. *Journal of Neuroscience Research* 88:3376 - 85

166. Zoltewicz J, Scharf D, Yang B, Chawla A, Newsom K, Fang L. 2012. Characterization of Antibodies that Detect Human GFAP after Traumatic Brain Injury. *Biomarker Insights* 7:71 - 9

Appendix 1: Technical validation of 6B3 anti-citrullinated protein antibody

Methodology: Citrullination of a mixture of known proteins: A mixture of seven known proteins (trypsinogen, glyceraldehyde 3-phosphate dehydrogenase, bovine albumin, trypsin inhibitor, alpha-lactalbumin, carbonic anhydrase, & egg albumin) was incubated with a cocktail of active PAD enzymes (SignalChem, P312-37C-25) in Tris buffer (50mM Tris HCl, pH 7.4) containing 5mM CaCl2 and 0.8mM DTT for 10 hours at 37C. The products of this reaction were fractionated by 1-D gel electrophoresis and visualized by anti-citrulline western blot analysis using a monoclonal anti-citrulline antibody, 6B3 "MAb a-citrulline, Cult Sup., 1995 batch, Lyoph May/20/2010," (1:20 dilution). Proteins making up the mixture, along with their respective masses, are shown in **Figure 1**. Their respective citrullination by the PAD Cocktail enzyme mixture is shown in the western blot (**Figure 2**) by comparing **Lane 3** (PAD-negative condition) to **Lane 4** (PAD-positive condition). Please note that carbonic anhydrase in the mixture was intentionally present in a higher concentration as compared to the other six proteins. This was done based on our previous finding that carbonic anhydrase is very susceptible to PAD-catalyzed citrullination and our hope to produce at least one citrulline-positive product.

Investigation of protein citrullination brains of control and TBI rats.

Proteins were prepared from the brains from adult control and TBI rats and evaluated by anti-citrulline western blot analysis as described above. In addition, we also examined a sample of brain homogenate prepared from neonatal (2 day) rat brain tissue.

Gel run protocol: MES buffer. 200 V, 400mA, 100w. 40 minutes. **Lane 1**: **Ladder**, BIORAD Prestained SDS-PAGE Standards, Low Range. 15ul ladder + 5ul loading buffer (reducing, 4x). **Lane 2**: **Neonatal mouse brain**, ~50ug + 5ul loading buffer (reducing, 4x). **Lane 3: Negative control for PAD-reacted sample (PAD-minus condition)**. 15ul negative control sample + 5ul loading buffer (reducing, 4x). Sample = 25ul collected from: 900ul protein mixture (225ug each of trypsinogen, glyceraldehyde 3-phosphate dehydrogenase, bovine albumin, trypsin inhibitor, alpha-lactalbumin, & egg albumin + 2475ug carbonic anhydrase) + 100ul of 0.5M Tris buffer / 50mM CaCl2 + 4ul 0.2M DTT. Carbonic anhydrase is present in a much higher concentration than the other proteins due to its relatively high degree of PAD-induced citrullination (previous findings). **Lane 4: PAD-reacted protein sample (PAD–plus condition)**: 15ul citrullinated sample + 5ul loading buffer (reducing, 4x). Sample = 900ul protein mixture (1575ug mixture of seven assorted proteins + 2250ug carbonic anhydrase)+ 100ul of 0.5M Tris buffer / 50mM CaCl2 + 4ul 0.2M DTT. Subtract 25ul taken for negative control. Added 25ul PAD cocktail, active. Incubated at 37C overnight. Spun in centrifuge at max speed, 5 min; supernatant removed and run on gel. **Lanes 5, 7, 9**: **Control rat brain samples**. 5ug each + 5ul loading buffer (reducing, 4x). **Lanes 6, 8, 10**: **TBI rat brain samples**, 5 days following TBI. 5ug each + 5ul loading buffer (reducing, 4x).

Gel: Gel was transferred to nitrocellulose for western blotting. After transfer, the residual proteins in the gel were visualized by Coomassie staining.

Blot: Gel transferred to nitrocellulose. Blot then blocked with 5% FBS / TBST for one hour. Probed overnight (4C, on shaker) with 1:20 6B3 MAb (brought up in 0.5ml glycerol / 0.5ml dH2O) in 5% FBS / TBST. Next day, washed three times, 20 minutes

each, with TBST. Probed with 1:5000 goat anti-mouse IgG secondary antibody (HRP labeled) in TBST for 1.5 hours. Washed three times, 20 minutes each, with TBST. Visualized with Novex ECL / HRP Chemiluminescent Substrate Reagent Kit.

Results

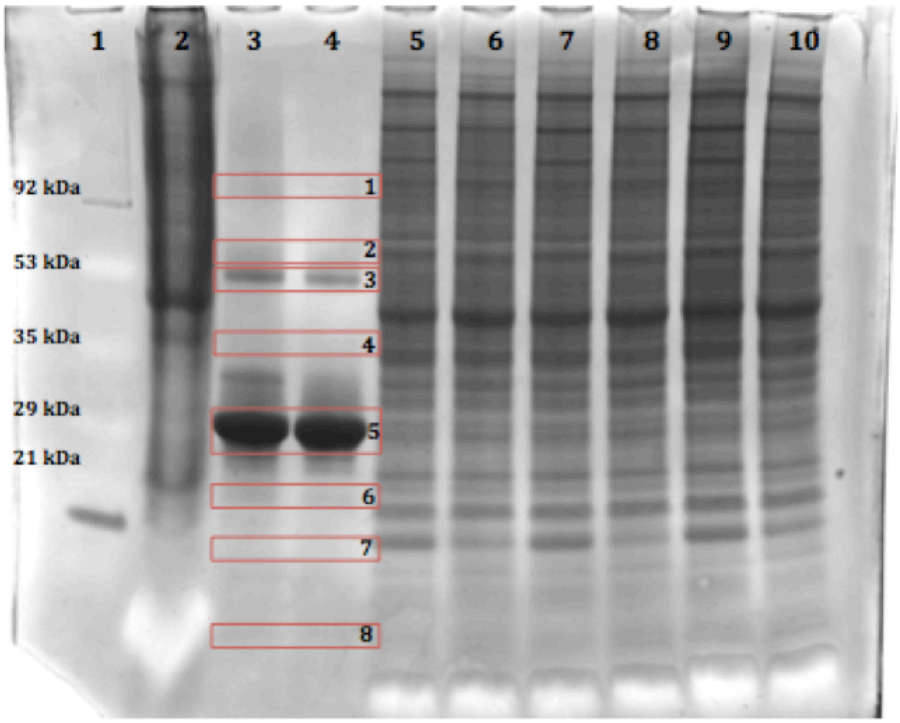

Appendix Figure 1. Coomassie-stained protein gel. After transfer, the gel was stained to visualize residual proteins. This figure shows: molecular weight markers in **Lane 1** (transfer virtually complete); overloading of neonatal (P2) brain sample (**Lane 2**); equivalent protein loading for PAD-negative (**Lane 3**) and PAD-positive (**Lane 4**) samples; and equivalent protein loading for the control (**Lanes 5, 7 & 9**) and TBI brain samples (**Lanes 6, 8 & 10**). Labeled proteins: **(1)** PAD proteins making up the Enzyme Cocktail, 95 – 100kDa; **(2)** Bovine serum albumin, 66kDa; **(3)** Egg albumin, 45kDa; **(4)** Glyceraldehyde 3- phosphate dehydrogenase, 36kDa; **(5)** Carbonic anhydrase, 29kDa; **(6)** Trypsinogen, 24kDa; **(7)** Trypsin inhibitor, 20.1kDa; **(8)** Alpha-lactalbumin, 14.2kDa.

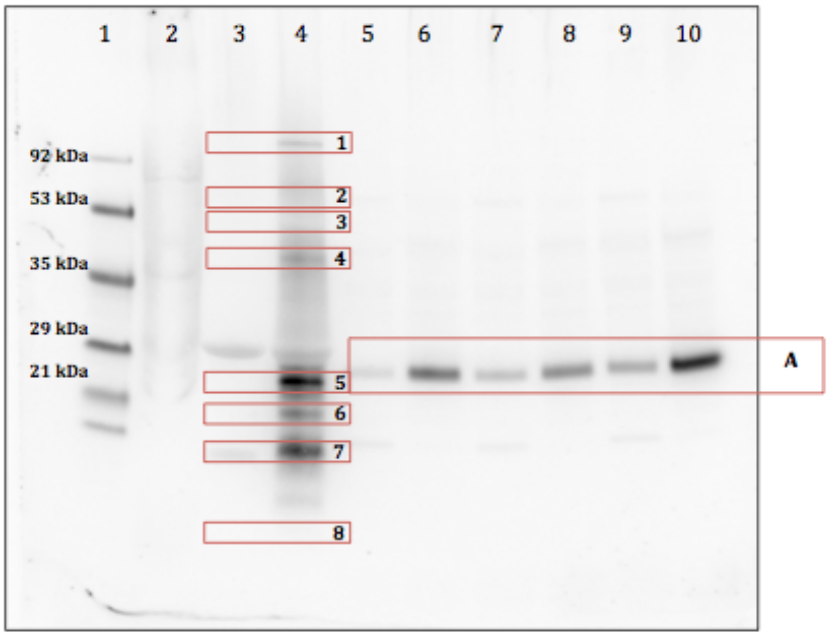

Appendix Figure 2. Visualized blot showing citrullinated proteins. After transfer, protein samples were visualized for citrullination using the monoclonal anti-citrulline antibody, 6B3 (1:20). This figure shows: molecular weight markers in **Lane 1**; over loaded neonatal (P2) brain sample (**Lane 2**); a relatively higher degree of protein citrullination in the PAD-positive (**Lane 4**) samples as compared to PAD- negative (**Lane 3**) samples; and a protein band at approximately 30kDa **("A")** that is significantly more citrullinated in TBI brain samples (**Lanes 6, 8 & 10**) than in control samples (**Lanes 5, 7 & 9).** Labeled proteins: **(1)** PAD Enzyme Cocktail, 95 – 100kDa; **(2)** Bovine albumin, 66kDa; **(3)** Egg albumin, 45kDa; **(4)** Glyceraldehyde 3-phosphate dehydrogenase, 36kDa; **(5)** Carbonic anhydrase, 29kDa; **(6)** Trypsinogen, 24kDa; **(7)** Trypsin inhibitor, 20.1kDa; **(8)** Alpha-lactalbumin, 14.2kDa. Proteins in **Lane 4** show differential susceptibility to citrullination, with proteins **(5)** carbonic anhydrase, **(6)** trypsinogen, and

(7) trypsin inhibitor containing relatively higher degrees of citrulline residues than the other processed proteins following PAD incubation.

Conclusions:

(1) PAD Cocktail citrullinated each of the seven proteins making up the protein mixture (**Lane 4**). Some proteins ((**5**) carbonic anhydrase, (**6**) trypsinogen, and (**7**) trypsin inhibitor) showed greater susceptibility to citrullination than other proteins in the mixture. This may be due to characteristics of tertiary structure, or possibly due to relatively greater arginine content. The PAD-negative control (**Lane 3**) is appropriately negative for citrullinated proteins.

(2) As tested here, the neonatal mouse brain contains no significantly citrullinated proteins. However, this sample lane was overloaded and subsequent tests with lower protein loads should be more informative.

(3) The control rat brain citrullinated proteome (**Figure 2. Lanes 5, 7, 9**) differs from injured rat brain citrullinated proteome (**Figure 2. Lanes 6, 8, 10**). Protein **A**, ~ 30 kDa, is significantly more citrullinated post-injury.